BINARY VAPOR-LIQUID PHASE EQUILIBRIUM FOR

METHANE IN SELECTED HEAVY NORMAL

PARAFFINS, NAPHTHENES, AND

AROMATICS

By

NAIF ABDELAZIZ DARWISH

Bachelor of Chemical Engineering
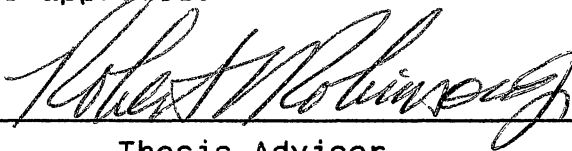University of Kuwait
Kuwait City, Kuwait
1981

Master of Mechanical Engineering
Yarmouk University
Irbid, Jordan
1983

Submitted to the Faculty of the
Graduate College of the
Oklahoma State University
in partial fulfillment of
the requirements for
the Degree of
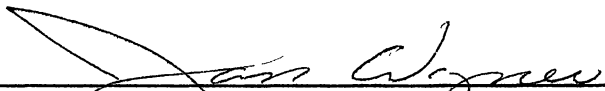DOCTOR OF PHILOSOPHY
May, 1991

BINARY VAPOR-LIQUID PHASE EQUILIBRIUM FOR

METHANE IN SELECTED HEAVY NORMAL

PARAFFINS, NAPHTHENES, AND

AROMATICS

Thesis approved:

_____
Thesis Advisor

_____

_____

_____

_____
Dean of the Graduate College

ii

PREFACE

An existing experimental apparatus was modified for the determination of bubble point pressures for binary mixtures of methane in paraffinic, naphthenic, and aromatic solvents at temperatures from 311 to 433 K and pressures to 113 bar. Precise bubble point data were obtained for methane binaries involving $n-C_{10}$, $n-C_{20}$, $n-C_{28}$, $n-C_{36}$, $n-C_{44}$, cyclohexane, t-decalin, benzene, naphthalene, phenanthrene, and pyrene. The solvents $n-C_{20}$, $n-C_{28}$, $n-C_{36}$, $n-C_{44}$, naphthalene, phenanthrene, and pyrene are solid at room temperature. Correlative efforts for methane + n-paraffins (C_3 and above) and methane + naphthenes and aromatics included: (1) Interaction parameters were determined for Soave-Redlich-Kwong (SRK) and Peng-Robinson (PR) equations of state using least squares regression of bubble point pressure data. (2) Several generalization schemes have been implemented for the SRK and PR interaction parameters in terms of pure hydrocarbon properties to extend the predictive capabilities of these equations to binary mixtures of methane + hydrocarbon solvents. (3) The new data and the data found in the literature were analyzed using the Krichevsky-Kasarnovsky model. This provided estimates of Henry's constants and infinite-dilution partial molar volumes of methane and demonstrated the internal consistency of the acquired data.

I wish to extend my sincere thanks and expressions of gratitude to Professor R. L. Robinson, Jr. for his advice, support and for the privilege of working under his supervision. His intelligent guidance, authoritative knowledge and depth of experience have significantly contributed to the completion of this study.

I would also like to thank and recognize Professor K. A. M. Gasem for the sacrifices he made during all phases of this study. He has proved indispensable as a guide and a mentor. Thanks are also extended to my advisory committee members Professor J. Wagner and Professor B. Ackerson for the time they spent in reading and criticizing this thesis.

Needless to say, this study was influenced by numerous contributions of so many, to those, to my teachers through the years, to my colleagues and to my friends goes my deepest sense of appreciation and indebtedness.

My greatest appreciation, thanks, and love go to my brothers: Abu Anas, Abu Malik, and Abu Jasim for their continued financial and moral support throughout the years.

My greatest appreciation and love go to my wife, for her patience and understanding, and to my children who make it all an enjoyable experience.

Most of all, to my mother, who wanted this more than I, I dedicate this humble work in recognition of her sacrifices and ever present love.

TABLE OF CONTENTS

TABLE OF CONTENTS (CONTINUED)

LIST OF TABLES

Table   Page

LIST OF TABLES (Continued)

LIST OF FIGURES

CHAPTER VII

CHAPTER I

INTRODUCTION

Problem and Importance

This study is concerned with the experimental determination of the solubility of methane in a number of hydrocarbon solvents, i.e., given the temperature and pressure of a certain binary mixture involving methane (e.g., CH_4 + $n-C_{10}$), the objective is to find the concentration (e.g., mole fraction) of methane dissolved in the liquid phase.

Phase equilibrium information (e.g., solubility in this case) is essential in many chemical engineering operations. Numerous separation processes such as distillation, absorption and extraction involve the transfer of chemical species between coexisting liquid and vapor phases. Rational design, operation, simulation, and optimization of such processes require the knowledge of equilibrium compositions of the existing phases over wide ranges of operating conditions of pressure and temperature. In the absence of reliable theoretical predictions, one has to resort to experimental data or to thermodynamic correlations derived from such data. Although multicomponent data are reported from time to time, the general practice is to investigate binary systems and estimate the behavior of multicomponent

1

systems on the basis of knowledge for the constituent binaries.

The study of phase equilibria for systems involving methane is motivated in part by interest in alternative fuels, especially, in view of price fluctuations and gradual depletion of light, high-quality crude oil. Alternative fuels include heavy crude oil, coal liquids, shale oil, and tar sands. The molecules in coal-derived fuels tend to be larger, more aromatic, and contain more oxygen, nitrogen, and sulfur than those in light crudes. During the initial stages of processing these heavy fossil fuels (e.g., dissolution of coal in a coal-derived recycle solvent), many light gases, such as CH_4, CO, CO_2, H_2S, H_2O, NH_3, and C_2-C_5, are produced thus creating a strong economic incentive for developing reliable thermodynamic data base for use in design and processing. An accurate and precise data base is also indispensable in testing, evaluating and developing solution theories. Binary mixtures of methane in heavy solvents, from the theoretical point of view, represents an attractive area of research because of the high nonideality of such mixtures which is a manifestation of the large difference in molecular size of the species involved.

Scope of the Present Work

The objective of the present work was to study, both experimentally and theoretically, the solubility of methane gas in systematically chosen sets of paraffinic, naphthenic,

and aromatic hydrocarbons.

Experimentally, the objectives were twofold: first, modification of an existing apparatus to accommodate methane systems and second, determination of methane solubilities (over the temperature range 100-320°F and mole fraction range of 0.0-0.3) in the following sets of hydrocarbons:

Paraffins: n-decane (n-C_{10}), n-eicosane (n-C_{20}), n-octaco-
             sane (n-C_{28}), n-hexatriacontane (n-C_{36}) and
             n-tetratetracontane (n-C_{44}). These paraffins,
             except n-decane, are solid at room temperature.

Naphthenes: Cyclohexane and trans-decalin, which are liquids
             at room temperature.

Aromatics: Benzene, naphthalene, phenanthrene, and pyrene.
             These aromatics, except benzene, are solid at
             room temperature.

These experiments were designed to investigate the effects of molecular size of the solvent on methane solubility and on our predictive abilities.

Our experimental data together with the available literature data were analyzed using Soave-Redlich-Kwong (SRK) and Peng-Robinson (PR) equations of state. Interaction parameters, C_{ij} and D_{ij}, for the SRK and the PR equations of state were obtained for the systems analyzed. The objectives here were to test the ability of cubic equations of state (EOS) in representing the experimental results and to explore the potentials of cubic EOS generalized predictions.

Organization of the Thesis

Chapter II describes the previous experimental work pertinent to the present study. Two areas of interest are reviewed briefly: high pressure experimental methods and experimental vapor-liquid equilibrium data involving methane and heavy hydrocarbons. The fundamental concepts in phase equilibrium problem, together with SRK and PR equations of state are reviewed in Chapter III. In Chapters IV and V, a detailed description of the modified apparatus and the experimental procedures used are presented. Presentation and analysis of our experimental data is the topic of Chapters VI, VII, and VIII. Correlations of methane solubilities in paraffins and other hydrocarbons are presented in Chapter IX. Analyses of systematic and random errors, together with the expected uncertainty in the measured values of the observables, are presented in Appendix A. In preparing this thesis a manuscript format was followed in writing chapters VI-IX, therefore, each of these chapters is a separate entity having its own tables, figures, symbols and references.

CHAPTER II

LITERATURE REVIEW

A comprehensive literature survey was conducted concerning the solubility of methane in hydrocarbons. The survey included Chemical Abstracts, Engineering Index, major data compilations such as that by Wichterle, et al. [1], and several specialized journals. The literature has been followed carefully for new contributions to the subject. Two distinct areas concerning this study will be reviewed briefly in this chapter: (1) experimental vapor-liquid equilibrium (VLE) data involving binary mixtures of methane in hydrocarbons, and (2) experimental apparatus which have been used in VLE data acquisition.

Experimental Data

Vapor liquid equilibria data of methane + hydrocarbons are of interest in a number of industrial processes, such as processing of petroleum products, and production of coal liquids. While several investigators [1-5] have compiled references for VLE data on methane + light hydrocarbon mixtures, data are scarce for systems involving methane and heavy hydrocarbon solvents which are solid at room temperature. At the inception of this work, no studies

(pertinent to our need) were found in the literature dealing
with the binary solubility of methane in any of the following
heavy hydrocarbon solvents: n-tetratetracontane ($n-C_{44}$), t-
decalin , naphthalene, phenanthrene and pyrene. More
recently, however, Malone and Kobayashi [6], reported binary
VLE data involving methane + phenanthrene. Literature
sources available on binary systems investigated in this
study, which are suitable for comparison purposes, are
presented in Table I. A specific literature set of binary
VLE data on methane + hydrocarbons will be considered later
(Chapter IX), when an attempt to generalize the equation-of-
state interaction parameters will be made.

Experimental Apparatus

In the last few years, different techniques for
experimental investigation of high pressure phase equilibria
have been proposed. A review covering the 1970s is given by
Eubank et al. [7] and a more recent review is given by
Fornari [4].

The experimental techniques used in VLE determinations
can be classified, according to the method employed to
determine compositions, as analytical and synthetic.

Analytical techniques require analysis of coexisting
phases following attainment of equilibrium. These could be
further categorized according to the methodology of attaining
equilibrium as static [8,18,9], continuous flow [10,11], and
circulation methods [12,13,14]. The latter two are dynamic

methods.

Synthetic techniques involve an indirect determination
of equilibrium compositions without sampling, so the
difficulties related to sampling process are avoided.
Recently analytic and synthetic methods were used incorporat-
ing the capacity for visual observations of phase behavior
where phase separation can be observed directly [15].

The experimental technique used in this study is a
synthetic one. The bubble point pressure of a synthetically
prepared binary mixture is identified graphically utilizing
the discontinuity in compressibility of the mixture as the
mixture crosses the liquid-vapor phase boundary [18]. This
method, therefore, consists of the introduction of known
amounts of well-degassed pure components into a variable-
volume thermostated equilibrium cell. The bubble point is
established by identifying the break point in a pressure-
volume curve. Reported methods for varying the volume in the
equilibrium cell include the use of a piston-cylinder
assembly [16] and the use of mercury as an incompressible,
involatile fluid piston [17]. The latter, used in this
study, is more suitable for high pressure, high temperature
operations since piston-cylinder assembly is more vulnerable
to leak problems due to thermal stresses.

Mechanical agitation of the cell contents is required
to ensure attainment of equilibrium in a reasonable time.
Several methods employed to accomplish this include rocking
the equilibrium cell [18] and magnetic stirring [19].

The mixing mode used in this study was rocking the cell from 45° below the horizontal level to 45° above horizontal level. The mixing was enhanced further by steel balls contained inside the cell.

Table I

Experimental Data for Methane + Hydrocarbons Used for Comparison Purposes in This Study

System	Temp. Range (°F)	CH₄ Mole Fraction Range	Reference Number
$CH_4 + n\text{-}C_{10}$	320 – 460	0.10 – 0.40	20
	77 – 302	0.03 – 0.30	21
	100 – 280	0.00 – 0.32	22
	100 – 220	0.05 – 0.44	23
$CH_4 + n\text{-}C_{20}$	212 – 392	0.05 – 0.20	24
$CH_4 + n\text{-}C_{28}$	212 – 392	0.05 – 0.25	25
$CH_4 + n\text{-}C_{36}$	212 – 392	0.06 – 0.27	26
$CH_4 +$ Cyclohexane	100 – 220	0.10 – 0.30	27
	100 – 220	0.37 – 0.45	28
	70 – 240	0.04 – 0.30	29
$CH_4 +$ Benzene	298 – 442	0.03 – 0.25	30
	100	0.20 – 0.53	31
	100 – 220	0.18 – 0.28	32
	150	0.01 – 0.21	33
	104	0.10 – 0.37	34
$CH_4 +$ Phenanthrene	257 – 302	0.02 – 0.18	35

CHAPTER III

A BRIEF REVIEW OF BASIC PRINCIPLES
IN PHASE EQUILIBRIA

The vapor-liquid phase equilibrium problem is reviewed briefly in this chapter with emphasis on the use of equations of state for both phases. For a more comprehensive treatment of the subject, reference could be made to fundamental texts on phase equilibria, in particular Van Ness and Abbott [36], Prausnitz [37], Prausnitz et al. [38], Chao and Robinson [39,40], Chao and Greenkorn [41], and Walas [42].

Phase Equilibrium Problem

When two phases containing N nonreacting chemical species are in equilibrium, the phase rule dictates that only N out of the 2N intensive variables (Temperature, T; Pressure, P; and N-1 mole fractions for each of the two phases) are independent and have to be specified for a full description of the system. The remaining N variables can be determined, in principle, by simultaneous solution of N equilibrium relations which can be stated as

$$f_i{}^v = f_i{}^l \qquad (i = 1, 2, 3,..., N) \qquad (1)$$

where $f_i{}^v$ and $f_i{}^l$ are the fugacities of component i in the

vapor and the liquid phases, respectively. Thus the solution of an equilibrium problem is reduced to the evaluation of fugacities (which have temperature, pressure and composition as the natural independent variables) of individual species in the coexisting phases. To evaluate fugacities in Equation 1, there are two basic thermodynamic procedures.

In the first alternative, an equation of state is assumed to be applicable to both phases and is used to evaluate f_i^v and f_i^l. In general, an equation of state, as referred to here, is an analytical expression that represents relations among volumetric properties, P, T, V for pure species and mixtures. In functional form this relation is

$$f(P,V,T,x) = 0 \qquad (2)$$

Usually, either P and T or T and V are chosen as independent variables of the equation of state, and V or P, respectively, is used as the dependent variable. Depending on this choice, the general algebraic forms of the derived quantities like fugacity are different, as discussed elsewhere [37]. With T and V as independent variables, the fugacities of species i can be evaluated from the exact thermodynamic relation [37]

$$RT \ln(f_i/x_i P) = \int_\infty^V [(\partial P/\partial n_i)_{T,V,n_j} - RT/V]dV - RT \ln(Z) \qquad (3)$$

where R is the gas constant, Z is the compressibility factor and n_i is the number of moles of species i. The terms $(\partial P/\partial n_i)_{T,V,n_j}$ and Z are evaluated using the equation of state.

In the second alternative, vapor phase fugacities are again
evaluated from an equation of state, but for the liquid phase
fugacities, an auxiliary function, activity coefficient, λ_i,
is defined so that

$$f_i = \lambda_i x_i f_i^{\,o} \tag{4}$$

where $f_i^{\,o}$ is the (standard state) fugacity of species i at
the system temperature and a certain standard pressure. In
principle, the use of equation of state for both phases has
several advantages over the activity coefficient method.
With the equation of state approach, the need for standard
states (which is often troublesome for systems containing
non-condensable components) is eliminated. Continuity at the
critical point is guaranteed since the same algebraic
equation is used for both phases. All necessary thermodynam-
ic relations may be derived from the same model. However,
this method is not free from limitations, since it requires
an equation of state which accurately represents volumetric
properties of both liquid and vapor phases throughout the
ranges of temperature, pressure, and composition of interest.
Also, extensions of equations of state to mixtures are not
always successful, since most of them are quite sensitive to
mixing rules.

SRK and PR Equations of State

Two equations of state used widely in industry are the Soave-Redlich-Kwong (SRK) and Peng-Robinson (PR) equations which are explicit in pressure, P, and cubic in volume, V. The SRK equation of state is [43]

$$P = \frac{RT}{V-b} - \frac{a(T)}{V(V+b)} \tag{5}$$

where

$$a(T) = a_c \alpha(T) \tag{6}$$

$$b = 0.08664\ RT_c/P_c \tag{7}$$

and

$$a_c = 0.42747\ R^2 T_c^2/P_c \tag{8}$$

$$\alpha(T)^{1/2} = 1 + k\ (1 - T_r^{1/2}) \tag{9}$$

$$k = 0.480 + 1.574\ w - 0.176\ w^2 \tag{10}$$

The PR equation of state is of similar form [44]

$$P = \frac{RT}{V-b} - \frac{a(T)}{V(V+b) + b(V-b)} \tag{11}$$

where a(T) and b are given as

$$a(T) = a_c \alpha(T) \tag{12}$$

$$b = 0.0778\ RT_c/P_c \tag{13}$$

$$a_c = 0.45724\ R^2 T_c^2/P_c \tag{14}$$

$$\alpha(T)^{1/2} = 1 + k\ (1 - T_r^{1/2}) \tag{15}$$

$$k = 0.37464 + 1.54226 \, w - 0.26992 \, w^2 \tag{16}$$

To apply the SRK or PR equations of state to mixtures, the values of a and b can be determined using the mixing rules [45]

$$a_m = \Sigma \, \Sigma \, z_i z_j (1 - C_{ij})(a_i a_j)^{1/2} \tag{17}$$

$$b_m = 0.5 \, \Sigma \, \Sigma \, z_i z_j (1 + D_{ij})(b_i + b_j) \tag{18}$$

In Equations 17 and 18 the summations are over all chemical species and C_{ij} and D_{ij} are empirical binary interaction parameters characterizing the binary interactions between components "i" and "j". Values of these parameters are typically determined by fitting experimental binary mixture data to minimize some objective function, SS, which, in this work, is the weighted sum of squared errors in predicted bubble point pressures

$$SS = \Sigma \, \frac{(P_{i\,exp} - P_{i\,calc})^2}{(\sigma_{ip})^2} \tag{19}$$

where

σ_{ip} is the uncertainty in the measured pressure (see Analysis of Experimental Errors - Appendix A) and the sum is over the data points analyzed. Further details of the data reduction techniques employed in this study are given by Gasem [18].

CHAPTER IV

EXPERIMENTAL APPARATUS USED IN THIS STUDY

The apparatus used in this study employs a variable
volume, static type, blind equilibrium cell for the
determination of bubble point pressures for synthetically
prepared mixtures of the solute gas (methane in this work)
and the respective solvent, which may be solid at room
conditions. The identification of the bubble point pressure
is achieved by following the compressibility of the mixture
as it changes abruptly across the liquid phase boundary. The
operation of the apparatus involves combining known amounts
of solute gas and a carefully degassed liquid solvent in a
thermostated equilibrium cell. The cell is rocked and the
contents are compressed by mercury so that the solute gas is
forced to dissolve in the solvent. The bubble point pressure
is taken as the pressure at which the gas phase disappears,
forming with the solvent, a homogeneous liquid phase.
Typical results of such a static experiment is an isothermal
p-x phase diagram.

The apparatus, as originally designed and built by
Gasem [18], employed a 90 cc equilibrium cell rocking between
the horizontal and the vertical positions. The effective
volume of the cell was varied by introducing mercury at the

bottom of the cell, while solvent and solute injections were made at the top of the cell. The equilibration time as reported by Gasem [18] was about 15-30 minutes for carbon dioxide solubility measurements. This means that more than 2 hours is needed to get a single bubble point on the p-x phase diagram. The apparatus, since then, has undergone an extensive modifications and reconstructions by a number of workers [19,46-49]. These modifications involved the equilibrium cell, the solute and solvent injection techniques the temperature and pressure instrumentations and control, and some other auxiliary circuits in the apparatus.

Most importantly, the rocking equilibrium cell was replaced by a stirred one, which reduced the equilibration time to 5 minutes for systems involving the solutes carbon dioxide and ethane [46]. This stirring technique, while adequate for carbon dioxide and ethane systems, resulted in poor mixing for methane in hydrocarbons heavier than n-octacosane (n-C_{28}) as revealed by equilibration times of the order of 30 minutes. To overcome the inadequate mixing in the stirred cell, different modes of mixing were tested. First, a vertically erected cell housing a steel ball driven by an external magnet was tested. The quality of mixing obtained by displacing the ball up and down the length of the equilibrium cell was poor in comparison with the stirring mechanism. A different approach was then employed to overcome the mixing problem and to avoid the use of mercury as a piston fluid. The proposed technique involved rocking

the equilibrium cell, which contains a certain binary mixture of known composition, in a temperature-programed liquid bath and using the solvent itself as the pressurizing medium to identify the break point in a pressure-volume curve. Once the bubble point is obtained at a given temperature, the exact amount of solvent in the cell is calculated and the composition is determined. The temperature then is dropped to the next desired temperature, thus flashing the previously liquid mixture into a vapor-liquid mixture. More solvent is injected to get the new bubble point and the procedure is repeated until the lowest desired temperature is reached. Upon completion of a run which may span four temperatures, the cell is cleaned and prepared for the next run. The procedure is repeated several times, starting each run with a different composition to cover the whole desired composition range. This technique was investigated for three different systems: ethane + n-hexane, methane + n-decane, and methane + n-hexatriacontane. Our results have indicated that identification of the bubble point pressure is a difficult and time consuming task in this approach. Further, while a glass windowed-cell could alleviate the problem in a well-designed equipment, it did not in our case. Other difficulties encountered in operating such an apparatus included the handling of solvents which are solids at room temperature. The storage cell of these solvents as well as the injection screw pump, must be placed in the liquid bath itself (or in another bath). This, combined with the high

probability of developing leaks due to thermal stresses, makes the technique somewhat difficult for solubility measurements of gases in heavy hydrocarbons which are solid at room temperature.

The implementation of the previous technique indicated that good mixing results from rocking the cell 90 degrees about the horizontal level. The combined effect of gravity on the steel balls inside the cell and the increased interfacial area between the two phases are perhaps responsible for the improved mixing. Therefore, it was decided to redesign and reconstruct the apparatus utilizing this method of mixing. Toward this end, three major modifications were implemented dealing specifically with:

1. The equilibrium cell: the stirred equilibrium cell was replaced by a rocking one. The cell, housing five steel balls, is designed to rock from 45° below to 45° above the horizontal level.

2. Dead volume: To a large extent, the dead volume was eliminated from the cell and the pertinent tubing and connections. This was achieved by injecting solute, solvent, and mercury through the same line at the bottom of the equilibrium cell, while having no connections at the other end of the cell. This also minimized leaking possibilities.

3. Cleaning and degassing circuits: Using the old cleaning procedure, the solvent, which could be solid at room temperature, could be easily trapped in some of lines outside the temperature bath, thus plugging these lines and

causing unnecessary delays.   This problem was alleviated in the new design by devising a different strategy for cleaning. Similarly, many redundant connections, fittings, and valves were eliminated to render degassing circuit more reliable and less prone to leaks.   The general layout of the apparatus is shown in Figure 1 and a detailed description of the important components is given below.

Equilibrium Cell

The central component of the apparatus is a variable volume, rocking equilibrium cell (EC). This is a 316 stainless steel tubular reactor (High Pressure Equipment Inc., Cat. No. MS-14) with an internal volume of 12.5 cc, a length of 10 in., an inside diameter, ID, of 5/16 in. and an outside diameter, OD of 9/16 in..   The equilibrium cell is connected at one "active" end to a simple pivoting assembly, while the other "dead" end is connected to an aluminum drive wheel, which is, in turn, driven by a 1/50 hp variable speed motor (Bodine Electric Company, type NSH-12R).   The end of the equilibrium cell is brought from a 45° above to 45° below the horizontal level at a controlled speed of about 15 rpm using a motor speed controller (Bodine Electric Company, model 901, type BSH-200).   Injections of solvent, solute, and mercury to the cell were made through a 1/16 in. OD, 0.03 in. ID stainless steel tubing welded to the pivoted end of the cell.   The effective volume of the cell can be varied by the introduction and withdrawal of mercury using a screw pump.

Five steel balls 3/16 in. in diameter are housed inside the cell to further promote mixing. Thus, the mercury acts in combination with the steel balls inside the cell to give excellent mixing.

Unique features of the equilibrium cell just described are its size and simplicity; being small in volume, the cell can be cleaned more efficiently, since all of its contents are disposed upon cleaning and no mercury from the previous run is retained in the cell for the next run, as was the case in the previous cells. Efficient cleaning of the cell is thought to be an important contribution toward the precision of data obtained in this study. Also, the cell is free of any unnecessary connections, which minimizes leaks.

The kind of mixing obtained from the cell described above has proved to be superior to that of the previous cells, as revealed by the equilibration time. For methane + n-hexatriacontane (n-C_{36}), the equilibration time was less than 5 minutes as compared to more than 30 minutes in the stirred cell previously used in the apparatus. Measuring the solubility of methane in pyrene would have been a very difficult task using the previous cells, using the present cell, however, an equilibration time of 5 minutes was observed.

Injection Pumps

Three injection pumps were used during the course of each run. A 10 cc positive displacement pump (HP, Figure 1) (Temco Incorporated, Model 10-1-12H), was used for measuring solvent injections as well as introducing and withdrawing mercury from the equilibrium cell during the experiment. The second injection pump was a 25 cc positive displacement pump (GP), (Temco Incorporated, Model 25-1-10HAT), used to inject solute gas into the equilibrium cell. Each pump was rated to 10,000 psia with a resolution of 0.005 cc. The third pump was a 500 cc positive displacement pump (CP), (Ruska Instruments Incorporated, Model 2210-801), rated to 12,000 psia with a resolution of 0.02 cc. This pump was used only for operations where precision was not required, as in cell cleanup.

Constant Temperature Baths

Two air baths were used in the operation of the apparatus. The first temperature controlled bath (Hotpack oven, Model 200001) houses the equilibrium cell (EC), the storage vessels (SV1 and SV2), and miscellaneous fittings, tubing, and valves. The second air bath was constructed of 1/2 in. plywood and used to house the two injection pumps (HP and GP) and pressure transducers (PT1 and PT2). Two proportional integral controllers (Halikainen, Model 1053 A), one in each bath, were used to maintain temperature within 0.1°C of the setpoint temperature. For the present study,

the temperature in the second air bath was set to 50°C.

The temperatures in the baths were measured using platinum resistance thermometers connected to digital readouts (Fluke Incorporated, Model 2180A), which have a resolution of 0.01°C.

Pressure Measurements

The pressure in the equilibrium cell was transmitted to a pressure transducer (PT1), (Sensotec Incorporated, Model ST5E1890) through mercury filled lines. The second transducer (PT2) was used to measure the solute gas pressure directly from the gas injection pump (GP). Each transducer has a range of 0 to 3000 psia and was calibrated regularly using a dead weight tester (Ruska Instrument Corporation, Model 2400.1). Pressure measurements were displayed on digital readouts (Sensotec Incorporated, Model 450D) with a resolution of 0.1 psia.

Vacuum System

The main components of the vacuum system are shown in Figure 2. Vacuum is achieved by a 100 1/m free air displacement mechanical vacuum pump (VP), (Sargent-Welch, Model 8811). A glass trap (GT) immersed in liquid nitrogen is used to trap condensable materials so they do not reach the vacuum pump. The vacuum level achieved is indicated by the vacuum meter (VM), (Sargent-Welch, Cat. No. S-39705-54), which receives its input signal from the vacuum gauge tube

(VG), (Sargent-Welch, Cat. No. S-39705-58), installed in the vacuum line. Vacuum levels down to 100 millitorr were achieved using this vacuum system.

Storage Vessels

Several vessels were used during the course of operation. The most important one is the solvent storage vessel (SV1). This is a high pressure reactor (High Pressure Equipment Inc., Model OC-3) which is used to store the degassed solvent at the operating temperature of the experiment for many runs.

Other vessels used included a 500 cc aluminum vessel used as a disposal vessel (TC1), a 250 cc mercury reservoir (MR), an 8 cc stainless steel vessel (SV2) and a 250 cc stainless steel vessel used during cleanup (SV3).

Fittings, Tubing, and Valves

All fittings, tubing, and valves used in the apparatus are made of 316 stainless steel and were supplied by the High Pressure Equipment Company. Sizes used include 1/16, 1/18, and 1/4 in., all rated at 15,000 psia.

Chemicals

All chemicals used in this study were provided by commercial suppliers. No further purification of the chemicals was attempted. The chemicals studied in this work, together with their reported purities and suppliers are presented in Table II.

Table II

Purities and Suppliers of Chemicals
Used in This Study

Chemicals	Supplier	Purity (mol%)
Methane	Big 3 Industries, Inc.	99.97+
Ammonia	Matheson	99.99+
n-Propane	Big 3 Industries, Inc.	99.99+
n-Pentane	Fisher Scientific	Spec.Grade
n-Decane	Aldrich Chemical Company	99.00+
n-Eicosane	Aldrich Chemical Company	99.00+
n-Octacosane	Aldrich Chemical Company	99.00+
n-Hexatriacontane	Aldrich Chemical Company	98.00+
n-Tetratetracontane	Alpha Morton Thiokol Inc.	96.00+
Benzene	J.T Baker Chemical Comp.	99.80+
Cyclohexane	Aldrich Chemical Company	99.90+
t-Decalin	Aldrich Chemical Company	99.00+
Naphthalene	Aldrich Chemical Company	99.00+
Phenanthrene	Aldrich Chemical Company	98.00+
Pyrene	Aldrich Chemical Company	99.00+

CP : Cleaning Pump
CR : Cleaning Reservoir
DWG: Dead Weight Gauge
EC : Equilibrium Cell
FW : Fly Wheel
GMI: Gas-Mercury Interface
GP : Gas Pump
HP : Hydrocarbon Pump
HT : Heating Tape
MR : Mercury Reservoir
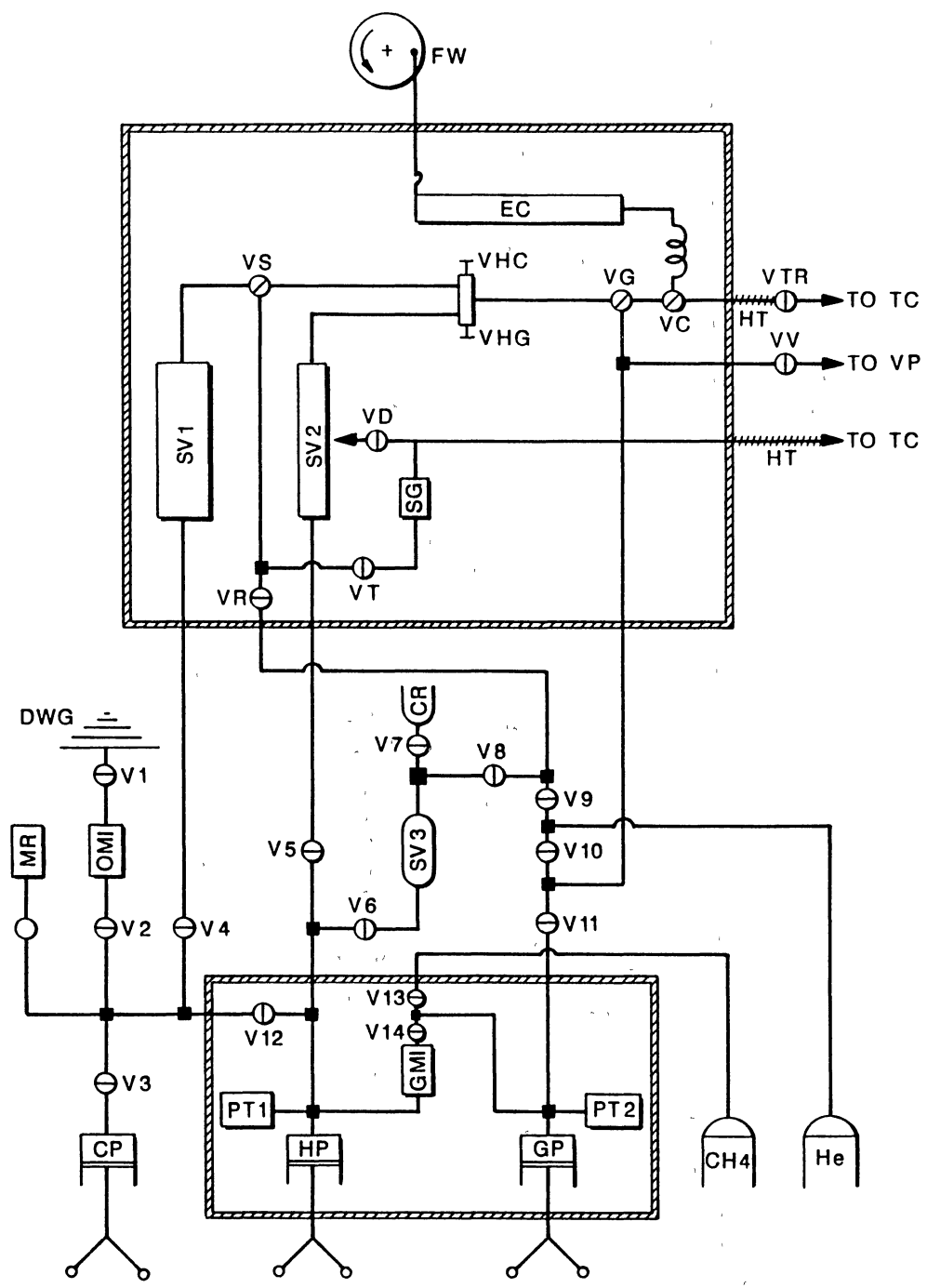
OMI: Oil-Mercury Interface
PT1: Pressure Transducer
PT2: Pressure Transducer
SG : Sight Glass
SV1: Storage Vessel
SV2: Storage Vessel
SV3: Storage Vessel
TC : Trash Can
VP : Vacuum Pump

Figure 1. Schematic Diagram of the Bubble Point Apparatus
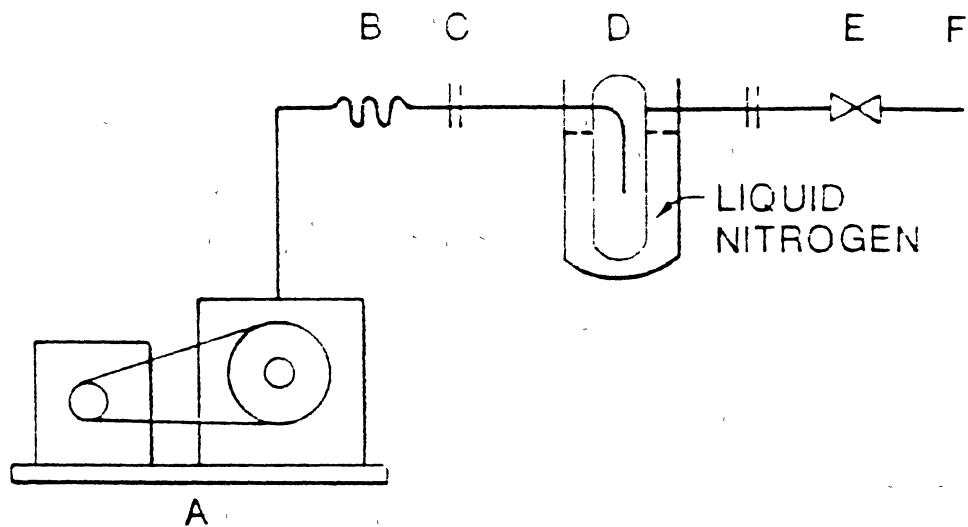
A. MECHANICAL VACUUM PUMP
B. CAJON FLEXIBLE BELLOWS TUBING
C. ULTRA-TORR UNIONS
D. GLASS COLD TRAP
E SHUTOFF VALVE
F. CONNECTION TO DEGASSING ASSEMBLY

Figure 2. Details of Vacuum System

CHAPTER V

EXPERIMENTAL PROCEDURES

This chapter describes the techniques and procedures used in operating the apparatus described in the previous chapter. Experimental procedures included apparatus clean-up, solvent preparations, solvent and solute injections, determination of bubble point pressure, calibration of pressure transducers, and pressure testing. Careful execution of each procedural step is an essential factor in determining the accuracy and the precision of the experimental data obtained; however, degassing and injection of solvent and solute need special attention. The validity of the experimental procedures was verified by reproducing well documented bubble point pressure data. A step-by-step description of each procedure follows. Unless otherwise stated, when a component of the equipment is mentioned, it refers to an item in Figure 1.

Apparatus Clean-up

The goal of apparatus clean-up is to remove any traces of chemicals from previous runs that may exist in the equilibrium cell, the storage cell, and any pertinent tubing and connections. The basic idea of cleaning is to empty the

cell, then rinse it (in situ) repeatedly with a solvent that dissolves the chemical to be washed out.

Cleaning of Equilibrium Cell (EC)

A completely clean equilibrium cell is the first requirement for accurate and precise experimental vapor-liquid equilibrium (VLE) data. The procedure used to clean the equilibrium cell (EC) was as follows:

1. If the solvent to be washed out from the equilibrium cell is solid at room temperature, turn on the heating tape (HT) and allow the cell to come to a temperature above the melting point of the solvent. Close valves V5, V4, V8, V9 and open valves V12, V6, and V7. Remove the stopper of cleaning reservoir (CR) which contains the cleaning fluid (pentane for paraffins and benzene for naphthenes and aromatics), and back the cleaning pump (CP) 120 turns (60 cc), allow fluid to drain into cleaning vessel (SV3). Close V7, V6 and open V5 to read the pressure inside the equilibrium cell (EC).

2. Set the equilibrium cell (EC) in the upright position and observe the reading on the injection pump (HP) to determine the amount of mercury injected into the cell during the previous run. Close VS, VG, VT, VR, VHC and, with VHG opened, back injection pump (HP) to a position such that about 1 cc of mercury is left in the equilibrium cell (EC).

Allow the pressure to stabilize.

3. Set EC in the lower position and open VC and VTR to release the gas that was injected into the cell. When dealing with a liquid solvent, the cell is set in the upper position, then VC and VTR are opened, thus the gas will drive the solvent out to the trash can (TC1).

4. Close VTR, V5 and open V6, V8, VR. Push the cleaning fluid into the equilibrium cell using the cleaning pump (CP) until about 300 psia pressure is reached in the equilibrium cell. Close V8 and back the cleaning pump 5 turns. Close V6 and open V5. Rock the cell for at least 5 minutes. Stop rocking while the cell is in the lower position and place an external magnet near the rocking end of the cell to prevent the steel balls from closing the active end of the cell. Set the cell in the upper position and open VTR, thus rejecting whatever is inside the cell to the trash can (TC1). If this is neither the first nor the second cycle of cleaning, the storage vessel (SV2) will have some cleaning fluid in it, and this fluid could be swept out using the hydrocarbon injection pump (HP) . It is essential that the cleaning fluid is in the liquid state while being pushed out from SV2. Close VTR and a full cycle of cleaning is done. If this is not the first cycle of cleaning, go to step 6 below.

5. Push used mercury (about 6 cc) from storage vessel SV2 to the equilibrium cell using the hydrocarbon injection pump (HP) and repeat step 4 above.

6. Back the hydrocarbon injection pump about 5 cc while valves VHG and V5 opened, and valves V4 and V6 closed. Wait for the pressure to stabilize. Go to step 4 above and repeat until five cycles are completed.

7. With V10 and VTR closed and the cell in the upper position, put about 700 psia of helium in the cell by opening V9 (the helium cylinder is assumed to be opened). Close V9 and release the pressure by opening VTR. Close VTR and repeat step 7 four more times. Repeat step 7 one more time releasing the gas through VT, then close VT. Close VC and turn off the heating tape.

8. With V11 closed, open VG and leave it opened. Put about 700 psia of helium in the cell by opening V10, then close it. Release the gas through VV. Repeat step 8 two more times and set the equilibrium cell in the lower position. Repeat step 8 one more time putting about 1500 psia of helium and test for leaks in the cell and the relevant valves and connections by checking the constancy of pressure over at least four hours. Fix leaks, if any, otherwise release pressure through VV (the vacuum rubber hose is assumed unhooked from the liquid nitrogen trap).

Flush the cell four times with low pressure (150 psia) methane as before.

9. Close valve VR and open valves VV, VG, and VHG. Turn on vacuum pump (VP) and be sure that the vacuum trap is immersed in liquid nitrogen. Solvent injection requires that the hydrocarbon injection pump be at a position where it can be advanced at least 7 cc. This step can be done by closing valves V4, V6 and opening valves V5, V12 and backing the hydrocarbon injection pump (HP) while simultaneously injecting mercury from the cleaning pump (CP).

To verify the effectiveness of this cleaning procedure the cell was cleaned as described above, then taken out of the apparatus, opened from both ends and examined. The cell, as well as the two caps, were clean and dry.

Cleaning of Solvent Storage Cell (SV1)

Care should be exercised in cleaning the solvent storage cell (SV1) since no mixing is available in it. Also, it is recommended that the temperature of the oven be adjusted to that of the lower isotherm of the solvent being cleaned. The procedure followed was as follows:

1. Close valves V5, V6, VR and VHC. Open valves V4, V12, VS, VT, and VD. Turn on the light inside the oven. An aluminum container is placed underneath valve VD to receive the ejected material. Push out the material that is inside the storage cell by

pumping mercury from the cleaning pump (CP) into storage vessel SV1 and thus receiving it in the portable aluminum vessel. Keep pumping until mercury is filling the sight glass which can be seen clearly through the oven glass window. Back the cleaning pump 150 turns and wait until pressure lines out at ambient pressure. Close valves VD and VT and dispose of the material collected in the container. In the previous design, the material to be removed was mixed with the cleaning fluid, and then pushed out through a heated trash line extending from valve VD to the trash can (TC2). Solidification of material inside that line, especially the portion penetrating the oven, was frequent and caused frequent delays. With the present strategy of cleaning, this problem was eliminated.

2. Close valves V4, V5, and V8 and open valves V6, V7, and V12. Remove the stopper from the cleaning fluid reservoir (CR) and, using the cleaning pump, inject mercury until it is seen rising in the cleaning fluid reservoir. Back the cleaning pump 80 turns (40 cc) and wait for pressure to line out. Back the pump 80 more turns and wait for pressure to line out. Close valves V7, V9, and VT and open valves V8, and VR.

3. Inject cleaning fluid into the storage cell (SV1) by

pumping mercury using the cleaning pump until the pressure reaches about 300 psia. Leave the cleaning fluid inside the cell for at least two hours to dissolve any traces of the previous solvent.

4. Close valves VR, V8, and V6 and open valves V4, and VT. Push out the cell contents by pumping mercury, using the cleaning pump, until mercury is seen rising in the sight glass. Set the helium cylinder to give 150 psia delivery pressure.

5. Close valve V10 and open valve V9. Slowly open valve VR to flush the lines with helium. Close valve VT and leave valve VR opened. Back the cleaning pump 150 turns and wait for pressure to line out. Close valve V9 and release the pressure through valve VT then close valve VT.

6. Repeat the cleaning procedure four times starting each time at step 2, above.

7. Set the equilibrium cell (EC) (which has already been cleaned) in the lower position. Close valves V5, V6, VR, V9, V11, and VV and open valves VG, VHG, and VHC.

8. Put about 500 psia of helium pressure on the storage cell, the equilibrium cell, and the pertinent connections by opening valve V10. Close V10 and release the gas through valve VV. Close VV and repeat step 8 four time. Repeat one more time with 800 psia helium and test for leaks in the

storage cell (SV1).

9. Repair any leaks, otherwise release gas through VV
    and connect the vacuum hose to the liquid nitrogen
    trap and apply vacuum for at least four hours.
    Close valve VV and unhook the hose. Put about one
    atmosphere of methane pressure on the cells and shut
    off the oven and allow it to cool down. The storage
    cell is now ready to accommodate the solvent.

Solvent Preparation

Two procedural steps will be discussed in this section;
filling the storage vessel with solvent, and degassing the
solvent.

Filling the Storage Vessel

Care must be taken during the removal of the cap of the
storage vessel to ensure that the sealing surface is not
scratched. To fill the storage vessel (SV1) with solvent,
the oven is cooled to room temperature and the cap of the
storage vessel is removed. The solvent (whether liquid or
solid at room temperature) is introduced directly into the
storage vessel in an amount sufficient for at least six
injections. About 15 cc of void space above the solvent
level is provided. The cap is replaced and air is removed by
purging the storage vessel with methane gas at low pressure.

Degassing Procedure

The major drawback of static methods in vapor-liquid equilibria (VLE) experimentation is the need for a highly degassed sample of the solvent [50,51], since incomplete degassing of the solvent can be a serious source of error [51,52]. Therefore, careful attention must be paid to this step. Degassing the solvent was carried out as follows:

1. The equilibrium cell (EC) is cleaned and the solvent added to the storage vessel (SV1), then the set-point temperature on the controller is adjusted to be about 5°C above the melting point of the solid solvent.

2. Vacuum is applied to the solid material (flakes or powder) in the storage vessel and the oven is turned on. To apply vacuum, close valves VT, VR and open valves VS, VHC, VG, VV. Connect the vacuum hose to the liquid nitrogen trap and turn on the mechanical vacuum pump. In this manner, the solvent is guaranteed to melt while under vacuum, so gas bubbles will not be trapped in liquid solvent. After about four hours, valve VS is closed and temperature in the oven is set to the required operating temperature. When temperature reaches steady state, vacuum is applied again to the solvent by opening VS for 10 to 15 minutes.

3. While valves VHC, VR, and V5 are closed, valves V4, and V12 are opened and the liquid solvent is

pressurized by pumping mercury into the bottom of the storage vessel (SV1), using the cleaning pump until a pressure of about 200 psia is obtained. The solvent is now completely prepared for injection.

Solvent and Solute Injections

No analytical methods to determine phase compositions are required in this experimental work. Instead, the mixture is synthesized volumetrically, using two screw pumps, one for the hydrocarbon solvent (HP), and another for the solute gas (GP). Sufficient time should be allowed for pressure and temperature stability before taking the reading of the screw pumps. Also, fluctuations in room temperature should be minimized by keeping the lab door closed, at least during solvent injection.

Solvent Injection

The basic idea in solvent injection is to transfer a known quantity of degassed solvent to the well evacuated equilibrium cell, which is isolated from vacuum at the instant of injection. The volume of the solvent injected is known from scale readings on the hydrocarbon injection pump (HP). Here we neglect variation of solvent density with pressure, which is justifiable for pressure ranges encountered during solvent injection [18].

The density of the solvent is needed to calculate the exact moles of that solvent. The densities used in this

study, together with their literature sources, are shown in Appendix B. The procedure followed for solvent injection was:

1. The solvent is degassed and pressurized to about 200 psia up to valve VHC as described above.

2. Close valves VHG, V4, and V6 and open valves V5, and V12, then, while the cell is under vacuum, fill the small storage vessel (SV2) with mercury to 200 psia by using the cleaning pump. Close valve V5.

3. Open valve V4 and close valves V1, V2 and V3. Allow sufficient time for the pressure to line out around 200 psia. Record pressure and initial position of the hydrocarbon injection pump (HP), together with the temperatures in both baths on the injection sheet.

4. The cell has now been under vacuum for at least the last three hours. Close the gas injection valve VG, thus isolating the cell from the vacuum pump. Open the hydrocarbon injection valve VHC, and inject, using the hydrocarbon injection pump, the desired volume of solvent (approximately) and immediately close valve VHC and adjust the pressure to the initial value recorded on the injection sheet.

5. Close valve VV and open valve V11, thus bringing solute gas up to the mouth of the equilibrium cell. (The gas pump is assumed charged with pure methane.)

6. Adjust the pressure in the storage vessel to its

initial value and record the final position of the
hydrocarbon injection pump. Calculate the exact
volume of the solvent injected (taking into account
correction needed because of the transfer of mercury
from one bath to another of different temperature).
The injected volume of the solvent, multiplied by
the molar density of the liquid solvent at the
operating temperature, gives the moles of solvent
injected into the cell. The required volume of
solute gas to give the desired mixture composition
is then calculated. Close valve V4 and proceed to
the solute injection.

Solute Injection

Solute injection is very similar to solvent injection;
however, the pressure readings and pump positions are those
of the gas pump (GP). The temperature of the methane gas
during this study was maintained at 50°C using a
proportional-integral controller. The pressure at which the
solute gas was injected lies in the range 500-800 psia, for
most of the times, however, gas injections were made at
pressures around 600 psia. The densities of the gas at the
injection conditions of temperature and pressure used in
calculating the moles of gas injected were the experimental
values of Schamp, et al. [54]. These densities were in
agreement with those of Goodwin [55] and the experimental
ones of Olds and Reamer [56]. The percentage uncertainty in

methane density at 50°C was calculated over a wide range of pressure from the modified Bender's equation of state of methane [53]. No specific pressure ranges (except at low pressures) were found over which the uncertainty is exceptionally high. The derivations and results of percentage uncertainty as a function of pressure at 50°C is shown in Appendix C (Fig. C-1).

The procedure of solute injection was as follows:

1. The pressure of the gas, together with the gas pump reading are recorded on the injection sheet, and the true gas pressure is calculated by applying the necessary corrections (see Appendix E). The pump is advanced until the volume change is equal to the volume of gas needed for injection.

2. The gas injection valve (VG) is opened slowly until the pressure in the gas pump falls to its original value or slightly below. The gas injection valve is closed and the gas pump (GP) is adjusted to give the initial pressure, which is recorded on the injection sheet. The volume of gas injected is equal to the difference between the final and initial pump readings. The moles of gas injected is simply the product of the volume of gas injected and the molar density of the gas.

Bubble Point Determination

The above procedures provide a binary mixture of known composition in the equilibrium cell. The next step is to determine the bubble point pressure of this mixture. This is done by measuring the pressure of the mixture as increments of mercury (0.01 cc) are injected into the cell. Above the bubble point, where the last bubble of the gas phase dissolves into the liquid phase, an increase in pressure is obtained indicating that the bubble point pressure has been passed. Accurate determination of the bubble point pressure is obtained from a plot such as that shown in Figure 3. Sometimes, however, plotting pressure vs volume of mercury injected does not help identifying the bubble point accurately, because of large pressure ranges involved. In this case, two least-squares linear equations are solved to give the intersection point that appears in Figure 3. To get the true bubble point pressure of the mixture, two corrections are required; the first comes from calibration of the pressure transducer (PT1) against a dead weight tester, and the second is due to the head of mercury between the cell and the pressure transducer. The procedure to account for these corrections is described in Appendix D. (Solubilities of the solvent and solute in mercury are assumed negligible under the experimental conditions of this study.)

The step-by-step procedure followed to determine the bubble point pressure of the mixture was as follows:

1. With valves V5, V4, and V6 closed, and valves V12,

and V3 opened, transfer about 7 cc of mercury from
the cleaning pump (CP) to the hydrocarbon injection
pump (HP). Close valve V12 and open valve V5 and
pressurize storage vessel SV2 to 700 psia.

2. Set the equilibrium cell in the upper position.
Open valve VHG and start injecting mercury into the
cell; after injecting about 4 cc begin rocking the
cell and keep injecting mercury while the cell is
rocking. Decrease the injection rate as the bubble
point is approached. Keep injecting mercury until a
sharp increase in pressure is obtained, at which
time stop rocking the cell while it is in the upper
position. Remove mercury so that at least 0.03 cc
of mercury will need to be injected before the
bubble point is reached. Start injecting increments
of 0.01 cc mercury into the cell while it is
rocking. Allow pressure to stabilize after each
injection and record the data on the P-V data sheet
until a minimum of three points are obtained at
pressures above the bubble point.

3. Set the equilibrium cell in the upper position.
Calculate the volume of solute gas needed for the
next desired mixture composition, and back the
injection pump to create clearance for the incoming
gas, then wait for pressure to stabilize. Close
valve VHG and proceed with the solute injection.

Calibration of Pressure Transducers

The hydrocarbon pressure transducer (PT1) was calibrated on a regular basis to assure proper pressure readings during operation. The gas pressure transducer (PT2) was then calibrated against the calibrated transducer (PT1). Calibration was performed using a dead weight pressure tester (Ruska Instrument Corporation, Mode 2400.1) connected directly to the hydrocarbon pressure transducer (PT1). The mercury level in the oil-gas interface (see Figure 1) should align with the black reference line marked on the outside glass window of the oil-gas interface. Note that the temperature in the bath containing the pressure transducers has to be stabilized at 50°C prior to calibration. The procedure followed was as follows:

1. The pressure transducer (PT1) is isolated from the rest of the apparatus by closing valves V5, V4, V6, V15, and V14. Valve V12 is then opened and the pressure is adjusted to about 150 psia with the cleaning pump. Valve V3 is then closed while valves V1, and V2 are opened. The dead weight gauge is now linked directly to the transducer (PT1). The dead weight tester is then turned on.

2. The ambient temperature and pressure are recorded and the calibration is begun by placing the proper disk weights on the floating piston of the dead weight tester and recording the pressure indicated by PT1, using the proper calibration sheet. The

choice of weights depends on the particular pressure range over which the apparatus will be operated.

3. Once the desired pressure range is covered, the pump on the dead weight tester is backed out to adjust the pressure to about 150 psia, and the dead weight gauge is isolated from the apparatus by closing valves V1, and V2. Valve V3 is then opened and valve V12 is closed to isolate the cleaning pump.

4. By comparing pressures displayed by the transducer with pressures generated by the dead weight tester, we are able to get corrections that should be made to the transducer readings. The calculation of these corrections is done in a simple computer program coded by Anderson [47] and a sample of typical corrections is shown in Table D-1 of Appendix D.

5. The gas pressure transducer (PT2) is calibrated against the already calibrated transducer (PT1) through a gas-mercury interface. The idea is to expose both transducers to the same pressure and compare the two readings. This is done by closing valves VG, V9, V13 and VV, while opening valves V11, V10, V15, and V14, thus exposing the gas pressure transducer (PT2) to pressures typical of those encountered during injection of the solute gas. The pressure is transmitted to the hydrocarbon pressure transducer through the gas-mercury interface. Valve

V11 is then closed while valve VV is opened (the vacuum hose should be unhooked from the liquid nitrogen trap) and the two pressures are recorded. A new set of pressures are obtained by releasing some of the helium gas through valve V11 until the desired pressure range is covered at which time valves V15, and V14 are closed.

Two kinds of corrections should be applied to the apparent pressure displayed by the digital readouts to get the true pressure; one correction coming from calibration and the other is a result of the mercury head in the gas-mercury interface. The procedure to account for these corrections to get the true pressure is presented in Appendix D.

Pressure Testing

One of the basic requirements for successful operation of static bubble point pressure apparatus is a leak-free system. To accomplish this, the equilibrium cell is pressurized with helium gas and a leak test is performed at room temperature using a highly sensitive helium leak detector (Gow Mac Instrument Co., Model 21-150). Next, the cell is pressurized with helium gas at the temperature of the experiment and a pressure test is carried out at a pressure level higher than those encountered during the experimental run. All elements of the pressure system are included in the test. Constancy of pressure over at least 4 hours is taken to be indicative of tightness of the system. Similar

procedures are followed to pressure test the solvent or the solute storage vessels.

One more test, to ensure absence of leaks in the cell, was carried out occasionally. This time, however, the test is for directional leaks of air into the evacuated cell. The test was performed by degassing the cell for at least three hours, isolating the cell from vacuum and leaving it overnight to check whether it retains vacuum.
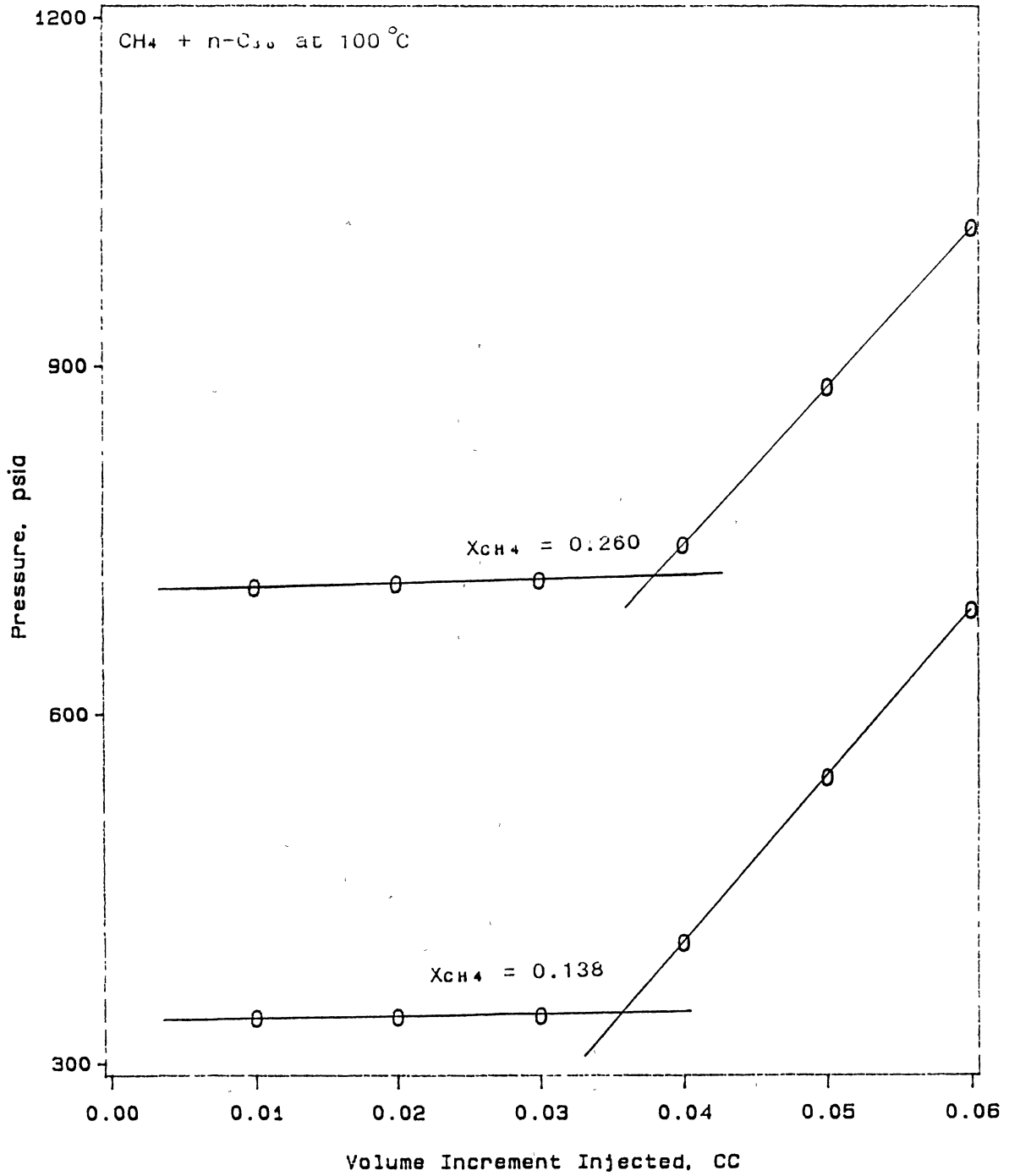
Figure 3. Graphical Determination of Bubble Point Pressure

CHAPTER VI

BINARY VAPOR-LIQUID PHASE EQUILIBRIUM

FOR METHANE + HEAVY

NORMAL PARAFFINS

Abstract

Binary solubility data are presented for methane in five heavy normal paraffins at temperatures from 311 to 423 K (100 to 302°F) and pressures up to 865 bar (1255 psia). The paraffins studied are: n-decane (n-C_{10}), n-eicosane (n-C_{20}), n-octacosane (n-C_{28}), n-hexatriacontane (n-C_{36}) and n-tetratetracontane (n-C_{44}). Data for methane + n-decane are in good agreement with the earlier measurements of Reamer, et al. and Lin, et al. but are in significant disagreement with the data obtained by Beaudoin and Lavender. The data obtained for the solubility of methane in n-C_{20}, n-C_{28}, and n-C_{36} are in good agreement with the earlier measurements of Chao and coworkers. The new data can be described with RMS errors of about 0.001 in mole fraction of methane by the Soave-Redlich-Kwong (SRK) or Peng-Robinson (PR) equation of state when two interaction parameters per isotherm are used. Henry's constants and partial molar volumes at infinite dilution are also evaluated from the data.

Introduction

The well-publicized energy situation in the United States has provided strong impetus toward the conversion of coal to liquid and gaseous products. Multiple phases are present in essentially all stages of feed preparation, conversion reactions, and product separation. For example, during the initial stages of coal dissolution in a coal-derived recycle solvent, many light gases are produced (e.g., CH_4, CO, CO_2, H_2S, H_2O, NH_3, and C_2-C_5) [1]. Therefore, the effective design and operation of such conversion processes require accurate knowledge of the phase behavior of the fluid mixtures encountered. Studies of the solubility of light gases in heavy hydrocarbons are also of interest in the processing of petroleum products, enhanced oil recovery and supercritical fluid processes. Moreover, such studies are valuable in the development and evaluation of solution theories.

Previously, we have reported and analyzed data on the solubility of carbon dioxide and ethane in a series of heavy hydrocarbons [2-6]. Recently, we have completed an experimental study on the solubility of methane in a series of heavy hydrocarbons (paraffins, naphthenes, and aromatics). Solubility data for the binary mixtures of methane with n-decane, n-eicosane, n-octacosane, n-hexatriacontane, and n-tetratetracontane are presented here and correlated using the Soave [7] and Peng-Robinson [8] equations of state. Solubilities were measured at temperatures from 311 to 423 K

(100 to 302°F) and pressures up to 865 bar (1255 psia).
These data should provide a valuable complement to the
available literature data and should prove useful in the
development and testing of correlations describing the phase
behavior of multicomponent systems involving methane.

Experimental Section

Apparatus and Procedure

The experimental apparatus used in this study is a
modified version of the apparatus used by Raff [6]. The
modifications resulted in a number of improvements including:
improved mixing, reduced dead volume, and improved procedures
for cleaning and degassing. A detailed description of the
apparatus and experimental procedure is given elsewhere [9].

Estimated uncertainties in experimental measurements are
0.1 K in temperature and less than 0.002 in mole fraction.
The uncertainty in the measured bubble point pressure depends
on the steepness of the p-x relation and is of the order of
0.35 bar (5 psia) [9].

Materials

The methane used in this study had a stated purity of
99.97+ mol% and was supplied by Matheson. N-decane,
n-eicosane, n-octacosane and n-hexatriacontane were from
Aldrich Chemical Company with quoted purities of 99+ mol%.
N-tetratetracontane was from Alfa Products with a stated

purity of 96+ mol%.   No further purification of the
chemicals was attempted.

Results and Discussion

Equilibrium Data

The experimental results are presented in Tables I-V. In
general, the lowest temperature at which each system was
studied was dictated by the melting point of the solvent.
For n-decane, however, measurements were conducted at
temperatures at which literature data are available for
comparison purposes. The first three isotherms of methane +
n-decane system were obtained using the apparatus described
by Raff [6]. These data, however, were verified using the
modified apparatus [9].

Equation of State Data Correlation

The experimental data have been correlated using the SRK
[7] and PR [8] cubic equations of state. Optimum binary
interaction parameters were obtained by minimizing the sum of
squares of pressure deviations from the experimental values.
Detailed procedure for data reduction is given by Gasem [10].
The input parameters for the pure components (acentric
factors, critical temperatures and critical pressures)
required by the SRK and PR equations of state, together with
the literature sources are presented in Table VI. The
parameters for components heavier than n-decane are those
used by Raff [6].

The effects of temperature and pressure on methane solubility (liquid phase mole fraction of methane) are evident in Figures 1-5. For a given pressure, the solubility of methane in a given n-paraffin decreases with increasing temperature, a behavior which is similar to that observed for carbon dioxide solubilities [10].

The effect of molecular weight of the solvent (or, equivalently, the carbon number) is displayed in Figure 6; For a given temperature and pressure, the solubility (on molar basis) of the gas increases with increasing molecular weight of the solvent.

The equation-of-state representations of the solubilities for the systems under study are documented in Tables VII-XI. The equations are capable of describing the data with RMS errors within 0.002 in mole fraction when a single pair of interaction parameters, C_{ij} and D_{ij}, is used over the complete temperature range for any system studied (except for methane + n-eicosane system which has an RMS error of 0.0036 in mole fraction). When two parameters are fitted to each isotherm, RMS errors are less than 0.0015 for all systems. These results illustrate both the ability of the equations of state and the precision of our reported data. The results in Tables IX-XI also reveal a certain degree of correlation between the C_{ij} and D_{ij} values. For example, the sensitivity of the optimized C_{ij} and the corresponding RMS errors (in methane mole fraction) to changes in D_{ij}, for methane + n-eicosane at 212°F, are shown

in Figure 7, where the very sharp minimum in the RMS vs D_{ij} plot signifies a high sensitivity of the model predictability to the interaction parameters. The rate of change of C_{ij} with respect to D_{ij} is high and equals -5 for this specific system with a clear optimum at C_{ij} = 0.096 and D_{ij} = -0.016. Similar behavior was observed for other binary mixtures of methane + n-paraffins where small changes in D_{ij} (from D_{ij} = 0 in the one parameter case) cause significant variations in C_{ij}.

Comparisons of our results with those reported by various investigators appear in Figures 8-16. The comparisons are shown in terms of deviations of the solubilities from values predicted using the SRK [7] equation of state. Interaction parameters employed in the equation-of-state predictions were obtained by fitting our data for each isotherm in each system. In cases where the literature data are reported at temperatures different from ours, solubility prediction were obtained using temperature independent parameters, C_{ij} and D_{ij}, regressed from our data over the complete range of temperature for the system. This method of comparison was employed because the interaction parameters, C_{ij} and D_{ij}, when regressed simultaneously, did not show, in general, a clear functionality in temperature and so interpolation becomes difficult.

Figures 8-13 show comparisons for methane + n-decane. The data obtained from the new apparatus are in excellent agreement with those obtained from the old apparatus for

methane + n-decane at 100, 160, and 220°F as shown in

Figures 8-10 where solubilities are predicted within 0.001.

Reasonable agreement is observed between the present study

and that of Reamer [11] at temperatures 160, 220 and 280;

solubilities, as shown in Figures 9-11, agree within 0.003

over the whole pressure range of this study. However, the

agreement is not as good at 100°F, as Figure 8 shows. At

temperatures higher than 280°F the agreement is reasonable

over the pressure range of this study. According to Mohindra

[12], Reamer's data at 100, 160, 220 were found to be

thermodynamically inconsistent. The best agreement between

this work and that of Reamer [12] is at 280°F where the

solubilities, as shown in Figure 11, agree within 0.0015.

Similarly, good agreement (solubility deviation within 0.002)

between this study and that of Lin [15] is revealed by Figure

12. Except at very low pressures (<100 psia), this study is

in significant disagreement with those of Lavender [13] and

Beaudoin [14], which were reported to be internally

inconsistent [12]. Figure 13 shows solubility deviation for

methane + n-decane when temperature independent parameters,

C_{ij} and D_{ij}, are used to fit the whole set of data of the

present work; solubilities of methane in n-decane are

predicted with RMS errors within 0.002.

Comparison of methane + n-eicosane (n-C_{20}) data appears

in Figure 14. Equation-of-state parameters regressed from

our data predict lower solubilities (higher bubble point

pressures) for the 392°F isotherm and higher solubilities

(lower bubble point pressures) for the 212°F isotherm than reported by Huang, et al [16]. Solubilities, as Figure 14 reveals, agree within 0.0025 for the 212°F isotherm and 0.004 for the 392°F isotherm.

Comparisons for methane + n-octacosane (n-C_{28}) and methane + n-hexatriacontane (n-C_{36}) are shown in Figures 15 and 16. The agreement between this study and those of Huang, et al. [17] for methane + n-C_{28} (in terms of solubility deviation) is within 0.004 for the 212°F isotherm and 0.002 for the 392°F isotherm. For methane + n-C_{36}, the agreement between this work and those of Tsai, et al. [18] is within 0.004 mole fraction, for the 212°F isotherm, and 0.003 mole fraction for the 392°F isotherm (Figure 16). For methane + n-tetratetracontane (n-C_{44}) no literature data are available for comparisons; the ability of the equation of states to represent our data is shown in Figure 17.

The effect of the carbon number of the paraffin on the optimum interaction parameters is shown in Figure 18. The standard deviation of any optimized parameter (whenever of adequate magnitude to be shown) is shown on the figures. The parameters, C_{ij} and D_{ij}, tend to increase linearly with carbon number (or, equivalently, with molecular weight). The effect of carbon number becomes more clear when optimizing only C_{ij} holding D_{ij} fixed (zero in this case) as Figure 19 shows. A constant value of 0.032 for C_{ij}, for the binary mixtures of methane in paraffinic solvents with carbon number less than or equal 30, is suggested by Figure 19. For

paraffinic solvents with higher carbon number, C_{ij} tends to increase linearly with carbon number for the set of critical properties and acentric factors used in this study. The corresponding RMS errors in solubility are shown in the same graph.

The effects of temperature and carbon number on C_{ij} and D_{ij}, when regressed simultaneously, are shown in Figure 20. For a given binary mixture (except methane + $n-C_{28}$) , C_{ij} increases with both, temperature and carbon number. No general conclusion can be drawn regarding the effects of temperature and carbon number on D_{ij} for this case as Figure 20 shows. When only C_{ij} is optimized setting D_{ij} at zero, no pronounced effects of temperature and carbon number are noticed for the binary mixtures of methane with $n-C_{10}$, $n-C_{20}$ and $n-C_{28}$ (Figure 21). However, for methane + $n-C_{36}$ and methane + $n-C_{44}$, C_{ij} increases with both, temperature and carbon number, which might be attributed to the uncertainty in their estimated critical properties.

Krichevsky-Kasarnovsky Analysis

In the range of methane mole fractions reported in this study, the binary solubilities of methane in $n-C_{10}$, $n-C_{20}$, $n-C_{28}$, $n-C_{36}$, and $n-C_{44}$ are represented within 0.0015 by the Krichevsky-Kasarnovsky (KK) equation [19] (definition of variables are given in the "List of Symbols"):

$$\ln(f_{CH_4}/x_{CH_4}) = \ln(H_{CH_4,P_{HC}}) + (v_{CH_4}/RT)(P-P_{HC}) \qquad (1)$$

Values of the methane fugacity, f_{CH_4}, required for the KK equation were obtained from Bender's equation of state for methane [20], since the vapor phase is essentially pure methane.

Solubility data for methane + n-paraffins of this work, as well as those found in the literature, were analyzed using Equation 1 above. The resultant Henry's constants and the infinite-dilution partial molar volumes of methane are presented in Table XII and Figures 22-25.

Comparisons of Henry's constants are shown in Figures 22 and 23. The Henry's constants of Chappelow [21] were obtained from equilibrium cell data, those of Ping [22] were obtained using gas chromatographic techniques, and those of the rest (including the present work) were obtained, as described above, by regression of solubility data using Equation 1. Henry's constants for methane + n-decane of this work agree within 10 bars with those of Lin [15], Beaudoin [14], Reamer [11] and Lavender [13]. For methane + n-C_{20}, our Henry's constants agree within 5 bars with those of Huang [16], and Chappelow [21]. Similar agreement is observed between Henry's constants of this work and other investigators [17,22,18] for methane + n-C_{28} and methane + n-C_{36}.

Figure 23 also shows the effects of the solvent carbon number and temperature on Henry's constants. For a given temperature, Henry's constant decreases with increasing carbon number of the solvent, and (for a given n-paraffinic

solvent over the temperature range of this work) increases with temperature, which is (in the light of Figures 1-6) an expected behavior.

Comparisons of infinite-dilution partial molar volumes, obtained from regression of solubility data using Equation 1 above, are shown in Figures 24 and 25. Care should be taken in attributing physical significance to these values which are considered less accurate than the corresponding Henry's constants.

Conclusions

Data have been obtained on the solubility of methane in each of the n-paraffin solvents n-decane, n-eicosane, n-octacosane, n-hexatriacontane and n-tetratetracontane at temperatures from 311 to 423 K (100 to 302°F) and pressures to 865 bar (1255 psia). These data are well described by the Soave-Redlich-Kwong and Peng-Robinson equations of states and the Krichevsky-Kasarnovsky correlation. These results will be of value in establishing interaction parameters in other equations of state for light gases in heavy hydrocarbon solvents.

List of Symbols

C_{ij}, D_{ij}	interaction parameters between components i and j in mixing rules for equation of state
f_{CH_4}	fugacity of methane in the liquid (or vapor) phase
p	pressure
P_{HC}	hydrocarbon vapor pressure
H_{CH_4}, P_{HC}	Henry's constant of methane
R	universal gas constant
T	temperature
v_{CH_4}	infinite dilution partial molar volume of methane
x	liquid phase mole fraction of methane (solubility)

References

1. Hensen, B. J.; Tarrer, A. R.; Curtis, C. W.; Guin, J., Ind. Eng. Chem. Process Des. Dev., 21, 575-579 (1982).

2. Robinson, R. L., Jr.; Anderson, J. M.; Barrick, M. W.; Bufkin, B. A.; Ross, C. H., " Phase behavior of Coal Fluids: Data for Correlation Development," DE-FG22-86PC90523, Final Report, Department of Energy, January (1987).

3. Gasem, K. A. M.; Robinson, R. L., Jr., J. Chem. Eng. Data, 30, 53-56 (1985).

4. Anderson, J. M.; Barrick, M. W.; Robinson, R. L., Jr., J. Chem. Eng. Data, 31, 172-175 (1986).

5. Gasem, K. A. M.; Bufkin, B. A.; Raff, A. M.; Robinson, R. L., Jr., J. Chem. Eng. Data, 34, 187-191 (1989).

6. Raff, A. M., M.S. Thesis, Oklahoma state University, Stillwater, Oklahoma (1989).

7. Soave, G., Chem. Eng. Sci., 27, 1197-1203 (1972).

8. Peng, Y. D.; Robinson, D. B., Ind. Eng. Chem. Fundam., 15, 59-64 (1976).

9. Darwish, N. A., Ph.D. Dissertation, Oklahoma State University, Stillwater, Oklahoma (1991).

10. Gasem, K. A. M., Ph.D. Dissertation, Oklahoma State University, Stillwater, Oklahoma (1986).

11. Reamer H. H.; Olds, R. H.; Sage, B. H.; Lacey, W. N., Ind. Eng. Chem., 34, 1526-31 (1942).

12. Mohindra, S., M.S. Thesis, University of Oklahoma, Norman, Oklahoma (1987).

13. Lavender, H. M.; Sage, B. H.; Lacey, W. N., The Oil and Gas Journal, 46-49, July (1940).

14. Beaudoin, J. M.; Kohn, J. P., J. Chem. Eng. Data, 12, 189-191 (1967).

15. Lin, H.-M.; Sebastian, H. M.; Simnick, J. J.; Chao, K. C., J. Chem. Eng. Data, 24, 146-149 (1979).

16. Huang, S. H.; Lin, H.-M.; Chao, K. C., J. Chem. Eng. Data, 33, 145-147 (1988).

17. Huang, S. H.; Lin, H.-M.; Chao, K. C., J. Chem. Eng.

Data, 33, 143-145 (1988).

18. Tsai, F.-N.; Huang, S. H.; Lin, H.-M.; Chao, K. C., J. Chem. Eng. Data, 32, 467-469 (1987).

19. Krichevsky, I. R.; Kasarnovsky, J. S., J. Am. Chem. Soc., 57, 2168-2171 (1935).

20. Sievers, U.; Schulz, S., Fluid Phase Equilibria, 5, 35-54 (1980).

21. Chappelow, C. C.; Prausnitz, J. M., AIChE J., 20, 1097-1104 (1974).

22. Ping, J. L.; Parcher, J. F., J. Chrom. Sci., 20, 33-38, January (1982).

23. Goodwin, R. D., "Thermophysical Properties of Methane from 90 to 500 K at Pressures to 700 Bar", NBS Technical Note 653, 22, April (1974).

24. Ely, J. F.; Hanley H. J. M., NBS Technical Note, 1039 (1981).

List of Tables

List of Figures

Table I

Solubility Data for Methane in n-Decane (n-C$_{10}$)

Mole Fraction Methane	Bubble Point Pressure bar	(psia)
310.9 K (37.8°C, 100°F)		
0.050	10.4	(151)
0.075	16.0	(232)
0.100	21.7	(315)
0.151	34.2	(495)
0.200	47.0	(682)
0.252	62.4	(905)
0.291	74.7	(1084)
0.308	80.4	(1166)
344.3 K (71.1°C, 160°F)		
0.051	12.2	(177)
0.074	17.9	(260)
0.096	23.9	(346)
0.127	32.1	(466)
0.154	39.5	(572)
0.201	53.5	(776)
0.227	61.7	(895)
0.248	68.7	(996)

Table I (Continued)

Solubility Data for Methane in n-Decane (n-C_{10}).

Mole Fraction Methane	Bubble Point Pressure bar	(psia)
377.6 K (104.4°C, 220°F)		
0.055	14.4	(209)
0.084	22.1	(320)
0.097	26.0	(377)
0.125	34.1	(495)
0.169	47.4	(688)
0.211	61.0	(884)
0.240	71.2	(1032)
0.276	83.5	(1212)
410.9 K (137.8°C, 280°F)		
0.074	20.6	(298)
0.126	35.8	(520)
0.152	43.7	(633)
0.176	51.5	(747)
0.202	60.2	(873)
0.226	68.6	(995)
0.251	77.5	(1124)
0.275	86.5	(1254)

Table II

Solubility Data for Methane in n-Eicosane (n-C_{20})

Mole Fraction Methane	Bubble Point Pressure	
	bar	(psia)
323.2 K (50.0°C, 122.0°F)		
0.051	9.5	(138)
0.099	18.9	(274)
0.119	23.2	(337)
0.150	30.2	(438)
0.177	36.8	(533)
0.212	45.5	(659)
373.2 K (100.0°C, 212.0°F)		
0.075	15.8	(230)
0.113	24.8	(359)
0.150	34.3	(498)
0.200	48.2	(699)
0.251	64.2	(930)
0.251	64.0	(929)
423.2 K (150.0°C, 302.0°F)		
0.074	16.8	(243)
0.156	38.5	(558)
0.200	51.6	(749)
0.250	67.7	(982)
0.251	67.9	(985)
0.275	76.7	(1113)
0.301	86.3	(1251)
0.350	106.9	(1550)

Table III

Solubility Data for Methane in n-Octacosane (n-C$_{28}$)

Mole Fraction Methane	Bubble Point Pressure bar	(psia)
348.2 K (75.0°C, 167.0°F)		
0.057	9.3	(134)
0.084	13.6	(197)
0.137	23.8	(345)
0.149	26.1	(379)
0.199	37.2	(540)
0.237	46.3	(672)
0.252	50.2	(728)
373.2 K (100.0°C, 212.0°F)		
0.074	12.6	(183)
0.127	23.6	(343)
0.152	28.4	(413)
0.175	34.3	(498)
0.277	61.7	(895)
0.325	77.4	(1123)
423.2 K (150.0°C, 302.0°F)		
0.074	14.1	(204)
0.109	21.3	(308)
0.154	31.6	(458)
0.202	43.3	(628)
0.251	56.7	(822)
0.299	70.9	(1029)

Table IV

Solubility Data for Methane in n-Hexatriacontane (n-C$_{36}$)

Mole Fraction Methane	Bubble Point Pressure bar	(psia)
373.2 K (100.0°C, 212.0°F)		
0.057	8.7	(126)
0.138	22.7	(329)
0.168	28.0	(407)
0.232	42.1	(610)
0.260	48.6	(705)
0.266	49.5	(719)
0.315	63.7	(924)
423.2 K (150.0°C, 302.0°F)		
0.051	8.4	(122)
0.102	17.4	(253)
0.152	26.7	(387)
0.198	36.9	(535)
0.248	48.9	(709)
0.300	63.1	(915)
0.351	79.3	(1150)

Table V

Solubility Data for Methane in n-Tetratetracontane (n-C_{44})

Mole Fraction Methane	Bubble Point Pressure bar	(psia)
373.2 K (100.0°C, 212.0°F)		
0.050	6.8	(98)
0.100	13.8	(200)
0.126	17.8	(256)
0.152	22.1	(321)
0.171	25.1	(363)
0.177	26.2	(379)
0.250	40.6	(589)
0.311	54.6	(792)
423.2 K (150.0°C, 302.0°F)		
0.086	12.5	(181)
0.121	18.1	(262)
0.157	24.2	(351)
0.211	34.2	(496)
0.254	43.7	(633)
0.279	48.9	(709)
0.304	55.7	(808)

Table VI

Critical Properties and Acentric Factors Used
in the SRK and PR Equations of State

Component	Pressure (bar)	Temperature (K)	Acentric Factor	Reference
Methane	46.60	190.5	0.0110	23
n-C_{10}	20.97	617.5	0.4885	24
n-C_{20}	10.69	766.6	0.8941	6
n-C_{28}	6.61	827.4	1.1617	6
n-C_{36}	4.28	864.0	1.4228	6
n-C_{44}	2.90	866.6	1.6664	6

Table VII

SRK and PR Equation-of-State Representations of Solubility of Methane in n-Decane

Temperature K (°F)	Soave Parameters (P-R Parameters) C_{12}	D_{12}	Error in Methane* Mole Fraction RMS	MAX
310.9 (100.0)	0.054	-0.009	0.0003	0.0005
	(0.054)	(-0.008)		
	0.033		0.0019	0.0028
	(0.037)			
344.3 (160.0)	0.046	-0.007	0.0003	0.0005
	(0.045)	(-0.006)		
	0.028		0.0009	0.0013
	(0.030)			
377.6 (220.0)	0.054	-0.010	0.0003	0.0005
	(0.053)	(-0.010)		
	0.031		0.0012	0.0019
	(0.030)			
410.9 (280.0)	0.069	-0.015	0.0004	0.0007
	(0.067)	(-0.017)		
	0.035		0.0013	0.0019
	(0.030)			
310.9, 344.3 377.6, 410.3	0.057	-0.011	0.0007	0.0017
	(0.057)	(-0.011)		
	0.032		0.0017	0.0032
	(0.033)			

* Errors are essentially identical for the SRK and PR EOS

Table VIII

SRK and PR Equation-of-State Representations of
Solubility of Methane in n-Eicosane

Temperature K (°F)	Soave Parameters (P-R Parameters) C_{12}	D_{12}	Error in Methane* Mole Fraction RMS	MAX
323.1 (122.0)	0.072	-0.008	0.0005	0.0007
	(0.069)	(-0.007)		
	0.029		0.0015	0.0024
	(0.031)			
373.1 (212.0)	0.096	-0.016	0.0002	0.0003
	(0.091)	(-0.016)		
	0.017		0.0032	0.0046
	(0.016)			
423.1 (302.0)	0.106	-0.020	0.0005	0.0008
	(0.101)	(-0.022)		
	0.021		0.0047	0.0067
	(0.015)			
323.1, 373.1 423.1	0.058	-0.008	0.0036	0.0070
	(0.039)	(-0.005)		
	0.022		0.0039	0.0066
	(0.019)			

* Errors are essentially identical for the SRK and PR EOS

Table IX

SRK and PR Equation-of-State Representations of Solubility of Methane in n-Octacosane

Temperature K (°F)	Soave Parameters (P-R Parameters) C_{12}	D_{12}	Error in Methane* Mole Fraction RMS	MAX
348.1 (167.0)	0.136	-0.013	0.0007	0.0016
	(0.127)	(-0.014)		
	0.033		0.0039	0.0056
	(0.029)			
373.1 (212.0)	0.170	-0.017	0.0009	0.0014
	(0.158)	(-0.018)		
	0.041		0.0057	0.0069
	(0.034)			
423.1 (302.0)	0.122	-0.012	0.0004	0.0007
	(0.112)	(-0.014)		
	0.025		0.0025	0.0038
	(0.012)			
348.1, 373.1 423.1	0.153	-0.015	0.0014	0.0028
	(0.140)	(-0.016)		
	0.034		0.0044	0.0098
	(0.027)			

* Errors are essentially identical for the SRK and PR EOS

Table X

SRK and PR Equation-of-State Representations of
Solubility of Methane in n-Hexatriacontane

Temperature K (°F)	Soave Parameters (P-R C_{12}	Parameters) D_{12}	Error in Methane* Mole Fraction RMS	MAX
373.1 (212.0)	0.192	-0.010	0.0013	0.0023
	(0.179)	(-0.012)		
	0.091		0.0042	0.0065
	(0.078)			
423.1 (302.0)	0.223	-0.012	0.0010	0.0016
	(0.208)	(-0.015)		
	0.110		0.0050	0.0074
	(0.092)			
373.1, 423.1	0.220	-0.013	0.0020	0.0040
	(0.201)	(-0.014)		
	0.099		0.0053	0.0110
	(0.084)			

* Errors are essentially identical for the SRK and PR EOS

Table XI

SRK and PR Equation-of-State Representations of
Solubility of Methane ın n-Tetratetracontane

Temperature K (°F)	Soave Parameters (P-R Parameters) C_{12}	D_{12}	Error ın Methane* Mole Fractıon RMS	MAX
373.1 (212.0)	0.243	-0.008	0.0009	0.0018
	(0.229)	(-0.009)		
	0.138		0.0040	0.0059
	(0.123)			
423.1 (302.0)	0.263	-0.008	0.0011	0.0017
	(0.249)	(-0.010)		
	0.161		0.0029	0.0041
	(0.139)			
373.1, 423.1	0.258	-0.008	0.0023	0.0040
	(0.242)	(-0.010)		
	0.148		0.0045	0.0079
	(0.130)			

* Errors are essentıally ıdentical for the SRK and PR EOS

Table XII

Henry's Constants and Infinite-Dilution Partial Molar Volumes for Methane in n-Paraffins (n-C_{10} to n-C_{44})

Temp. K	Ref.	Henry's Cons. bar	Partial Mol. Vol. cm^3/g-mole	RMS Error Mole Fraction
			n-Decane (C_{10})	
298.2	14	199 ($\pm$1)*	735 ($\pm$30)*	0.0015
310.9	This Work	203 ($\pm$4)	695 ($\pm$13)	0.0002
310.9	11	195 ($\pm$1)	960 ($\pm$35)	0.0023
310.9	13	196 ($\pm$3)	980 ($\pm$70)	0.0080
323.2	14	217 ($\pm$1)	875 ($\pm$18)	0.0014
344.3	This Work	233 ($\pm$1)	665 ($\pm$32)	0.0003
344.3	11	221 ($\pm$1)	950 ($\pm$25)	0.0013
344.3	13	220 ($\pm$3)	1100 ($\pm$65)	0.0060
348.2	14	240 ($\pm$1)	855 ($\pm$30)	0.0013
373.2	14	261 ($\pm$2)	850 ($\pm$55)	0.0019
377.6	This Work	252 ($\pm$1)	750 ($\pm$23)	0.0003
377.6	11	251 ($\pm$2)	760 ($\pm$75)	0.0007
377.6	13	250 ($\pm$4)	1050 ($\pm$110)	0.0037
410.9	This Work	266 ($\pm$1)	770 ($\pm$40)	0.0006
410.9	11	293 ($\pm$1)	128 ($\pm$290)	0.0046
423.2	15	270 ($\pm$5)	765 ($\pm$180)	0.0013
423.2	14	305 ($\pm$3)	93 ($\pm$135)	0.0015

Table XII (Continued)

Henry's Constants and Infinite-Dilution Partial Molar Volumes for Methane in n-Paraffins (n-C_{10} to n-C_{44})

Temp. K	Ref.	Henry's Cons. bar	Partial Mol. Vol. cm^3/g-mole	RMS Error Mole Fraction
			n-Eicosane (C_{20})	
323.2	This Work	178 ($\pm$1)	1230 ($\pm$80)	0.0005
373.2	This Work	199 ($\pm$1)	1470 ($\pm$25)	0.0003
373.4	16	208 ($\pm$1)	1075 ($\pm$45)	0.0003
423.2	This Work	217 ($\pm$1)	1520 ($\pm$25)	0.0007
473.5	16	226 ($\pm$3)	1490 ($\pm$220)	0.0009
			n-Octacosane (C_{28})	
348.2	This Work	153 ($\pm$1)	1855 ($\pm$110)	0.0007
373.2	This Work	162 ($\pm$2)	2080 ($\pm$150)	0.0013
373.4	17	165 ($\pm$2)	1720 ($\pm$200)	0.0014
423.2	This Work	179 ($\pm$1)	1950 ($\pm$75)	0.0005
473.5	17	192 ($\pm$3)	1740 ($\pm$230)	0.0012
			n-Hexatriacontane (C_{36})	
373.2	This Work	147 ($\pm$1)	2000 ($\pm$50)	0.0010
373.4	18	143 ($\pm$2)	2075 ($\pm$155)	0.0013
423.2	This Work	157 ($\pm$1)	2195 ($\pm$40)	0.0006
473.5	18	159 ($\pm$3)	2420 ($\pm$290)	0.0019
			n-Tetratetracontane (C_{44})	
373.2	This Work	128 ($\pm$1)	2270 ($\pm$90)	0.0009
423.2	This Work	135 ($\pm$1)	2585 ($\pm$60)	0.0009

* Values in parentheses are the standard deviation in the estimated parameters
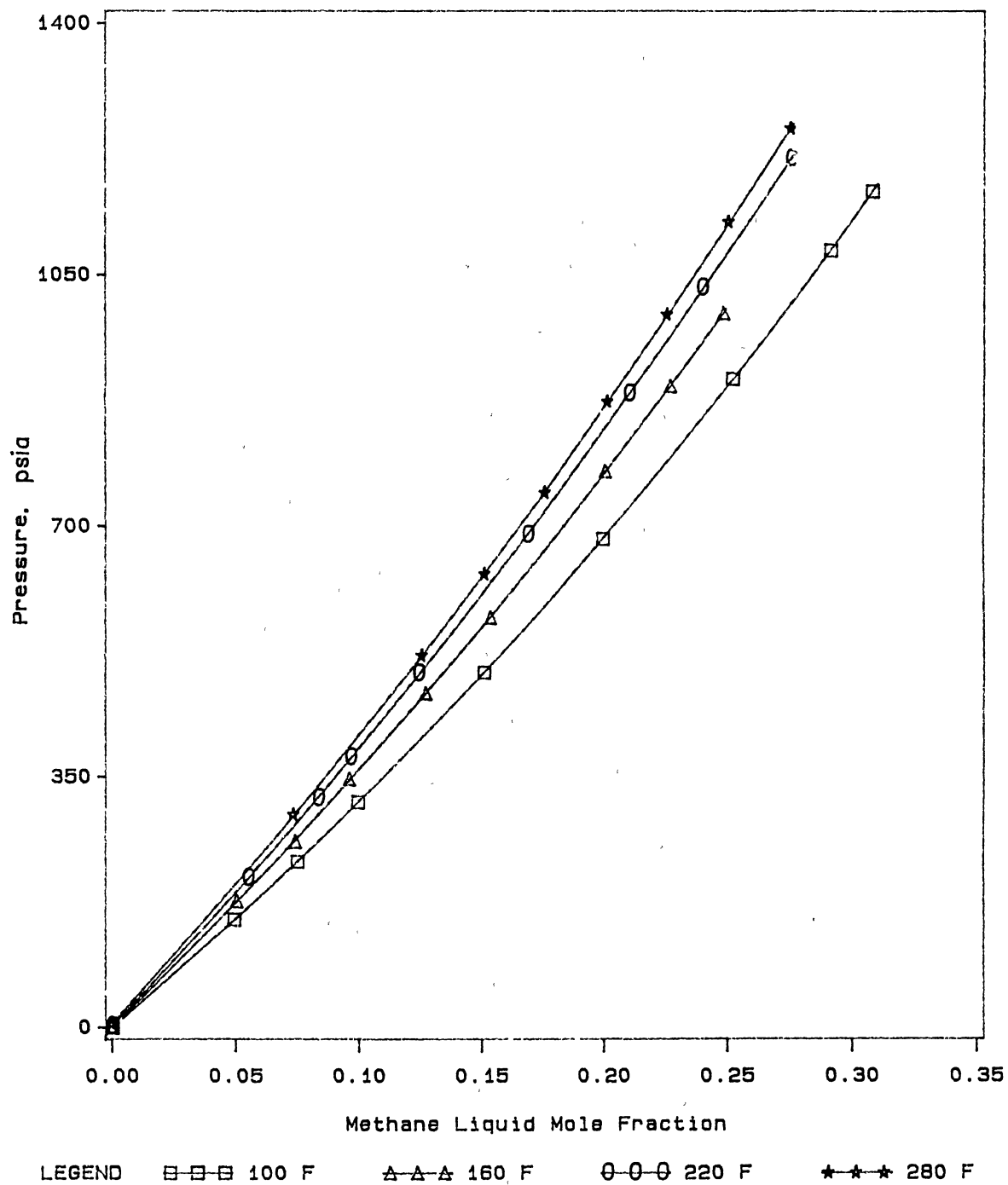
Figure 1

Bubble Point Pressure Data for Methane + n—Decane
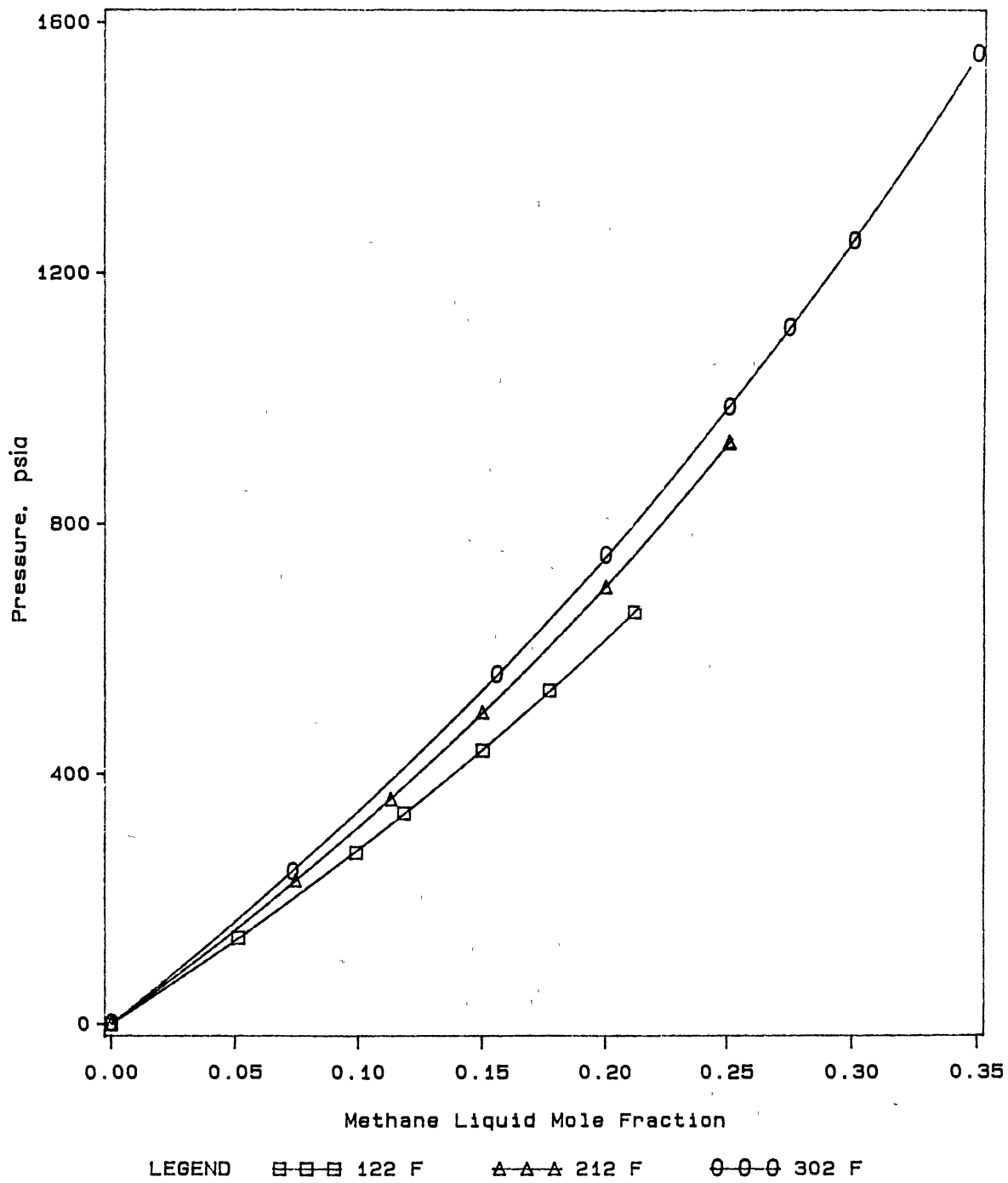
Figure 2

Bubble Point Pressure Data for Methane + n-Eicosane
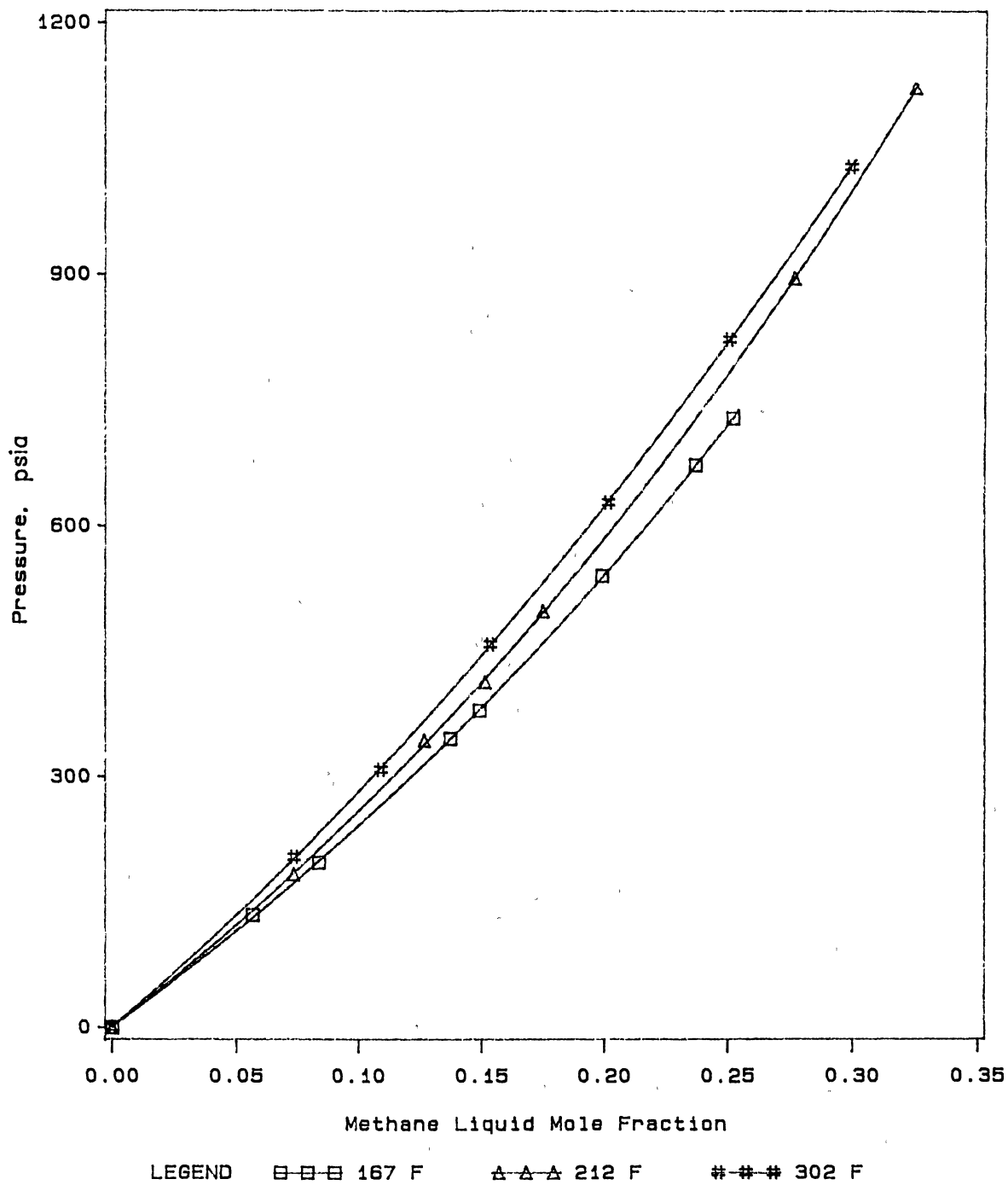
Figure 3

Bubble Point Pressure Data for Methane + n—Octacosane
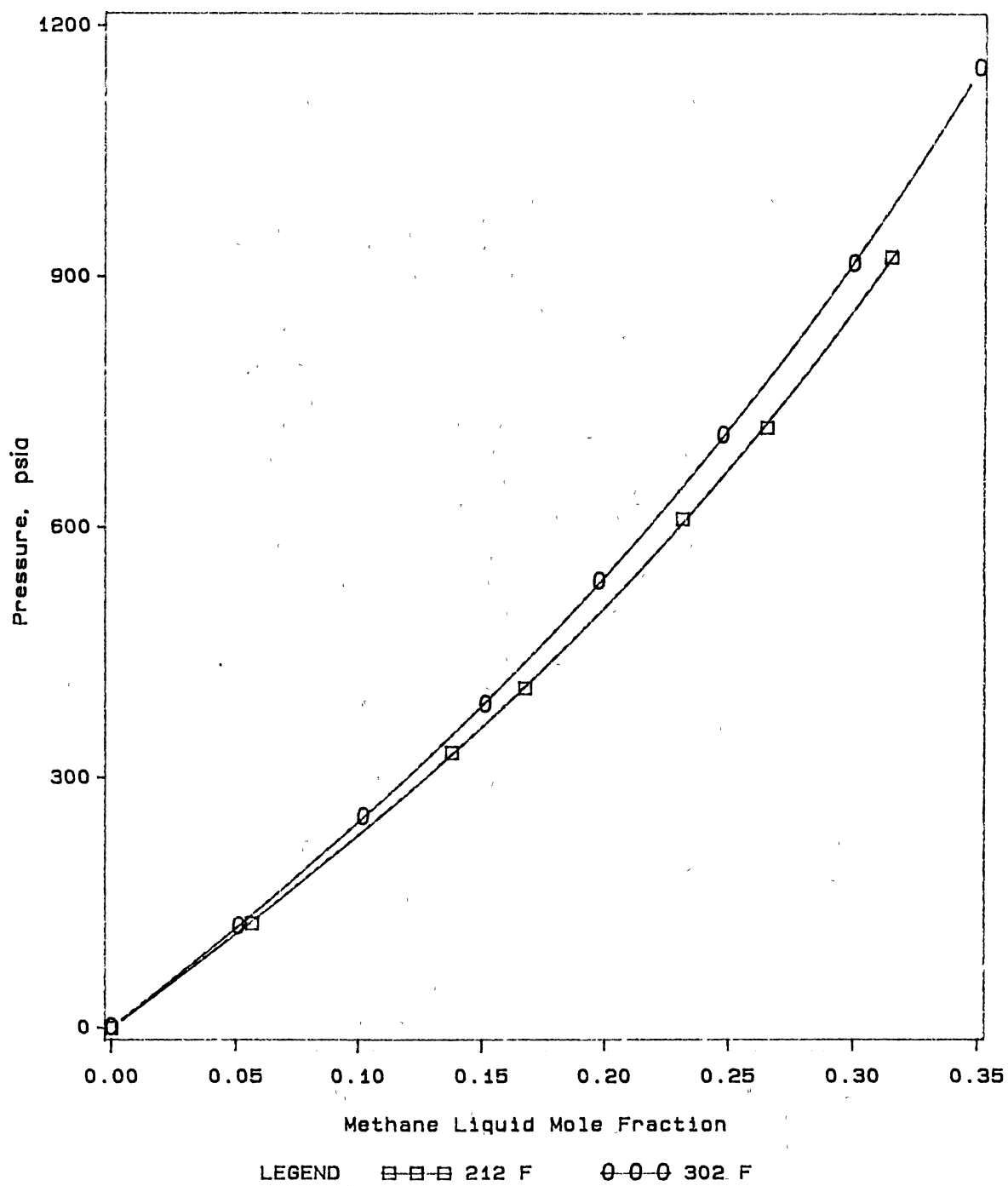
Figure 4

Bubble Point Pressure Data for Methane + n—Hexatriacontane
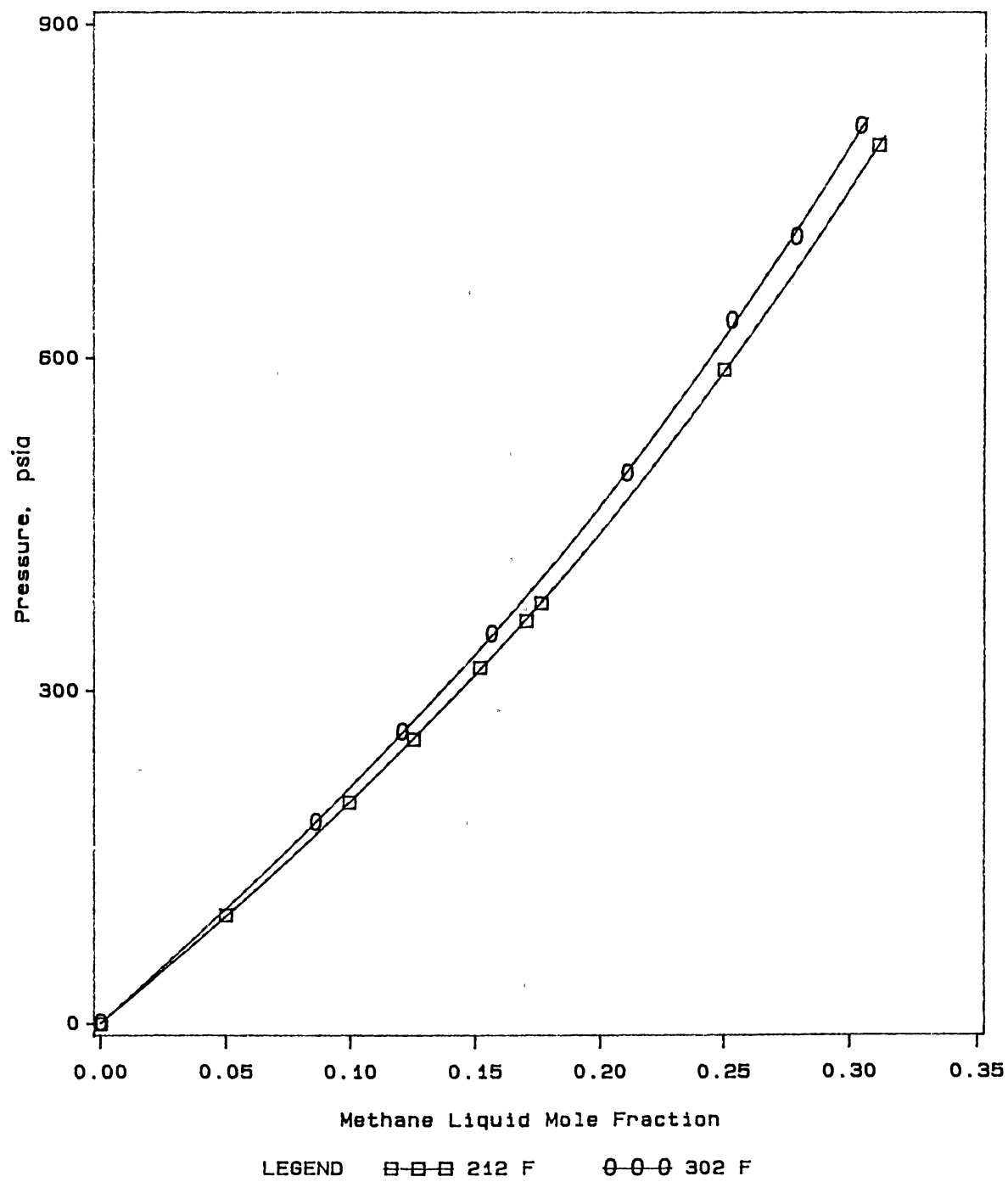
Figure 5

Bubble Point Pressure Data for Methane + n—Tetratetracontane
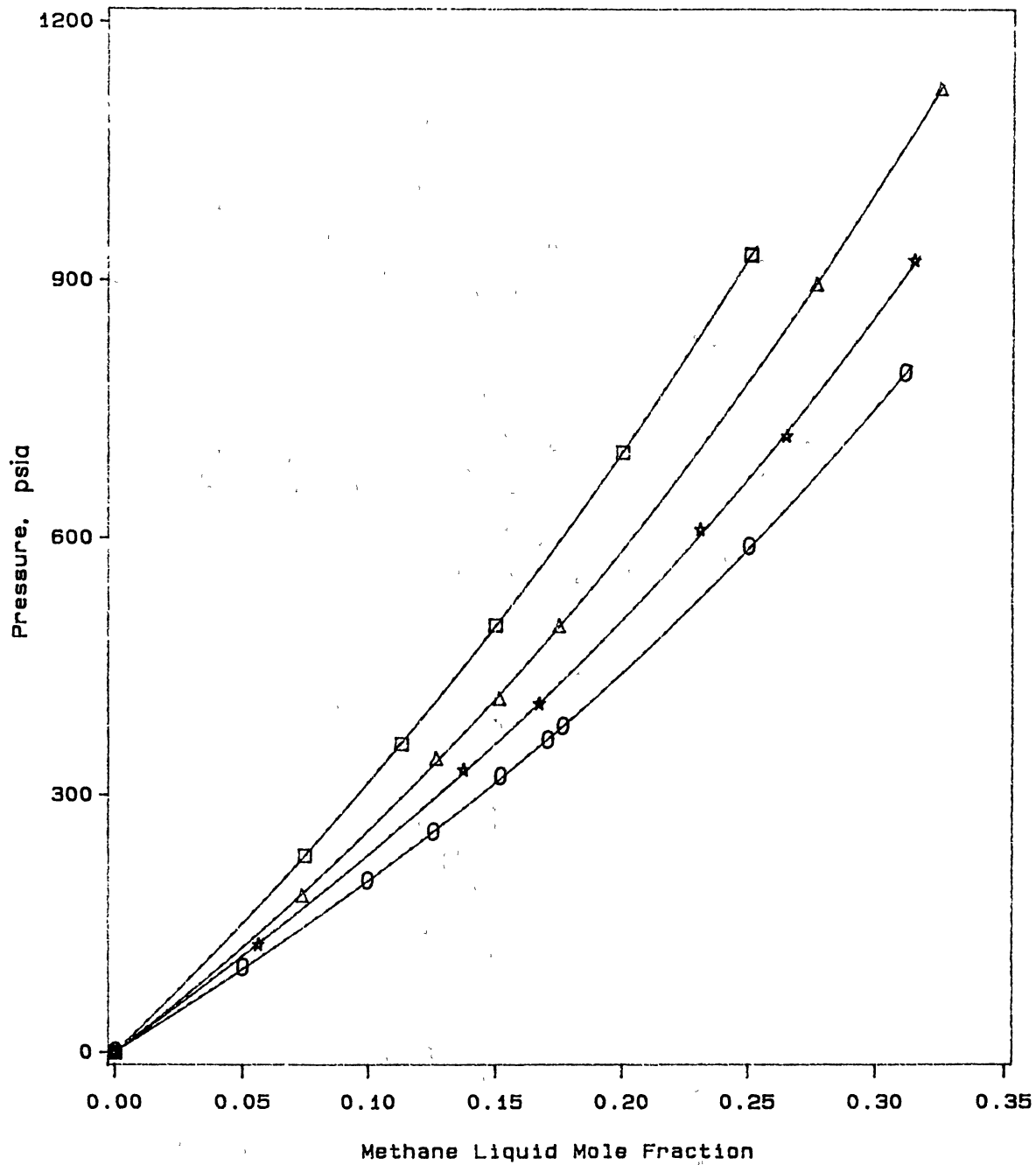
Figure 6

Bubble Point Pressure Data for Methane + n—Paraffins at 212 F
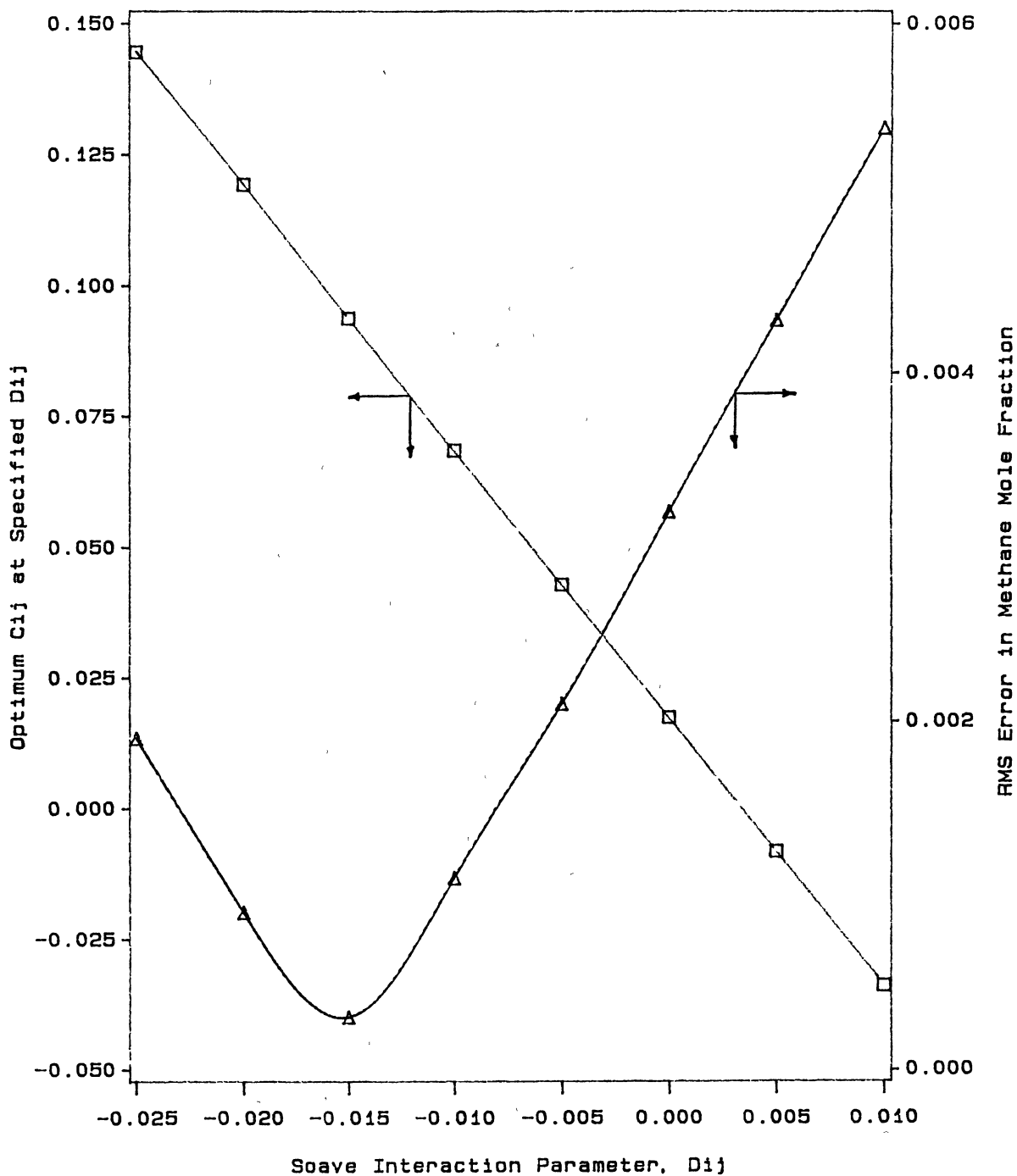
Figure 7

Sensitivity of Optimized Cij and Corresponding RMS Errors in Mole Fraction
to Dij for Methane + n—Eicosane at 212 F
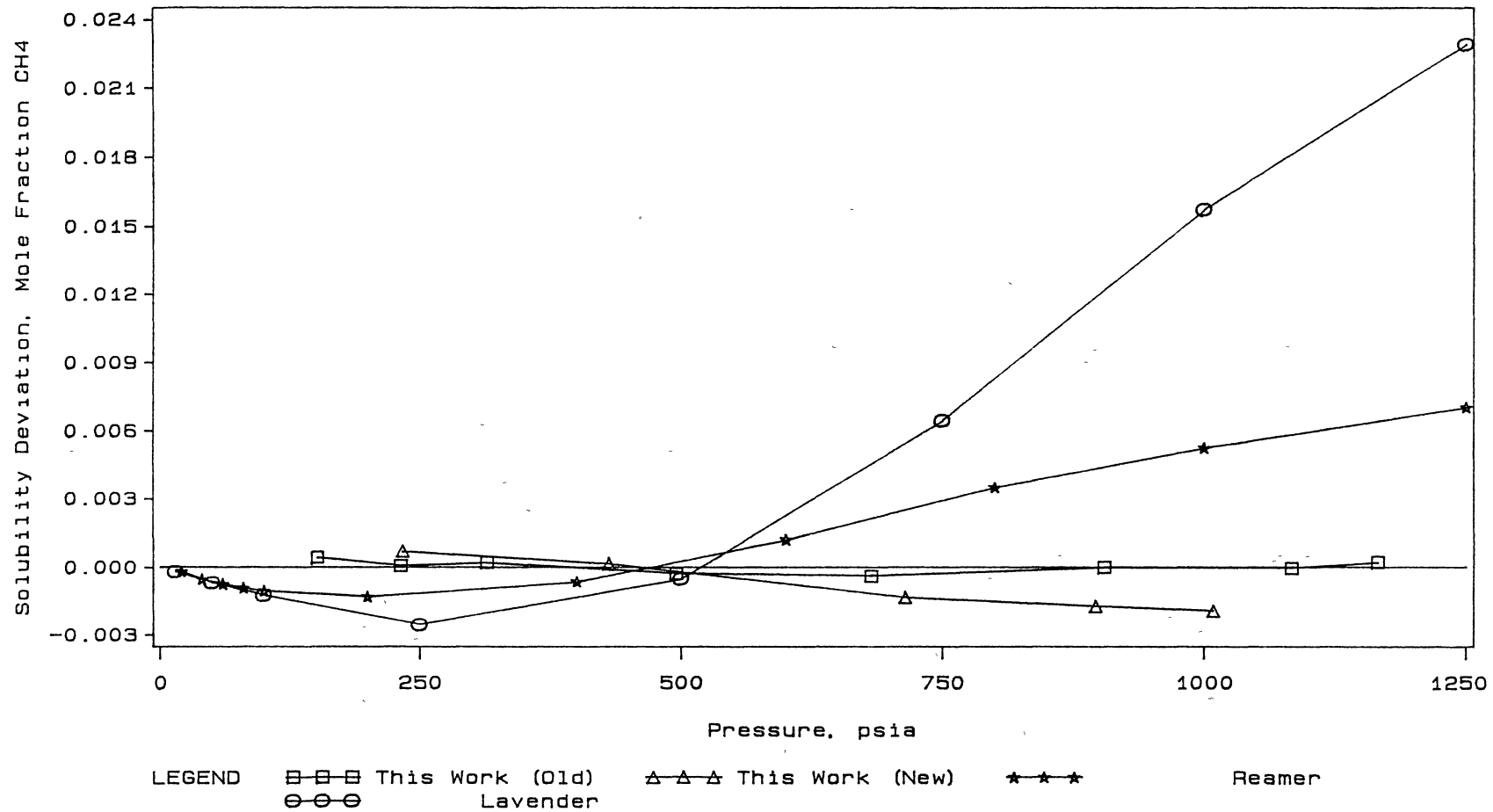
Figure 8.

Comparison of Methane Solubilities in n—Decane at 100 F
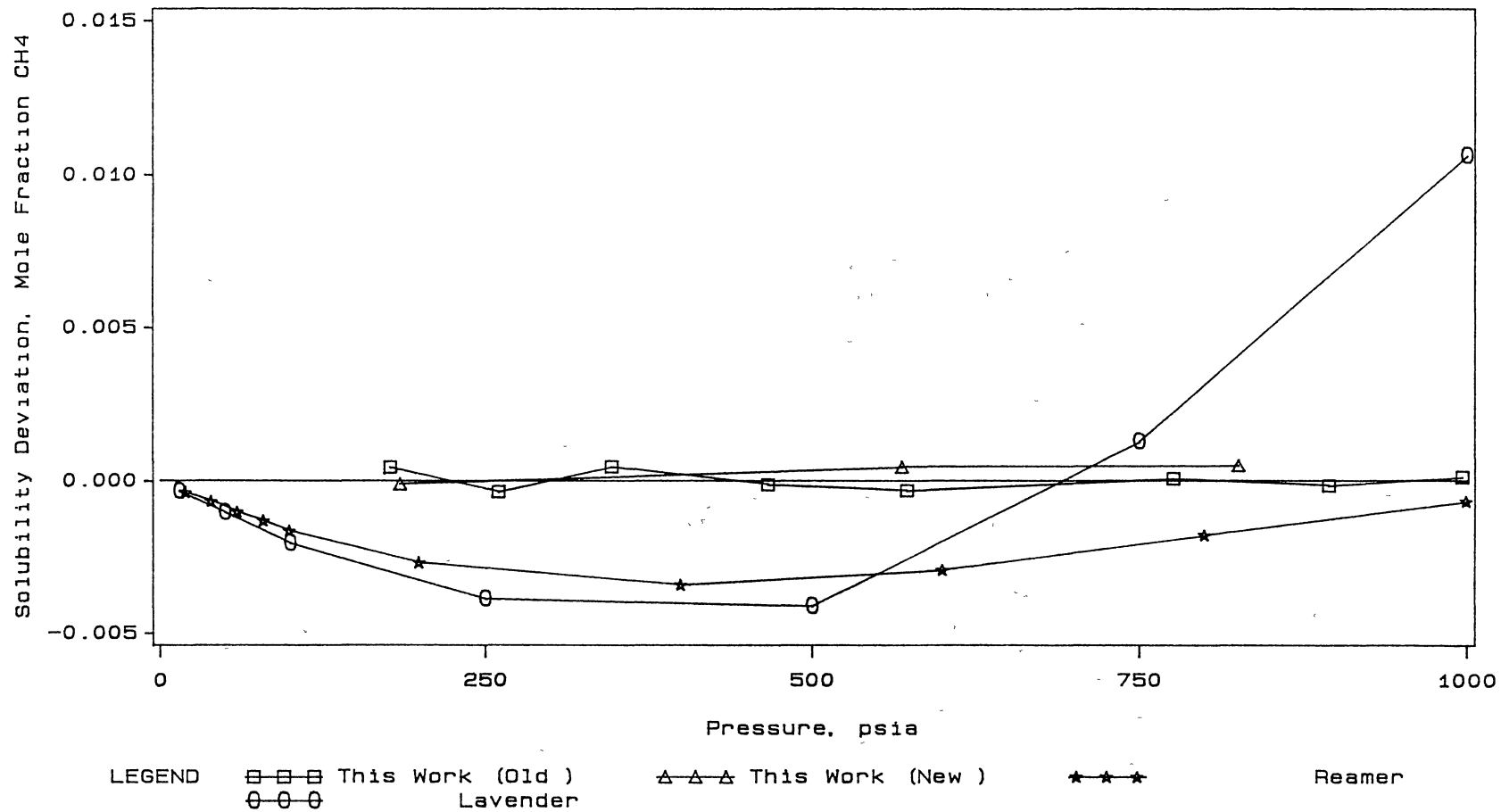
Figure 9.

Comparison of Methane Solubilities in n—Decane at 160 F
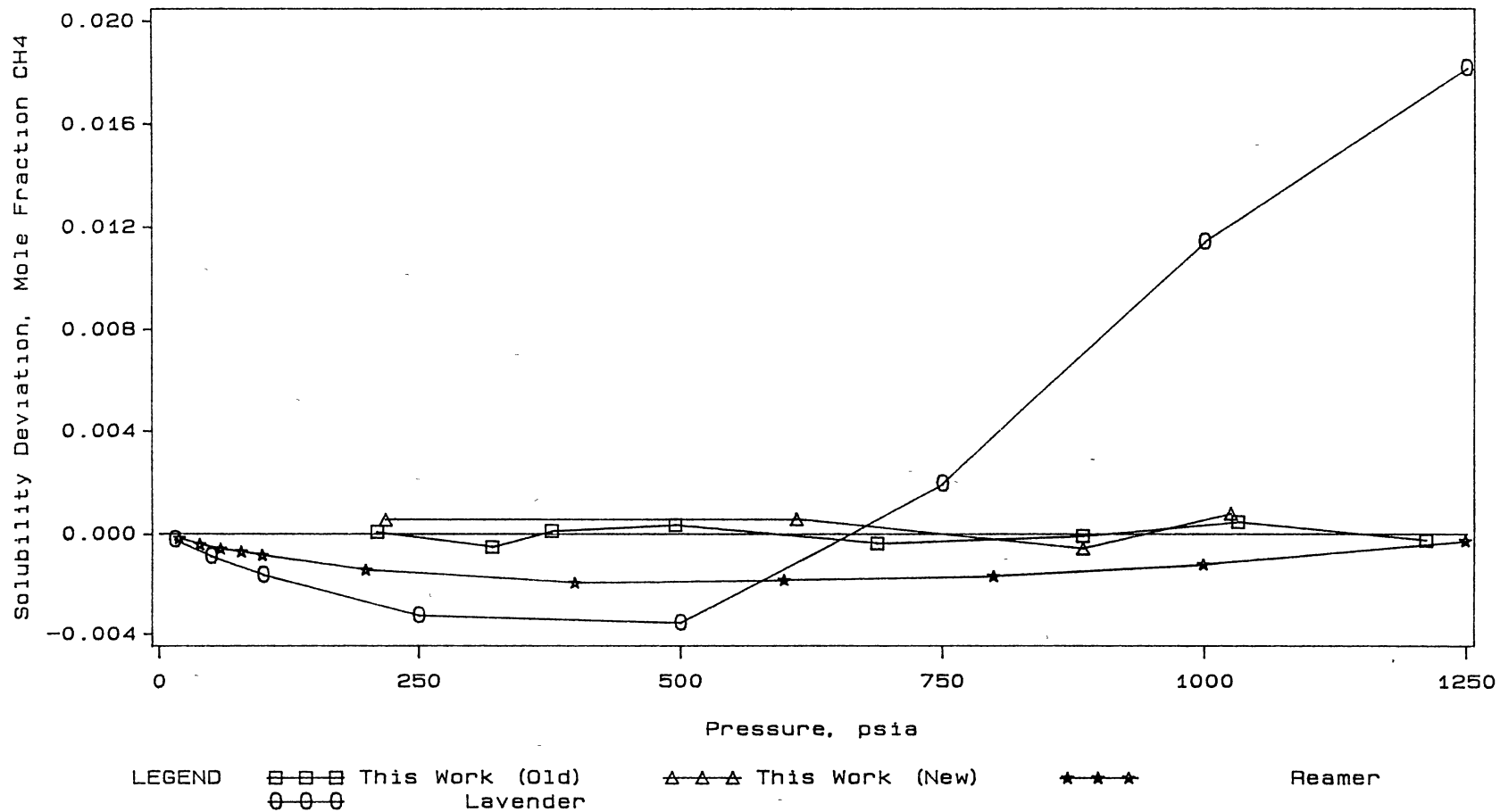
Figure 10.

Comparison of Methane Solubilities in n—Decane at 220 F
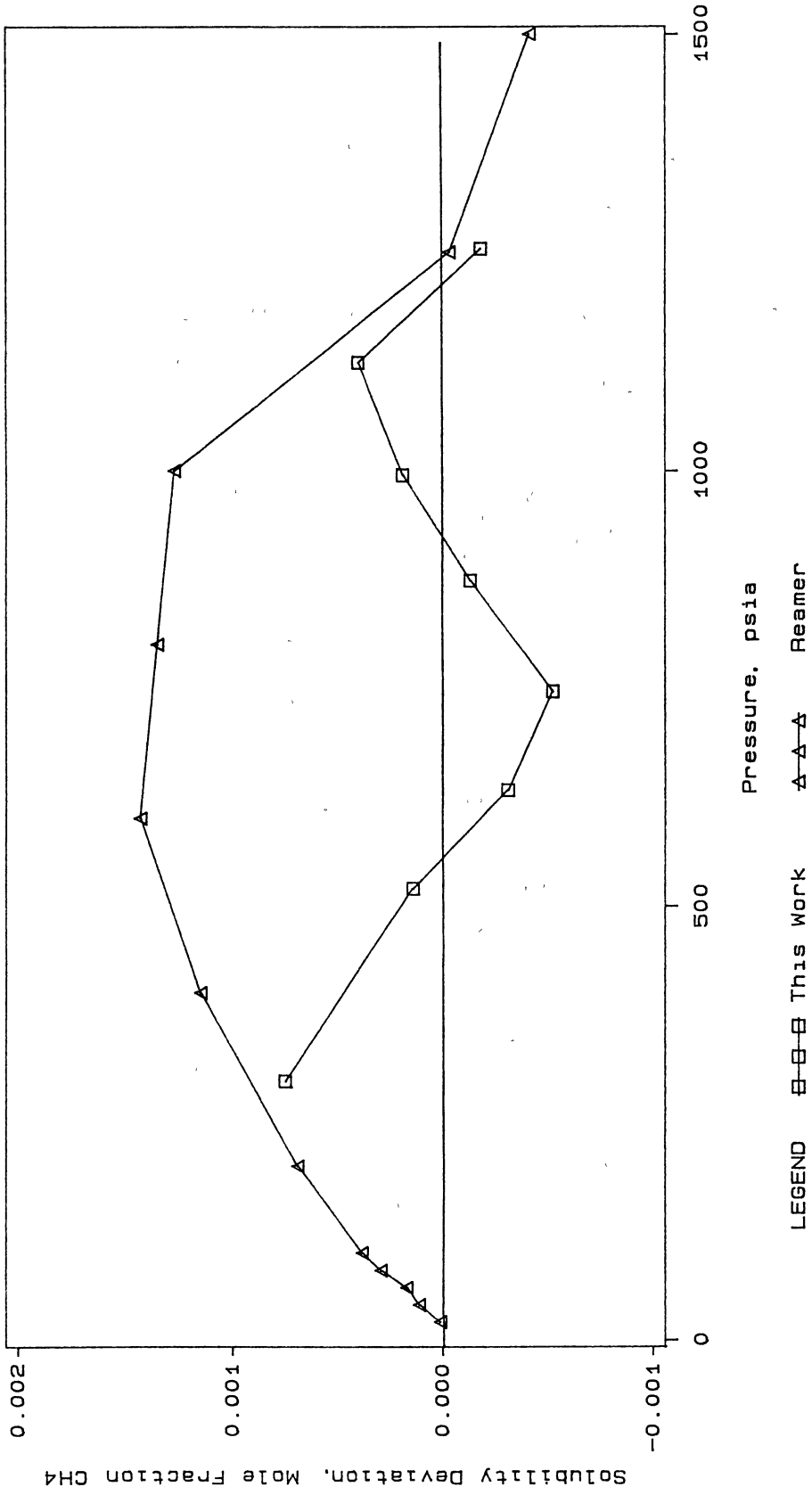
Figure 11.

Comparison of Methane Solubilities in n—Decane at 280 F
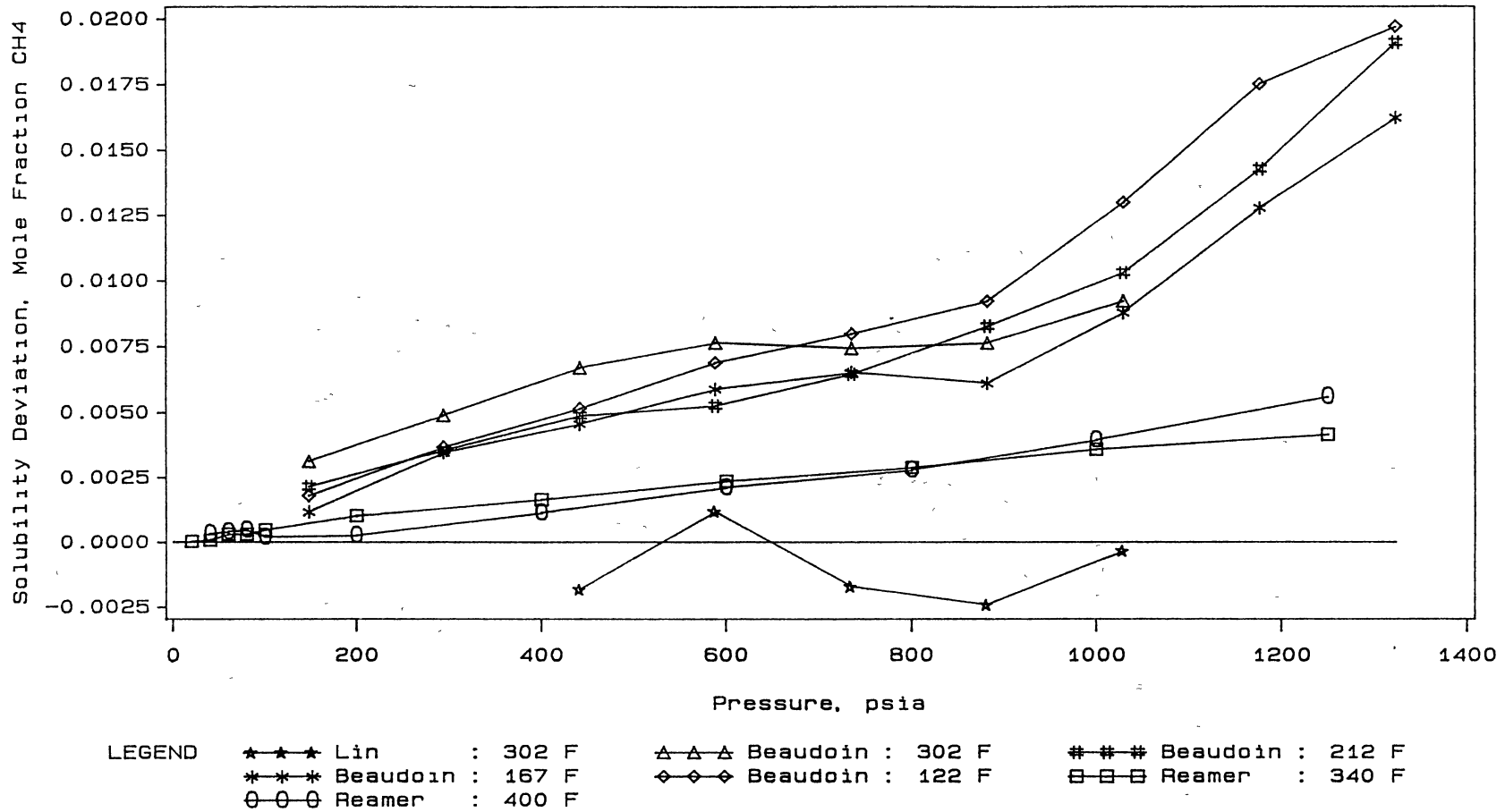
Figure 12.

Comparison of Methane Solubilities in n—Decane for Studies Performed
at Temperatures Different from the Present Work
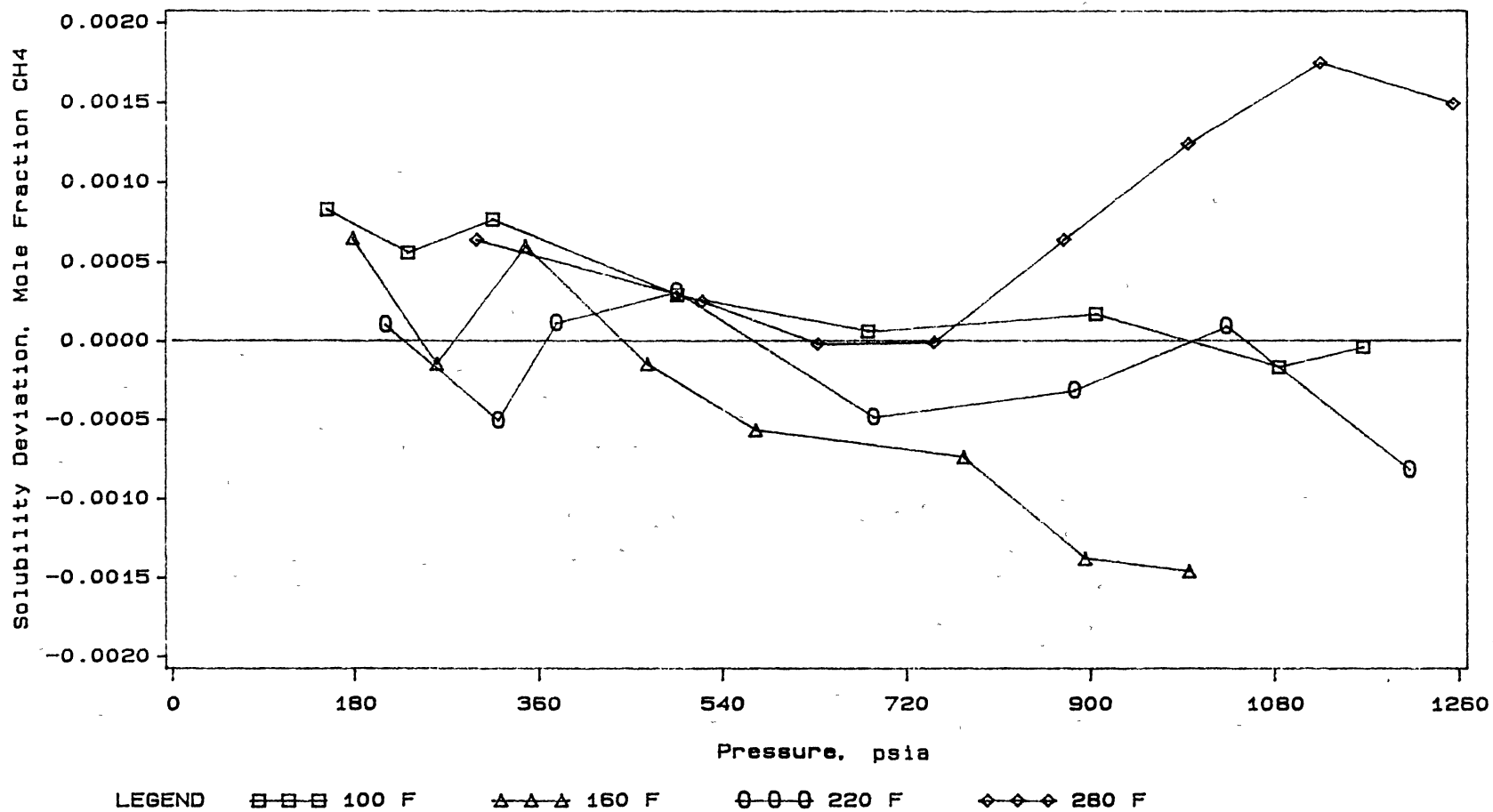
Figure 13

Comparison of Methane Solubilities in n—Decane Using Lumped Parameters, Cij and Dij, of the Present Work
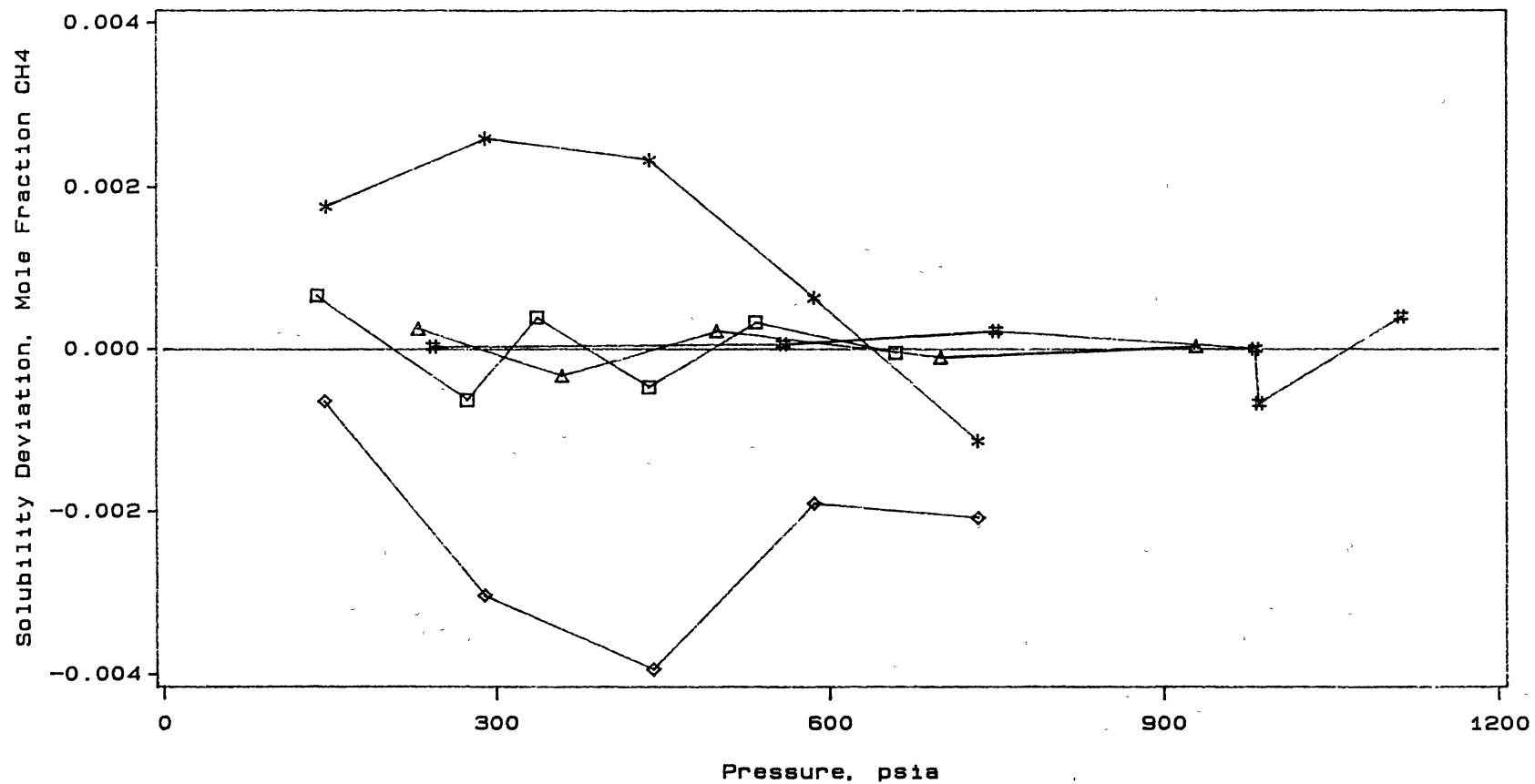
Figure 14.

Comparison of Methane Solubilities in n—Eicosane
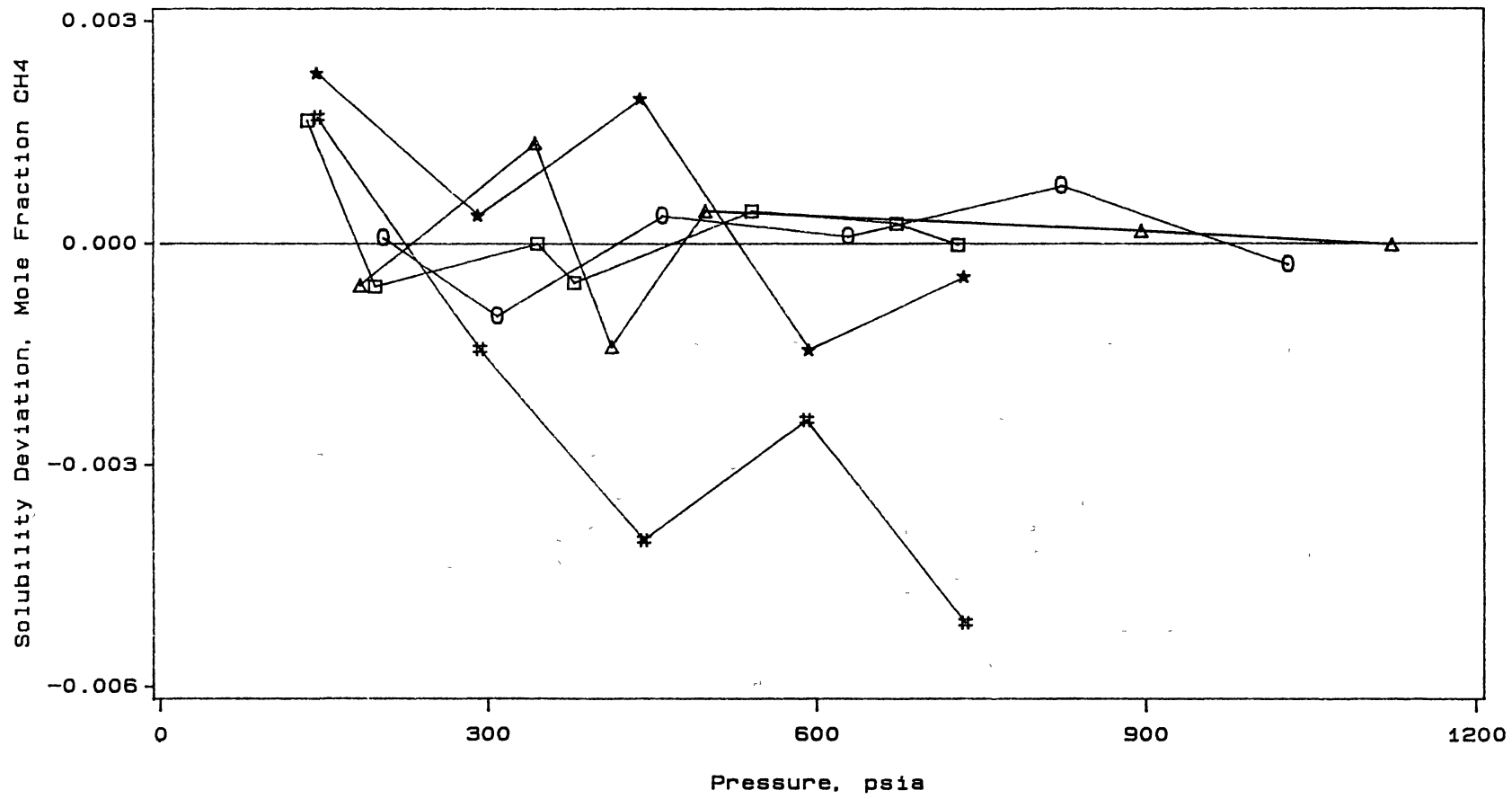
Figure 15.

Comparison of Methane Solubilities in n—Octacosane

Figure 16.

Comparison of Methane Solubilities in n–Hexatriacontane
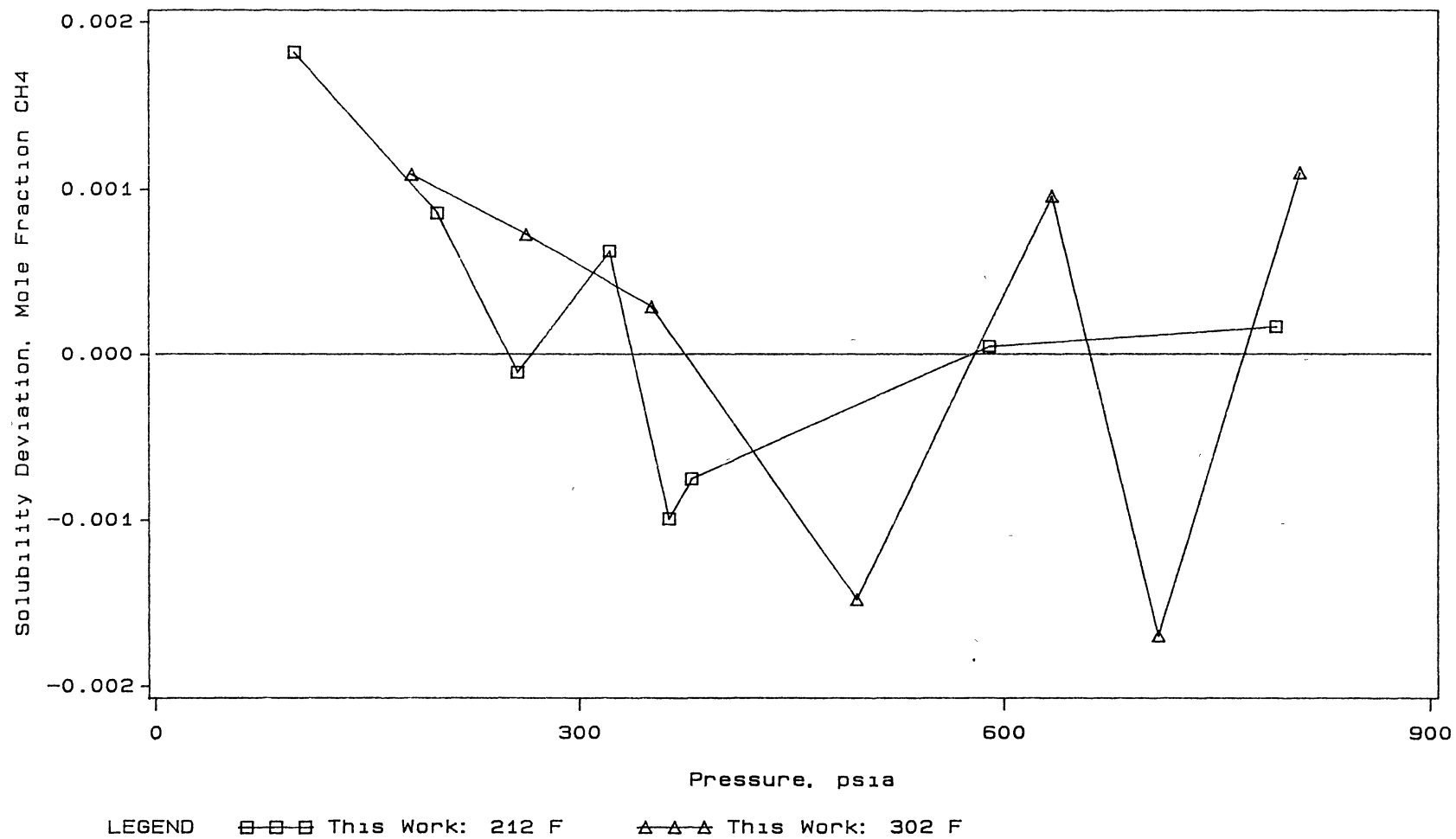
Figure 17.

Comparison of Methane Solubilities in n—Tetratetracontane
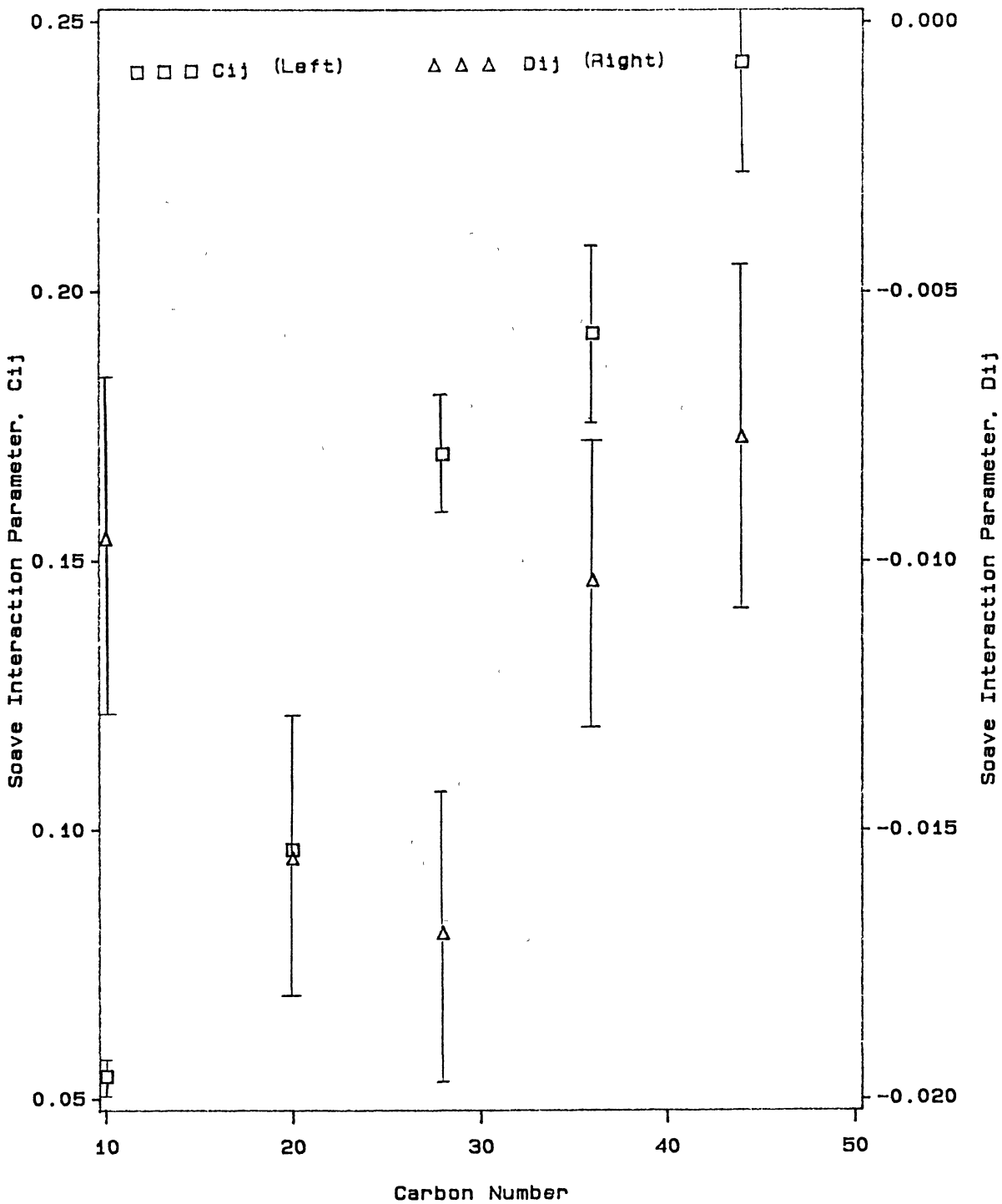
Figure 18

Soave Interaction Parameters, Cij and Dij, for Methane + n—Paraffins at 212 F
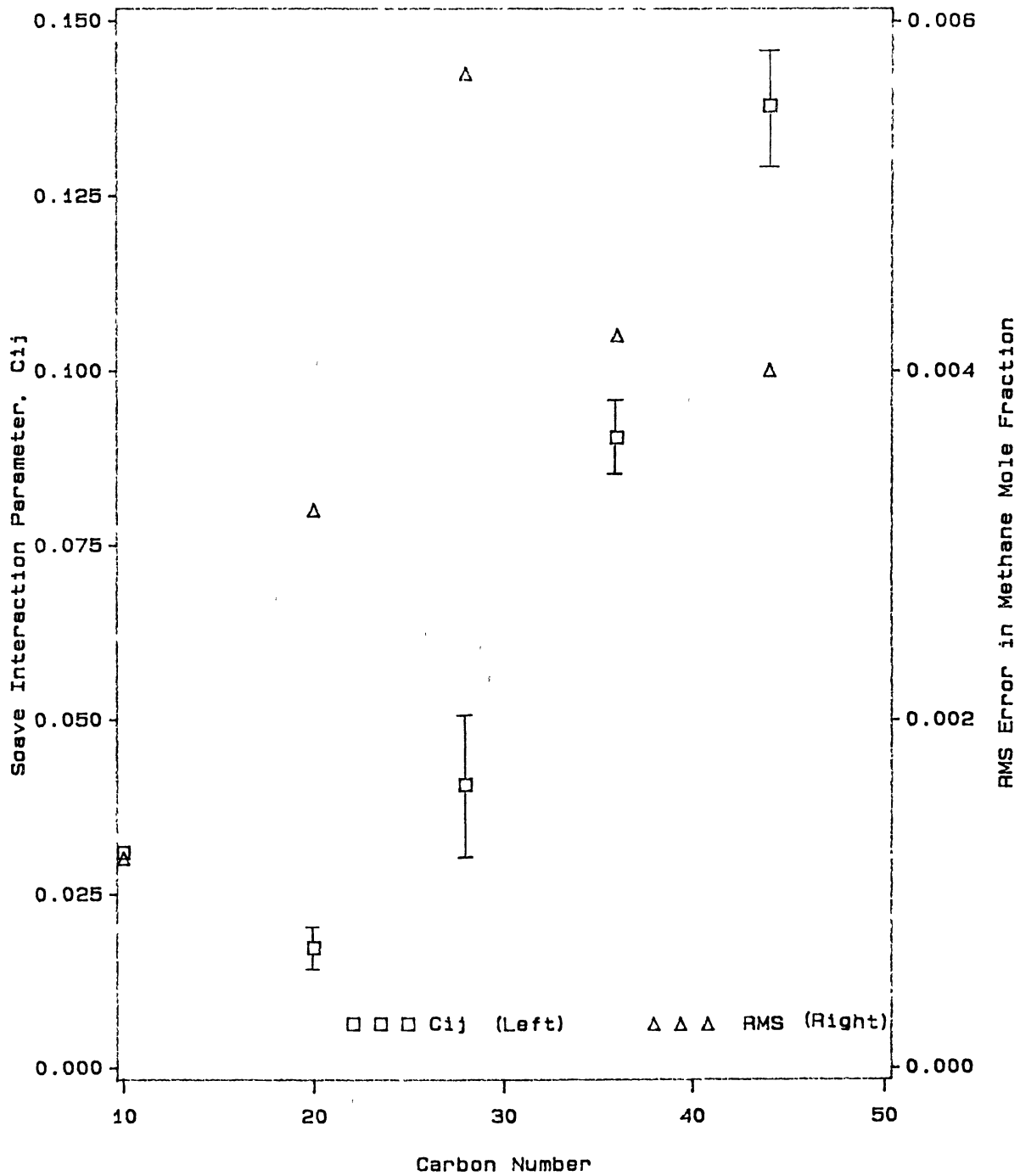
Figure 19

Soave Interaction Parameter, Cij, and Corresponding RMS Errors for
Methane + n—Paraffins at 212 F
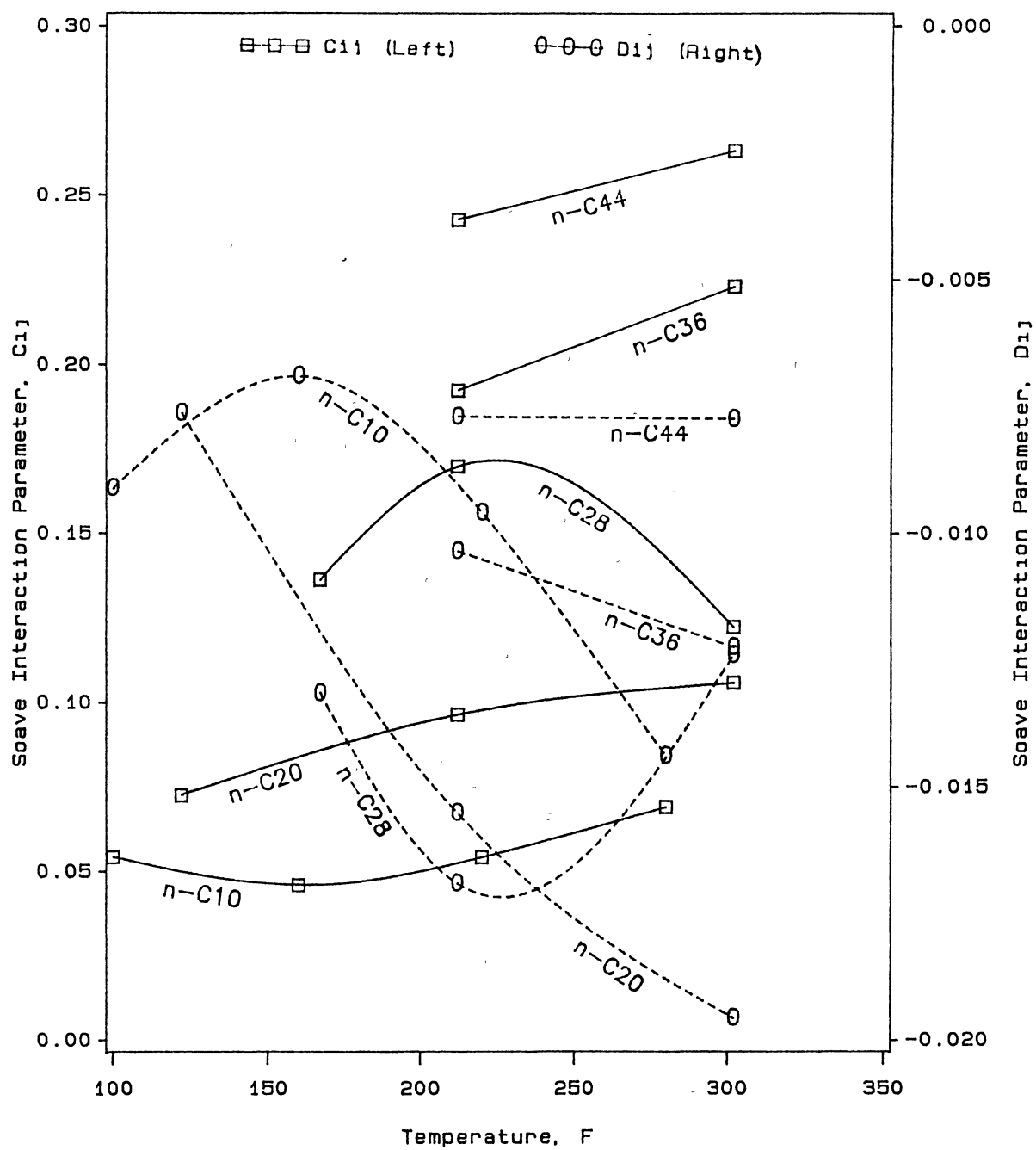
Figure 20.

Soave Interaction Parameters, Cij and Dij, for Methane + n—Paraffins
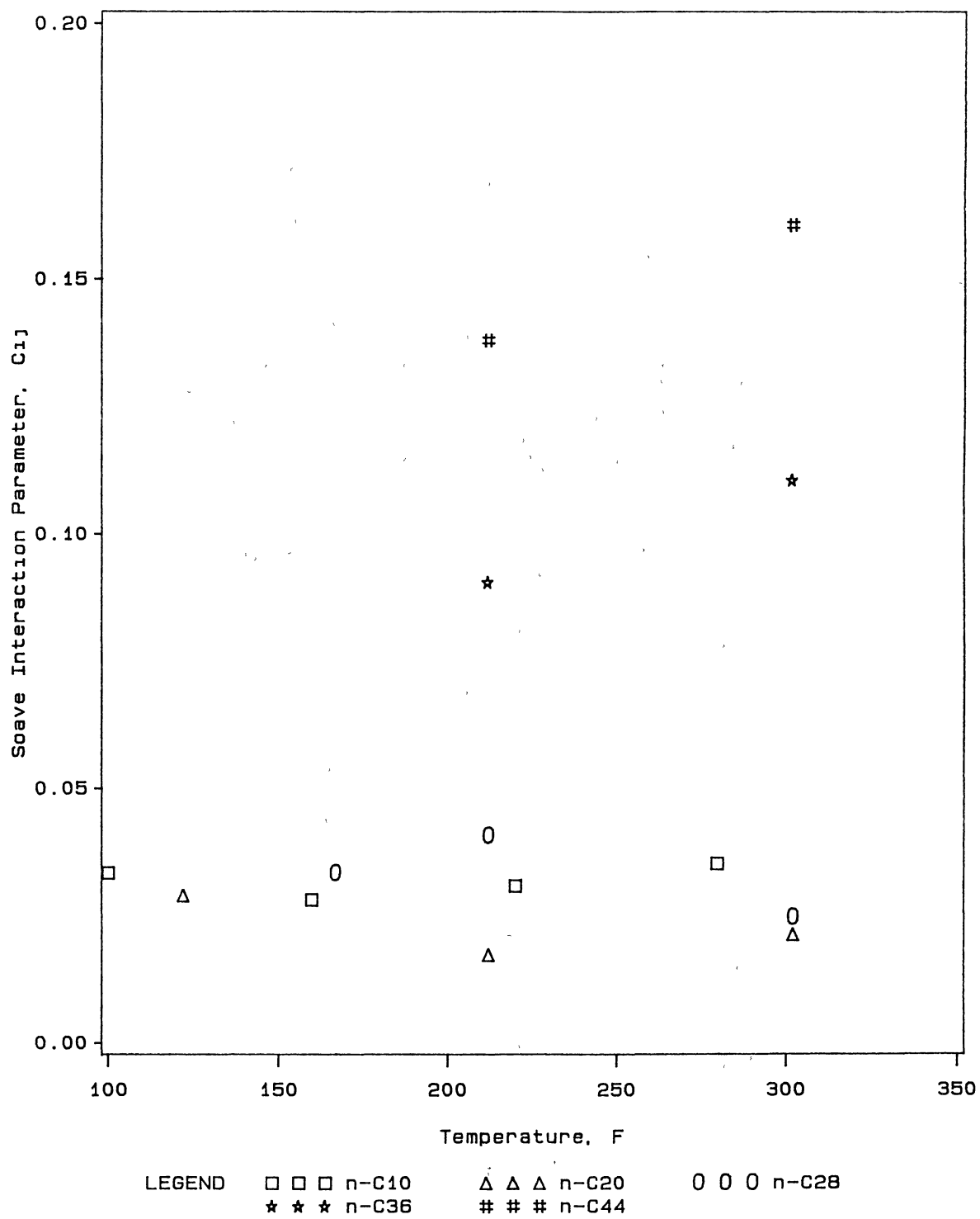
Figure 21.

Soave Interaction Parameter, Cij, for Methane + n—Paraffins
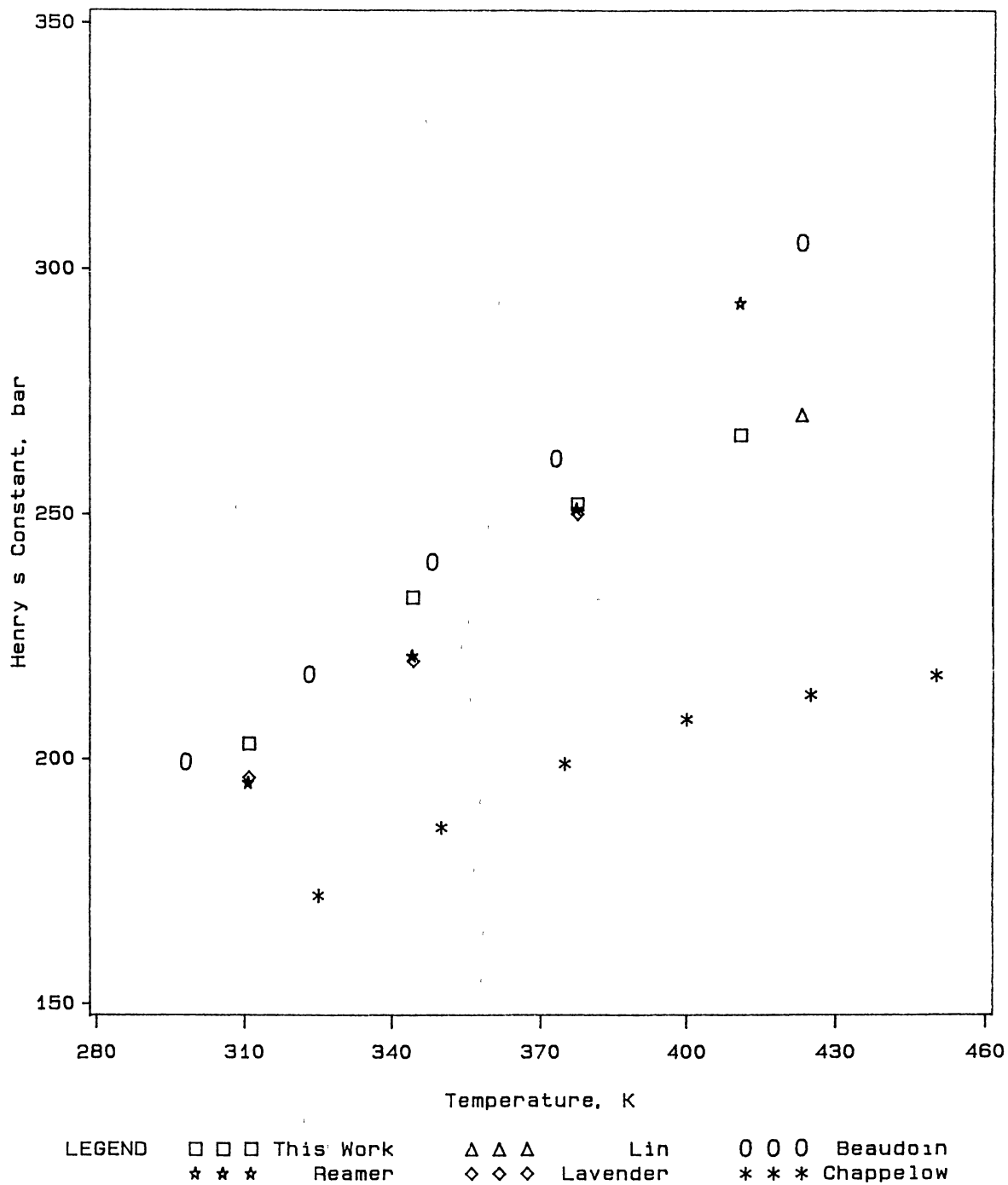
Figure 22.

Comparison of Henry s Constants of Methane in n—Decane
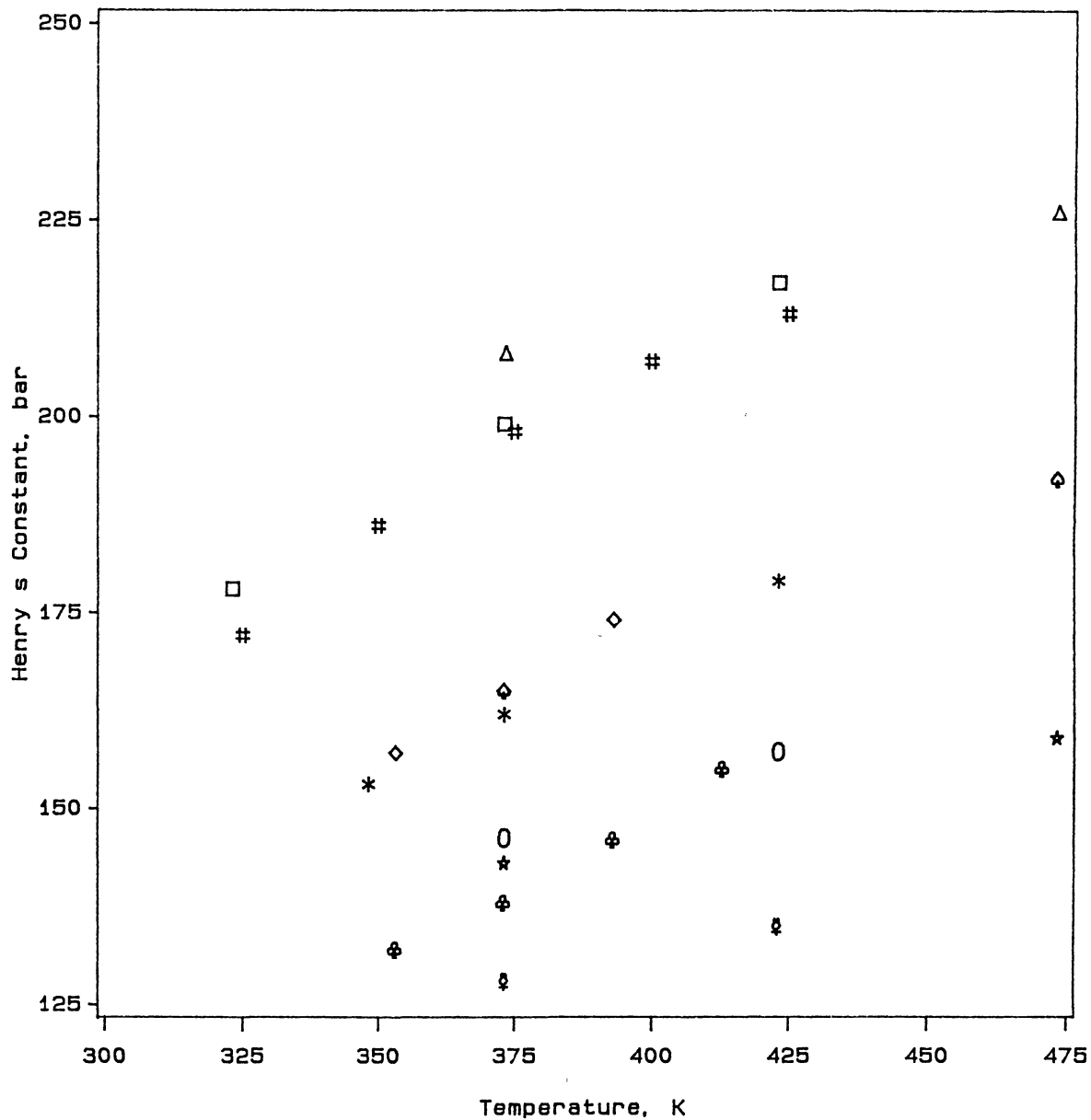
Figure 23.

Comparison of Henry s Constants of Methane in n—Paraffins
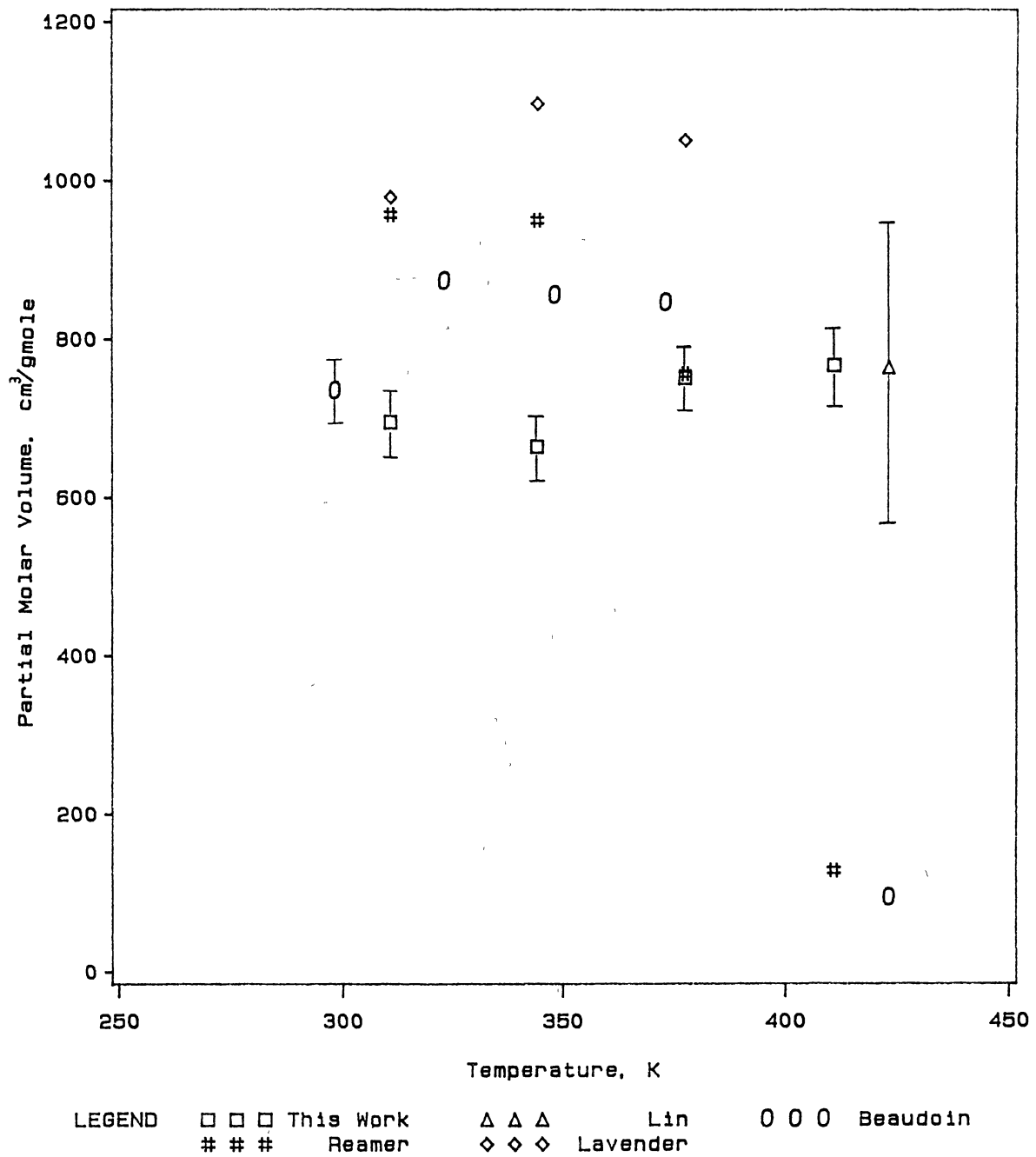
Figure 24

Comparison of Infinite—Dilution Partial Molar Volumes
of Methane in n—Decane
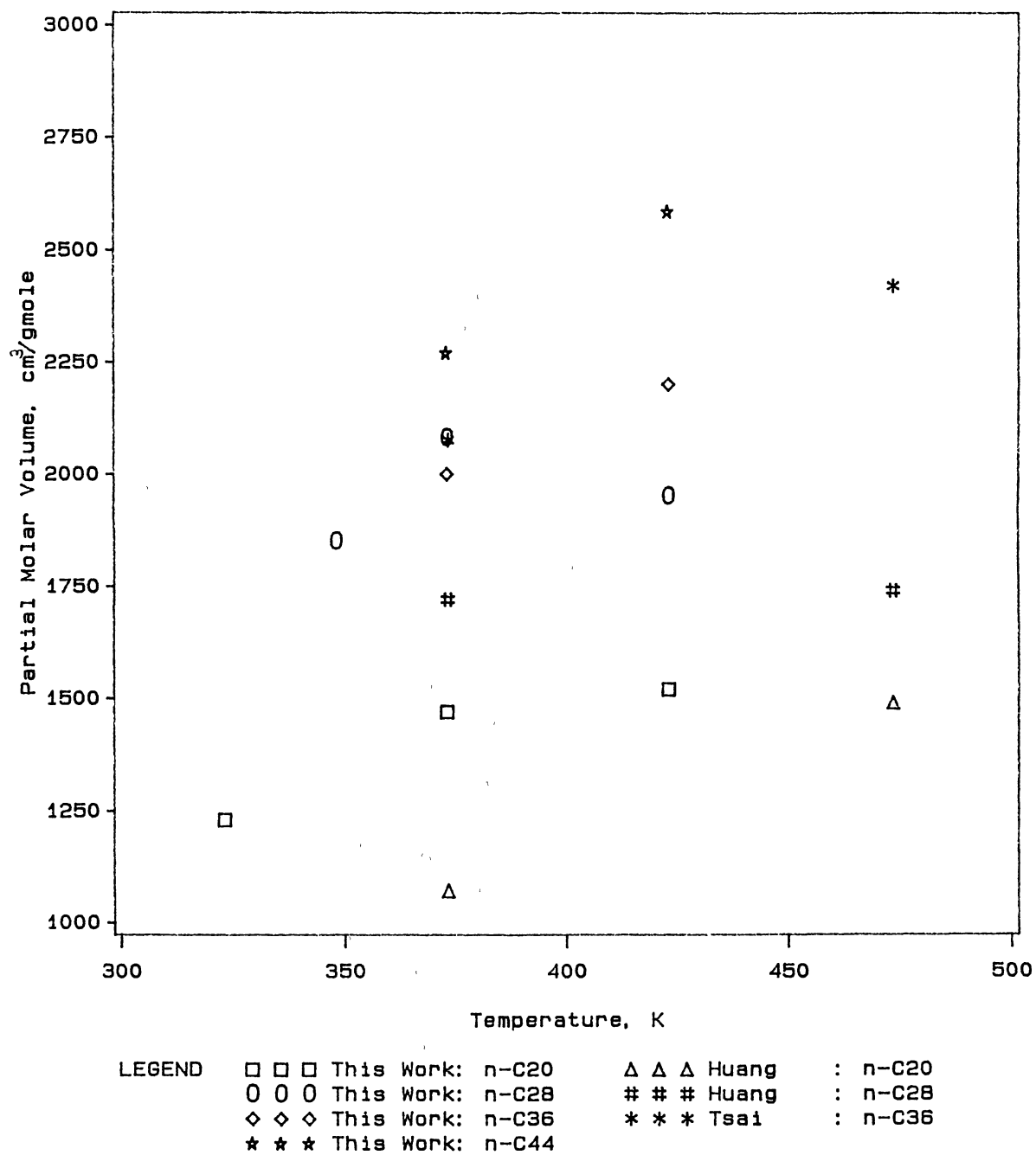
Figure 25.

Comparison of Infinite—Dilution Partial Molar Volumes
of Methane in n—Paraffins

CHAPTER VII

BINARY VAPOR-LIQUID PHASE EQUILIBRIUM
FOR METHANE + CYCLOHEXANE AND
METHANE + TRANS-DECALIN

Abstract

Binary solubility data are presented for methane + cyclohexane and methane + trans-decalin at temperatures from 323 to 423 K (122 to 302°F) and pressures to 965 bar (1400 psia). Our data for methane + cyclohexane are in reasonable agreement with the earlier measurements of Reamer but they are in significant disagreement with some of the data of Schoch. The new data can be described with RMS errors less than 0.0005 in mole fraction by the Soave-Redlich-Kwong (SRK) and Peng-Robinson (PR) equations of state when two interaction parameters per isotherm are employed in the equations.

Introduction

Solubility data for methane in naphthenic solvents are of interest in a number of engineering applications. Experimental data are needed for developing and testing viable correlations and describing the phase behavior of methane mixtures.

Essentially all state-of-the-art models for phase behavior contain one [1,2], two [3] or three [4] interaction parameters to account for unlike molecular pair interactions. These "empirical" interaction parameters have a dramatic effect on the predicted properties of mixtures and are thus required for accurate predictions. In most instances, successful modeling of the behavior of complex multicomponent mixtures requires accurate information on the pure compounds and on the binary interactions that exist between the different molecular species. Experimental measurements made on systematically chosen mixtures can be used to evaluate interaction parameters and, more importantly, furnish the basis for generalization of the parameters to allow interpolation (and perhaps extrapolation) to other solvents in the same homologous series. Toward this end, we have previously reported and analyzed data on the solubility of carbon dioxide and ethane in a series of hydrocarbons [5-8]. Recently we have completed an experimental study of the solubility of methane in a series of hydrocarbons (aromatic, paraffinic, and naphthenic solvents). Solubility data for the binary systems of methane in n-decane, n-eicosane,

n-octacosane, n-hexatriacontane, and n-tetratetracontane have been presented [9]. In the present work, solubility data for the binary systems of methane + cyclohexane and methane + trans-decalin are presented and correlated using SRK [1] and PR [2] equations of state (EOS). Solubilities were measured at temperatures from 323 to 423 K (122 to 302°F) and pressures to 965 bar (1400 psia). These data should provide a valuable complement to the available literature data and prove useful in the development and testing of correlations describing the phase behavior of multicomponent systems involving methane.

Experimental Section

Apparatus and Procedure

The experimental apparatus used in this study is a modified version of the apparatus used by Raff [10]. The modifications resulted in a number of improvements including improved mixing, reduced dead volumes, and improved design and procedures for cleaning and degassing. A detailed description of the apparatus and the experimental procedure is given elsewhere [9].

Estimated uncertainties in experimental measurements are 0.1 K in temperature and less than 0.001 in mole fraction. It should be noted that the uncertainty in the solute mole fraction depends (among other variables) on the amount of gas required (for a given mole fraction), which, in turn, depends on the solvent molecular weight. The lower the molecular

weight of the solvent, the higher is the amount of gas needed
for a given composition, and thus the better is the estimated
uncertainty in the solute mole fraction [9]. The estimated
uncertainties in the measured bubble point pressures depend
on the steepness of the p-x relation and are of the order of
0.35 bar (5 psia) [9].

Materials

The methane had a stated purity of 99.97+ mol% and was
supplied by Matheson. Cyclohexane and trans-decalin were
from Aldrich Chemical Company with quoted purities of 99+
mol%. No further purification of the chemicals was
attempted.

Results and Discussion

The experimental data (presented in Tables I and II)
have been correlated using SRK and PR cubic equation of
state. Optimum binary interaction parameters were obtained
by minimizing the sum of squares of pressure deviations from
the experimental values. The detailed procedure for data
reduction is given by Gasem [11]. The input parameters of
the pure components (acentric factors, critical temperatures
and critical pressures) required by the SRK and PR equations
of state, together with the literature sources are presented
in Table III.

Figures 1 and 2 show the effects of temperature and
pressure on methane solubility (liquid phase mole fraction of

the solute) . For a given total pressure, solubility of the gas decreases with increasing temperature which is the same behavior observed for carbon dioxide and methane solubilities in heavy normal paraffins [11,9].

The effect of molecular weight of the solvent on the gas solubility is displayed in Figure 3. For a given temperature and pressure, solubility of the gas increases with decreasing molecular weight of the solvent.

The equation-of-state representations of the solubilities for the systems under study are documented in Tables IV and V. The Peng-Robinson (PR) equation of state is capable of describing the data with RMS errors within 0.002 in mole fraction when a single interaction parameters, C_{ij}, is used over the complete temperature range of the systems studied. Using an additional interaction parameter, D_{ij}, in PR equation produces no further improvements as shown in Tables IV and V for the case of temperature-independent interaction parameters. In contrast, the SRK equation of state does not represent the data as well and, as shown in Tables IV and V, the PR equation with one parameter represents the data better than the SRK equation with two parameters. When two parameters are fitted to each isotherm, the RMS errors are less than 0.0005 and the two equations give comparable representation of the data. These results illustrate both the ability of the equations of state and the precision of our reported data.

Comparisons of our results with those reported by

various investigators appear in Figures 4-11. The
comparisons are shown in terms of deviations of the
solubilities from values predicted using the PR equation of
state [2]. The available literature data for methane +
cyclohexane are reported at temperatures different
from ours. Therefore, the prediction of solubilities is
performed using temperature independent parameters, C_{ij} and
D_{ij}, obtained from our data.

Comparisons for methane + cyclohexane are shown in
Figures 4 and 5. Good agreement (solubility deviation within
0.002) is observed between the present data and those of
Reamer [12] at temperatures 160, 220, and 280°F. However,
the agreement is not as good at 100 and 340°F, as shown in
Figure 4. Excellent agreement is observed between this work
and that of Schoch, et al. [13], at 220°F, since solubility
deviation is within 0.001 (Figure 5). Significant
disagreement, however, is observed at 100 and 160°F as shown
in Figure 5. Not much can be said regarding the disagreement
with those data of Sage [14] which are outside the range of
pressure of this study. For methane + trans-decalin, no
literature data are available for comparisons; the ability of
the equation of state to represent our data is displayed in
Figure 6.

The effects of temperature on C_{ij} and D_{ij} for methane +
cyclohexane, when regressed simultaneously, are shown in
Figure 7. The standard deviation (uncertainty) of any
optimized parameter (whenever of adequate magnitude to be

shown) is shown on the figures. The parameters exhibit a
minimum at a temperature around 170°F, which is the same
behavior observed when only one parameter, C_{ij} is regressed
holding the other, D_{ij}, constant (zero in this case) as
Figure 8 shows. The same trend is observed for the parameter
C_{ij} regressed from Reamer's data (Figure 8). Also shown are
the corresponding RMS prediction errors of our data and those
of Reamer over the same pressure range. The high precision
of the present data is evident from Figure 8.

When C_{ij} and D_{ij} for methane + trans-decalin are
regressed simultaneously, the two parameters exhibit
opposite behaviors with temperature. While D_{ij} shows a
minimum , C_{ij} exhibits a maximum as indicated in Figure 9.
Simpler dependence of C_{ij} on temperature, for methane + t-
decalin, is observed when only C_{ij} is optimized. In this
case, C_{ij} shows a monotonic behavior with temperature as is
shown in Figure 10, indicating a certain degree of
correlation between C_{ij} and D_{ij}. The sensitivity of C_{ij} and
the corresponding RMS errors in solubility to changes in D_{ij},
for methane + cyclohexane and methane + t-decalin, are shown
in Figures 11 and 12. The rate of change of C_{ij} with respect
to D_{ij} is almost the same (-1.7) for different temperatures.
More importantly, the sharp minima in the RMS vs D_{ij} plot for
methane + cyclohexane is indicative of a high sensitivity of
the model (SRK) to the interaction parameters. The
sensitivity is less severe for methane + t-decalin as
revealed by the shallow minima in Figure 12.

The influence of the chemical structure of the solvent on the parameter C_{ij} is shown in Figure 13. C_{ij} assumes higher values with higher molecular weight solvent which is expected.

Conclusions

Data have been obtained on the solubility for methane + cyclohexane and methane + trans-decalin at temperatures from 323 to 423 K (122 to 302°F) and pressures to 895 bar (1400 psia). These data are well described by the Soave-Redlich-Kwong and Peng-Robinson equations of states. These results can be of value in establishing equation-of-state interaction parameters for light gases in naphthenic hydrocarbon liquids.

References

1. Soave, G., Chem. Eng. Sci., 27, 1197-1203 (1972).

2. Peng, Y. D.; Robinson, D. B., Ind. Eng. Chem. Fundam., 15, 59-64 (1976).

3. Turek, E. A.; Metcalfe, R. S.; Yarborough, L.; Robinson, R. L., Jr., J. Soc. Petrol. Eng., 24, 308-324 (1984).

4. Assadipour, H.; Hajela, V., "New Mixing Rules for Parameters of a three-Parameter Equation of State", Paper presented at AIChE Meeting, New Orleans, April 6-10 (1986).

5. Robinson, R. L., Jr.; Anderson, J. M.; Barrick, M. W.; Bufkin, B. A.; Ross, C. H., " Phase behavior of Coal Fluids: Data for Correlation Development," DE-FG22-86PC90523, Final Report, Department of Energy, January (1987).

6. Gasem, K. A. M.; Robinson, R. L., Jr., J. Chem. Eng. Data, 30, 53-56 (1985).

7. Anderson, J. M.; Barrick, M. W.; Robinson, R. L., Jr., J. Chem. Eng. Data, 31, 172-175 (1986).

8. Gasem, K. A. M.; Bufkin, B. A.; Raff, A. M.; Robinson, R. L., Jr., J. Chem. Eng. Data, 34, 187-191 (1989).

9. Darwish, N. A., Ph.D. Dissertation, Oklahoma State University, Stillwater, Oklahoma (1991).

10. Raff, A. M., M.S. Thesis, Oklahoma state University, Stillwater, Oklahoma (1989).

11. Gasem, K. A. M., Ph.D. Dissertation, Oklahoma State University, Stillwater, Oklahoma (1986).

12. Reamer, H. H; Sage, B. H.; Lacey, W. N., Ind. Eng. Chem., (Chemical and Engineering Data Series), 3, 240-245 (1958).

13. Schoch, E. D.; Hoffmann, A. E.; Mayfield, F. D., Ind. Eng. Chem., 32, 1351-1353 (1940).

14. Sage, B. H.; Webester, D. C.; Lacey, W. N., Ind. Eng. Chem., 28, 1045-1047 (1936).

15. Goodwin, R. D., "Thermophysical Properties of Methane from 90 to 500 K at Pressures to 700 Bar", NBS Technical Note 653, 22, April (1974).

16. "Lange's Handbook of Chemistry", 12th Edition, Dean, J. D., (Editor), McGraw-Hill Book Company, New York, (1979).

List of Tables

I.   Solubility Data for Methane + Cyclohexane.

II.   Solubility Data for Methane + t-Decalin.

III.   Critical Properties and Acentric Factors Used in the SRK and PR Equations of State.

IV.   SRK and PR Equation-of-State Representations of Solubility of Methane in Cyclohexane.

V.   SRK and PR Equation-of-State Representations of Solubility of Methane in t-Decalin.

List of Figures

Table I

Solubility Data of Methane in Cyclohexane

Mole Fraction Methane	Bubble Point Pressure bar	(psia)
323.2 K (50.0°C, 122.0°F)		
0.042	14.1	(201)
0.069	23.5	(341)
0.098	33.4	(484)
0.124	42.5	(616)
0.155	54.0	(783)
0.174	61.0	(885)
0.207	73.8	(1071)
373.2 K (100.0°C, 212.0°F)		
0.029	12.5	(181)
0.052	20.9	(303)
0.083	32.4	(469)
0.100	39.1	(567)
0.138	54.0	(783)
0.152	59.1	(858)
0.178	70.2	(1018)
0.194	76.3	(1106)
0.201	79.4	(1151)
0.212	84.1	(1220)

Table I (Continued)

Solubility Data of Methane in Cyclohexane

Mole Fraction Methane	Bubble Point Pressure bar	(psia)
	423.2 K (150.0°C, 302.0°F)	
0.027	16.0	(232)
0.051	25.1	(365)
0.065	30.4	(441)
0.075	35.0	(508)
0.088	40.1	(582)
0.101	45.0	(653)
0.129	56.4	(818)
0.151	65.2	(945)
0.176	75.4	(1094)
0.201	85.9	(1246)
0.222	94.3	(1368)

Table II

Solubility Data of Methane in t-Decalin

Mole Fraction Methane	Bubble Point Pressure bar	(psia)
323.2 K (50.0°C, 122.0°F)		
0.026	8.9	(129)
0.050	17.5	(253)
0.075	26.6	(385)
0.100	36.7	(532)
0.134	50.1	(726)
0.150	57.3	(832)
373.2 K (100.0°C, 212.0°F)		
0.050	20.4	(296)
0.100	42.0	(609)
0.120	51.1	(741)
0.150	65.7	(953)
0.170	75.3	(1092)
0.180	81.1	(1176)
0.200	91.1	(1322)
423.2 K (150.0°C, 302.0°F)		
0.030	13.5	(196)
0.075	33.9	(492)
0.100	46.0	(667)
0.127	58.6	(850)
0.135	63.0	(914)
0.176	83.6	(1213)
0.200	96.2	(1396)

Table III

Critical Properties and Acentric Factors Used in the SRK and PR Equations of State

Component	Pressure (bar)	Temperature (K)	Acentric Factor	Reference
Methane	46.60	190.5	0.011	15
Cyclohexane	40.66	553.4	0.213	16
t-Decalin	29.08	681.5	0.286	16

Table IV

SRK and PR Equation-of-State Representations of Solubility of Methane in Cyclohexane

Temperature K (°F)	Soave Parameters (P-R Parameters)		Error in Methane* Mole Fraction	
	C_{12}	D_{12}	RMS	MAX
323.2 (122.0)	0.023	0.005	0.0002	0.0003
	(0.028)	(0.008)		
	0.032		0.0004	0.0006
	(0.042)			
373.2 (212.0)	0.023	0.004	0.0003	0.0005
	(0.027)	(0.005)		
	0.029		0.0004	0.0006
	(0.036)			
423.2 (302.0)	0.034	0.010	0.0004	0.0007
	(0.038)	(0.008)		
	0.050		0.0006	0.0010
	(0.050)			
323.2, 373.2 423.2	0.040	-0.003	0.0026	0.0049
	(0.035)	(0.004)	(0.0020)	(0.0038)
	0.034		0.0026	0.0053
	(0.041)		0.0020	(0.0034)

* Errors are essentially identical for the SRK and PR EOS

Table V

SRK and PR Equation-of-State Representations of Solubility of Methane in t-Decalin

Temperature K (°F)	Soave Parameters (P-R Parameters)		Error in Methane* Mole Fraction	
	C_{12}	D_{12}	RMS	MAX
323.2 (122.0)	0.073	0.002	0.0003	0.0005
	(0.073)	(0.004)		
	0.078		0.0004	0.0006
	(0.084)			
373.2 (212.0)	0.096	-0.004	0.0004	0.0005
	(0.094)	(-0.003)		
	0.085		0.0004	0.0007
	(0.087)			
423.2 (302.0)	0.079	0.007	0.0002	0.0004
	(0.080)	(0.006)		
	0.098		0.0005	0.0007
	(0.095)			
323.2, 373.2 423.2	0.115	-0.011	0.0022	0.0037
	(0.102)	(-0.005)	(0.0014)	(0.0023)
	0.087		0.0023	0.0039
	(0.088)		0.0014	(0.0024)

* Errors are essentially identical for the SRK and PR EOS
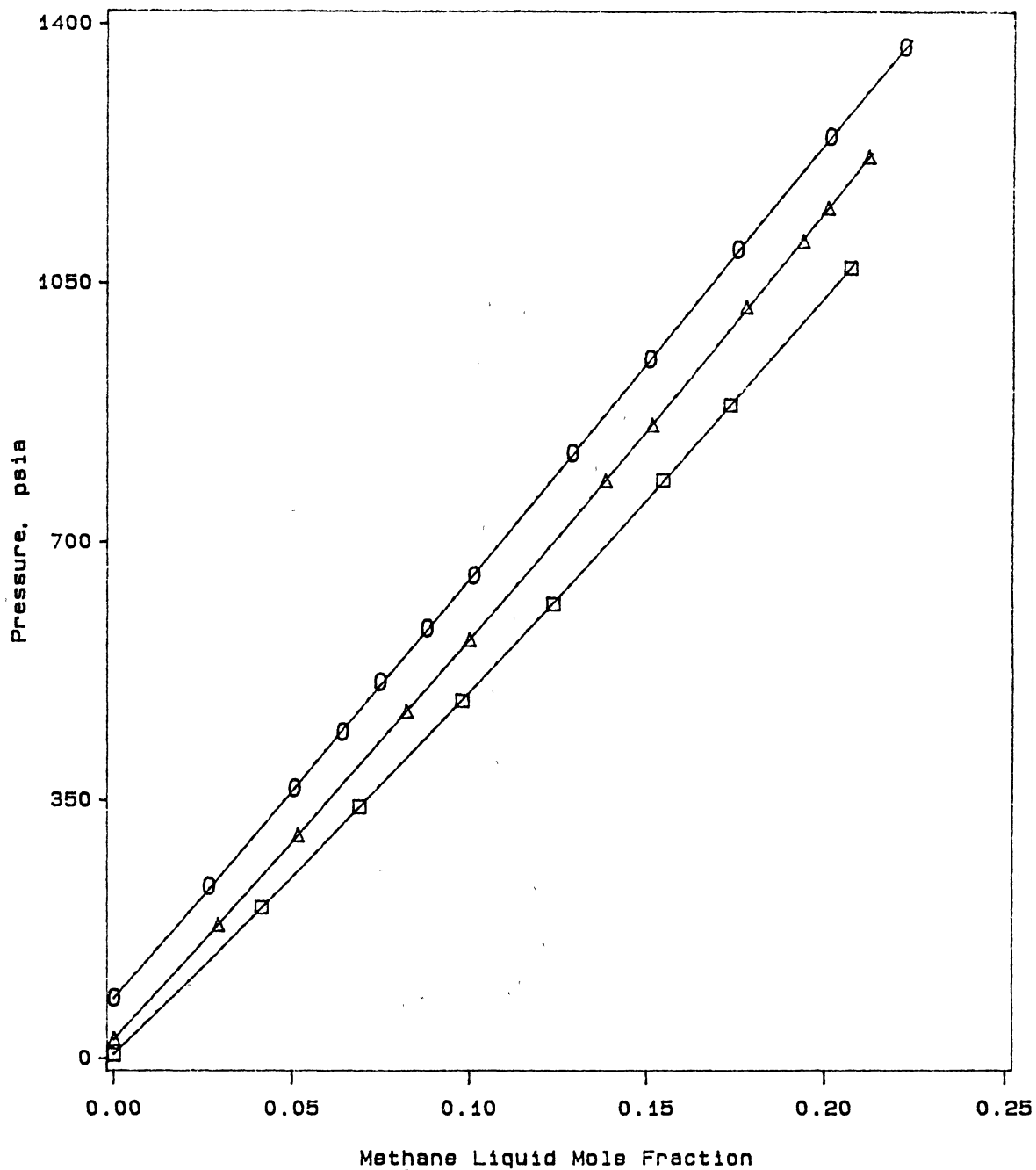
Figure 1

Bubble Point Pressure Data for Methane + Cyclohexane
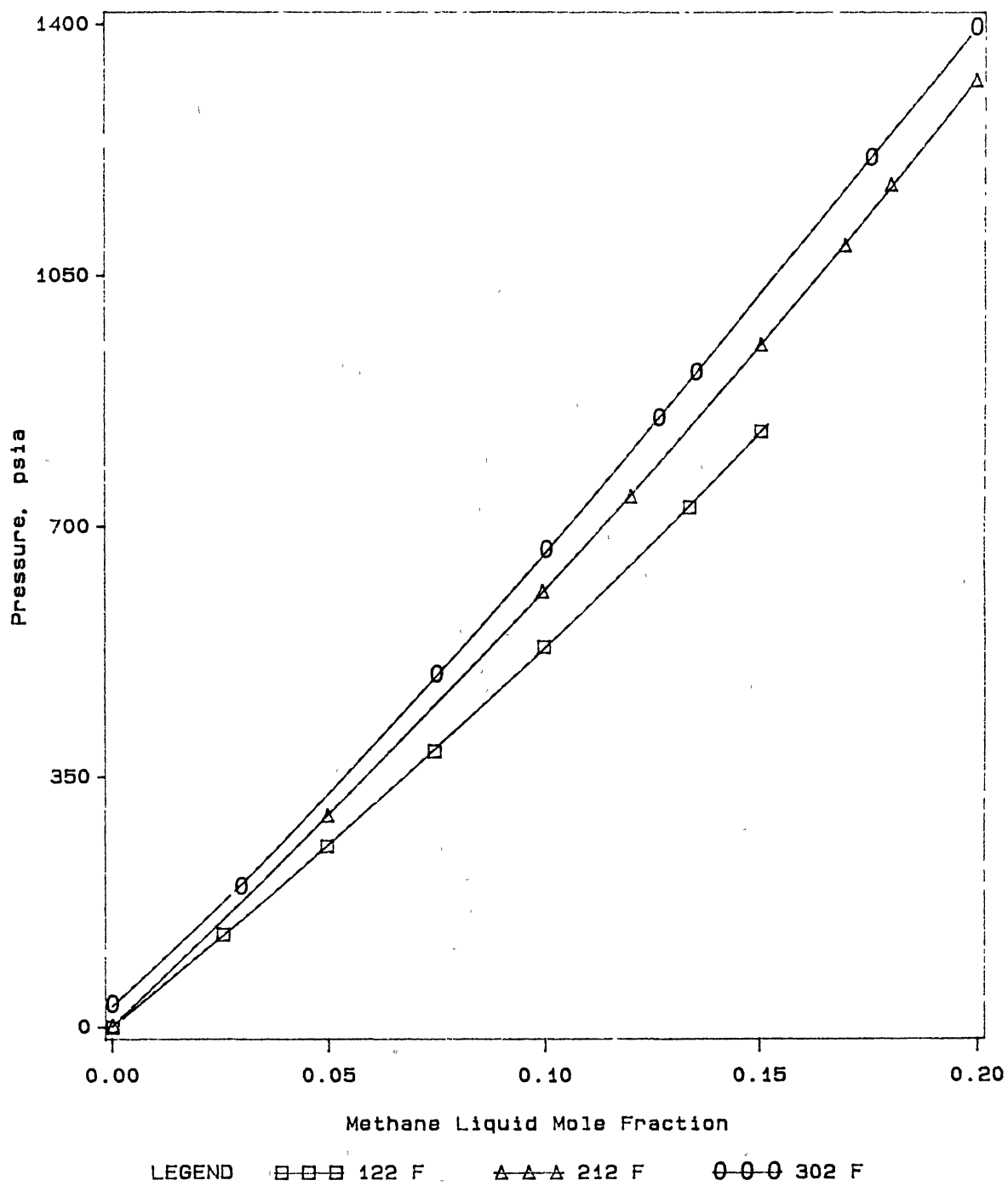
Figure 2

Bubble Point Pressure Data for Methane + t—Decalin
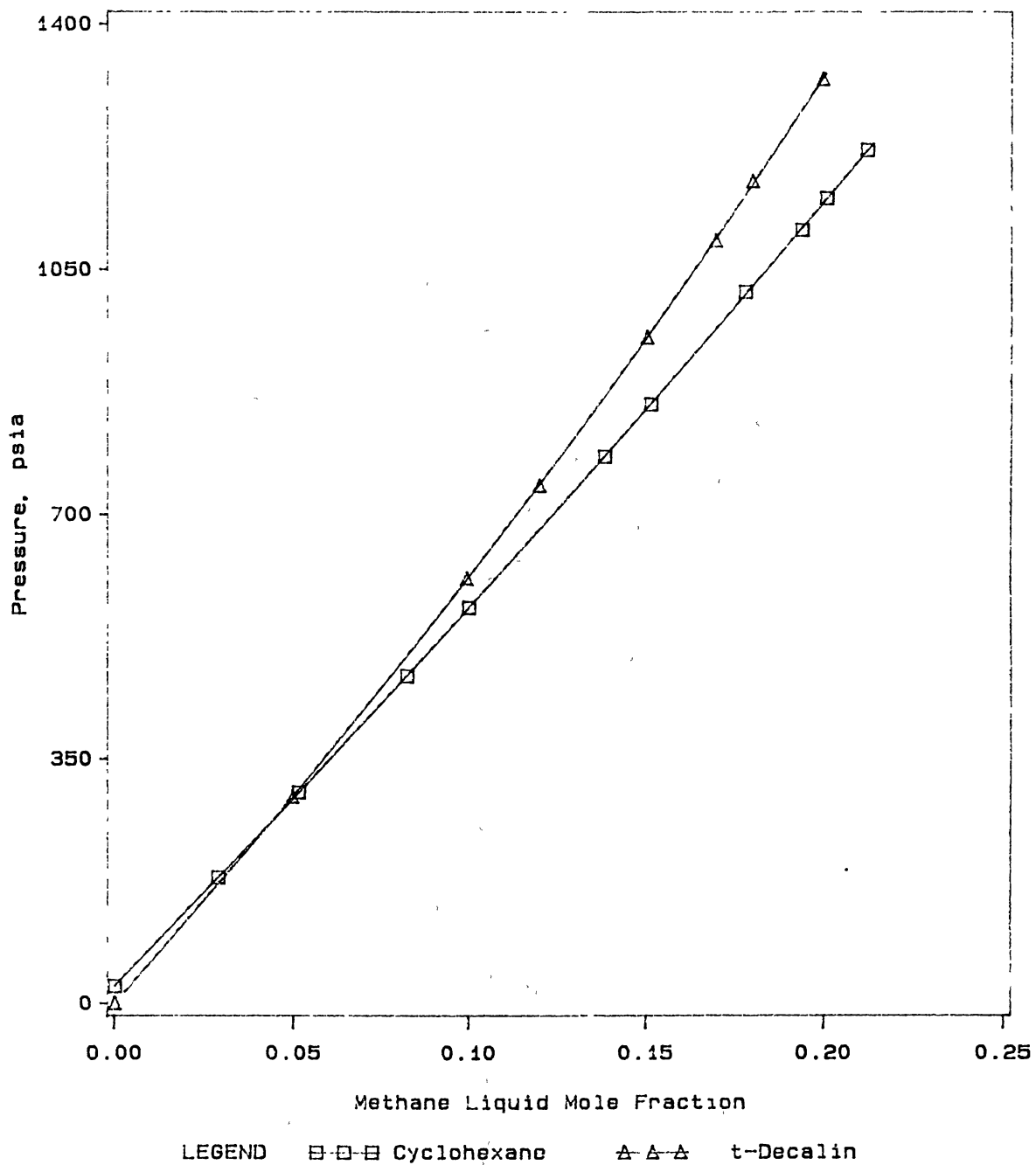
Figure 3

Bubble Point Pressure Data for Methane + Cyclohexane and
Methane + t-Decalin at 212 F
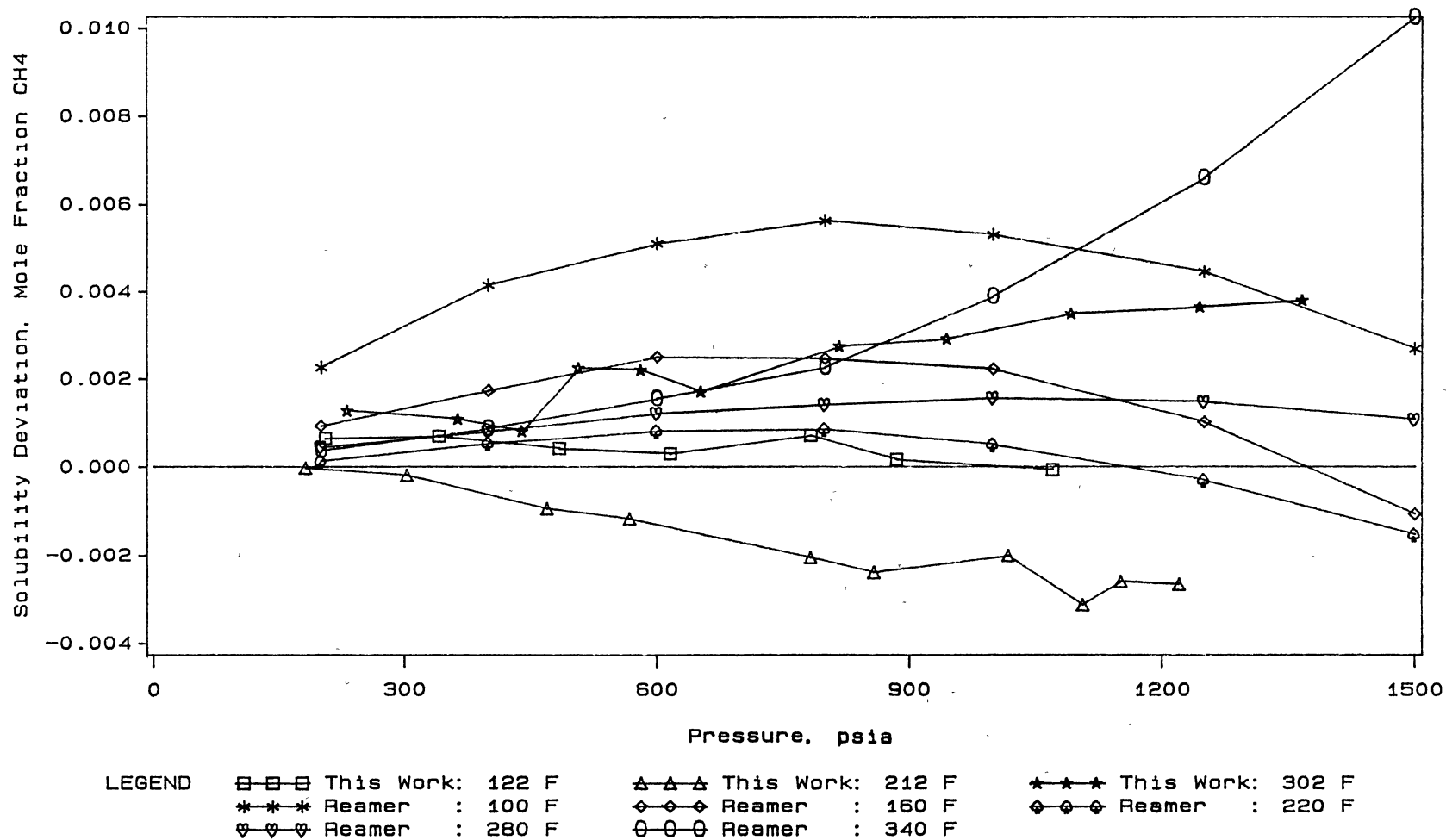
Figure 4.

Comparison of Methane Solubilities in Cyclohexane
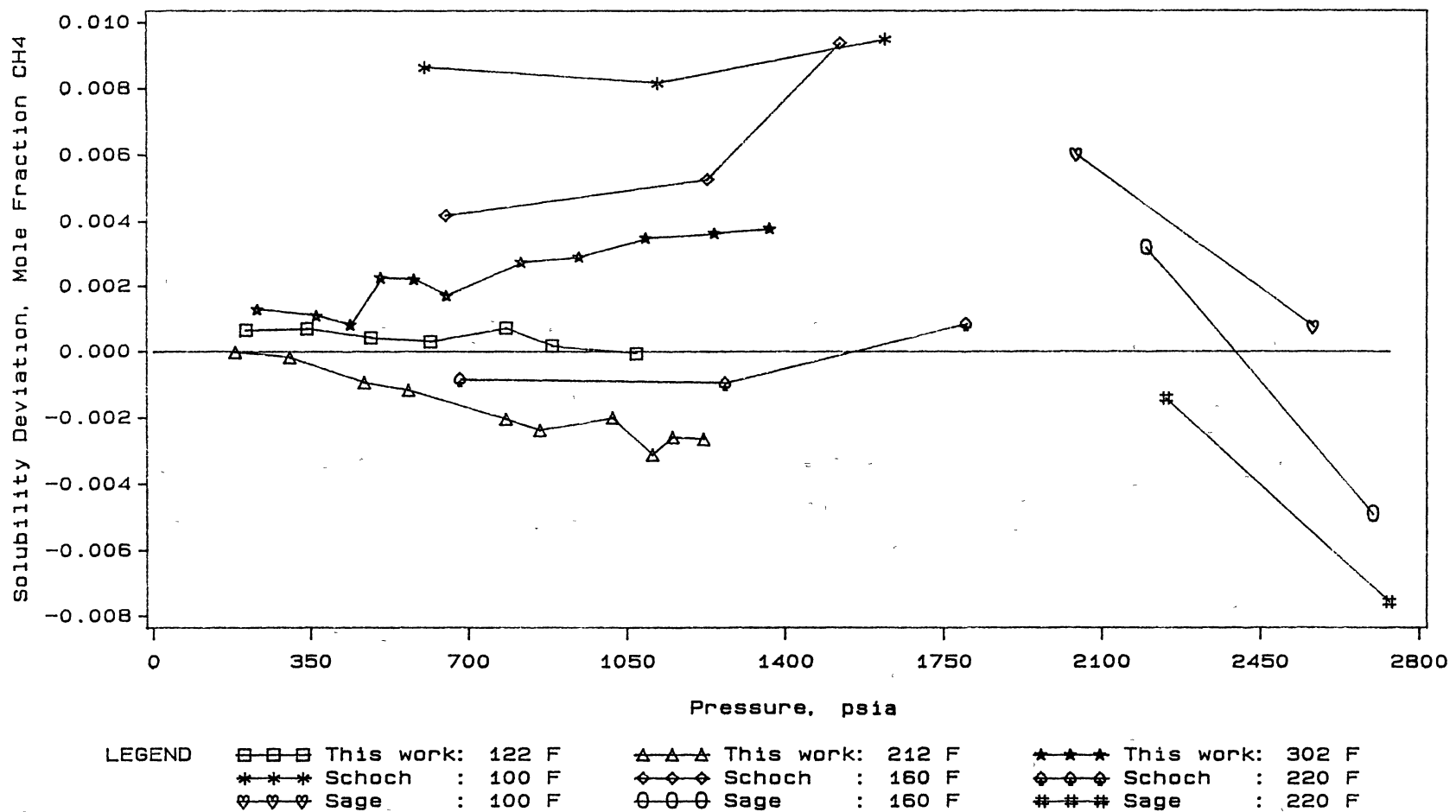
Figure 5.

Comparison of Methane Solubilities in Cyclohexane Using Lumped Parameters of This Work
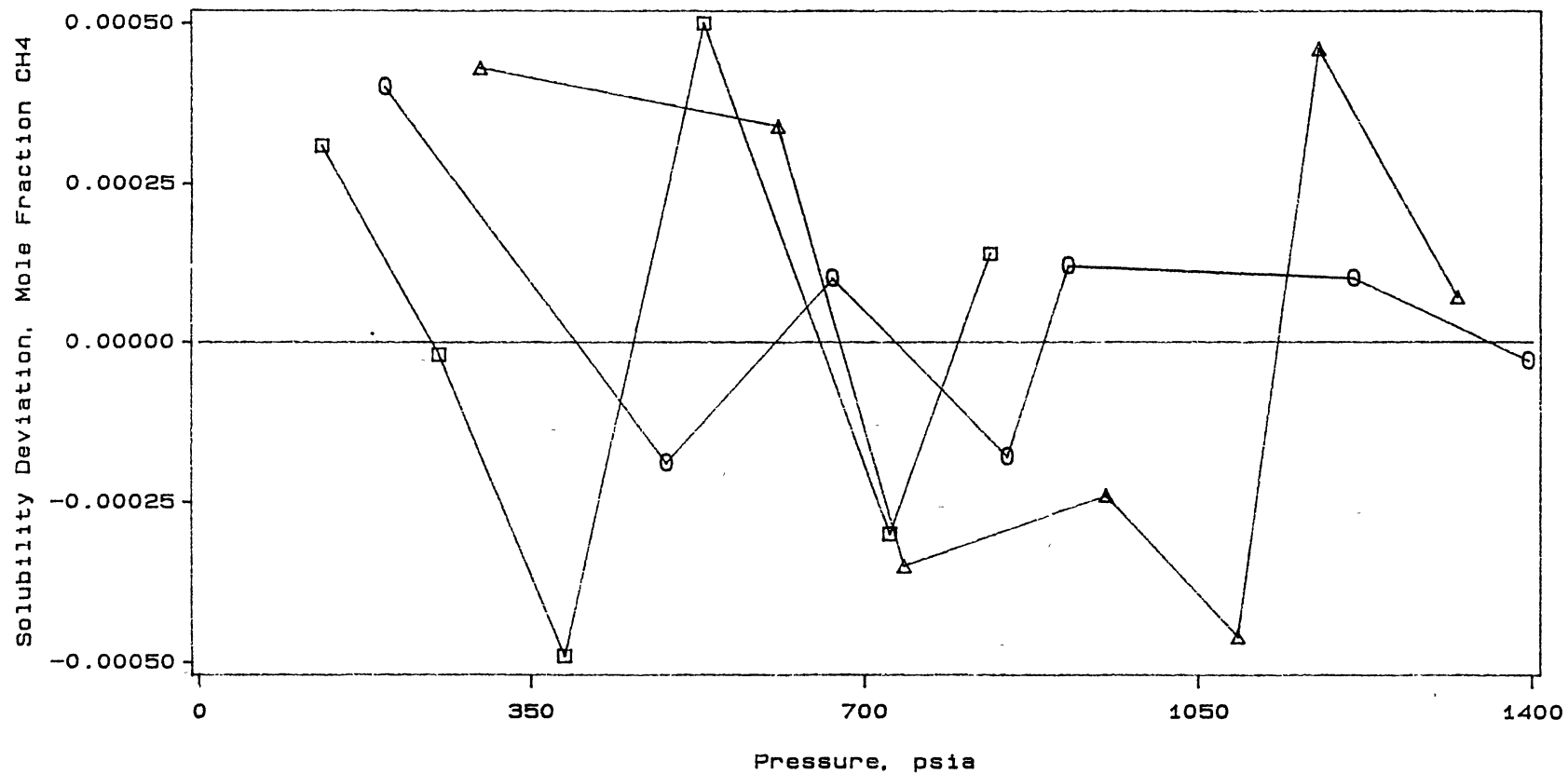
Figure 6.

Comparison of Methane Solubilities in t—Decalin
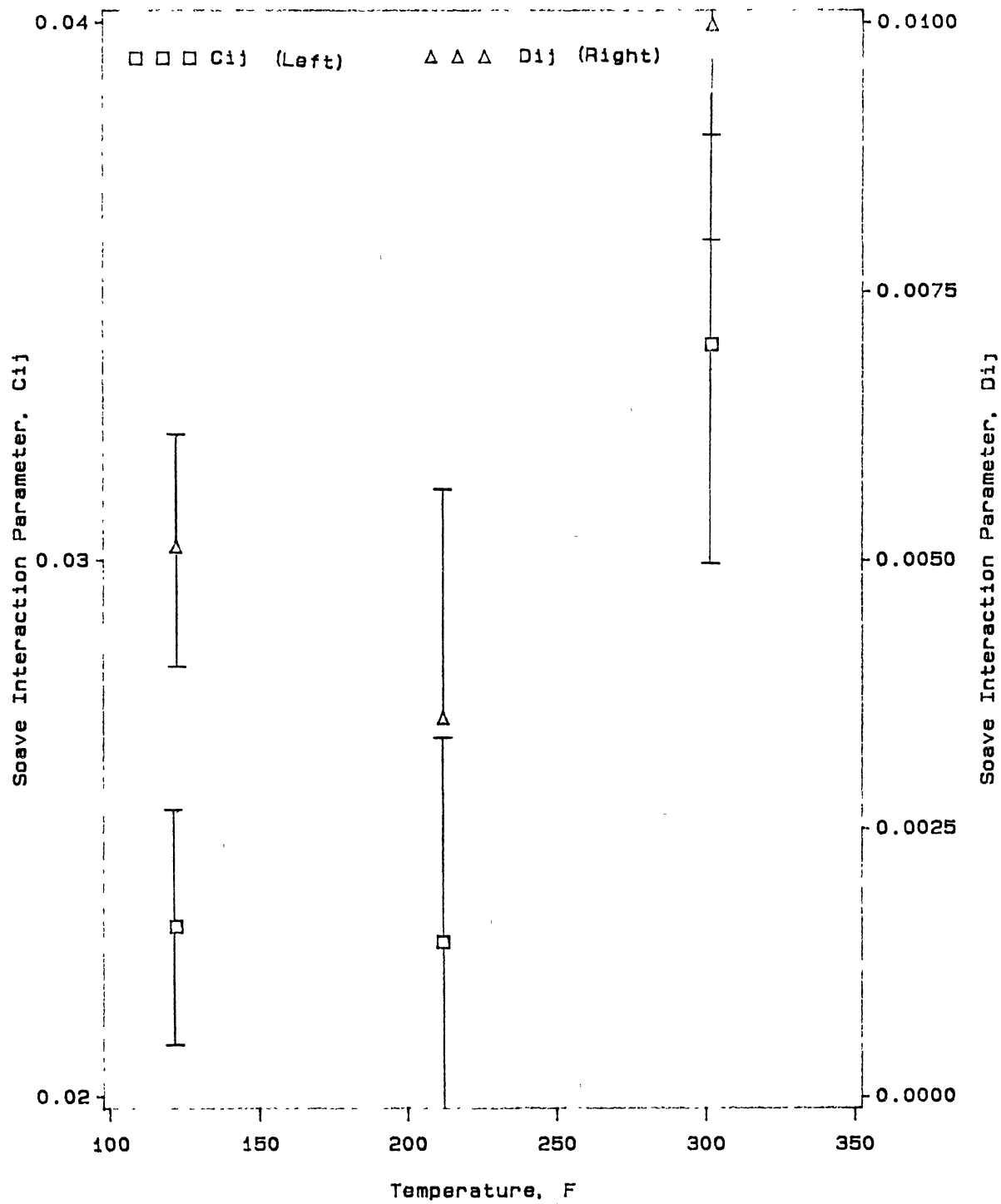
Figure 7

Soave Interaction Parameters, Cij and Dij ,for Methane + Cyclohexane
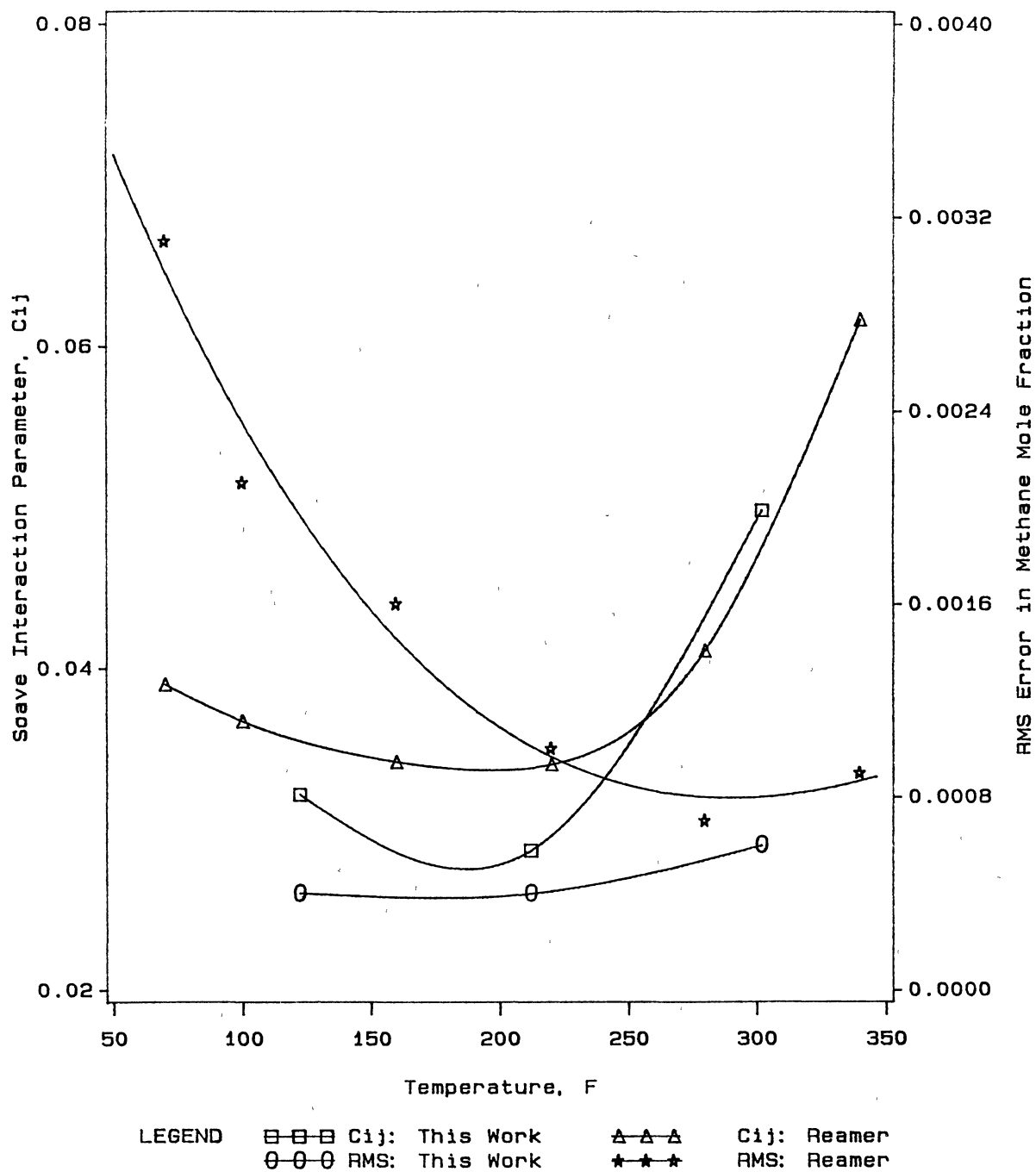
Figure 8

Soave Interaction Parameter, Cij, and Corresponding
RMS Errors for Methane + Cyclohexane
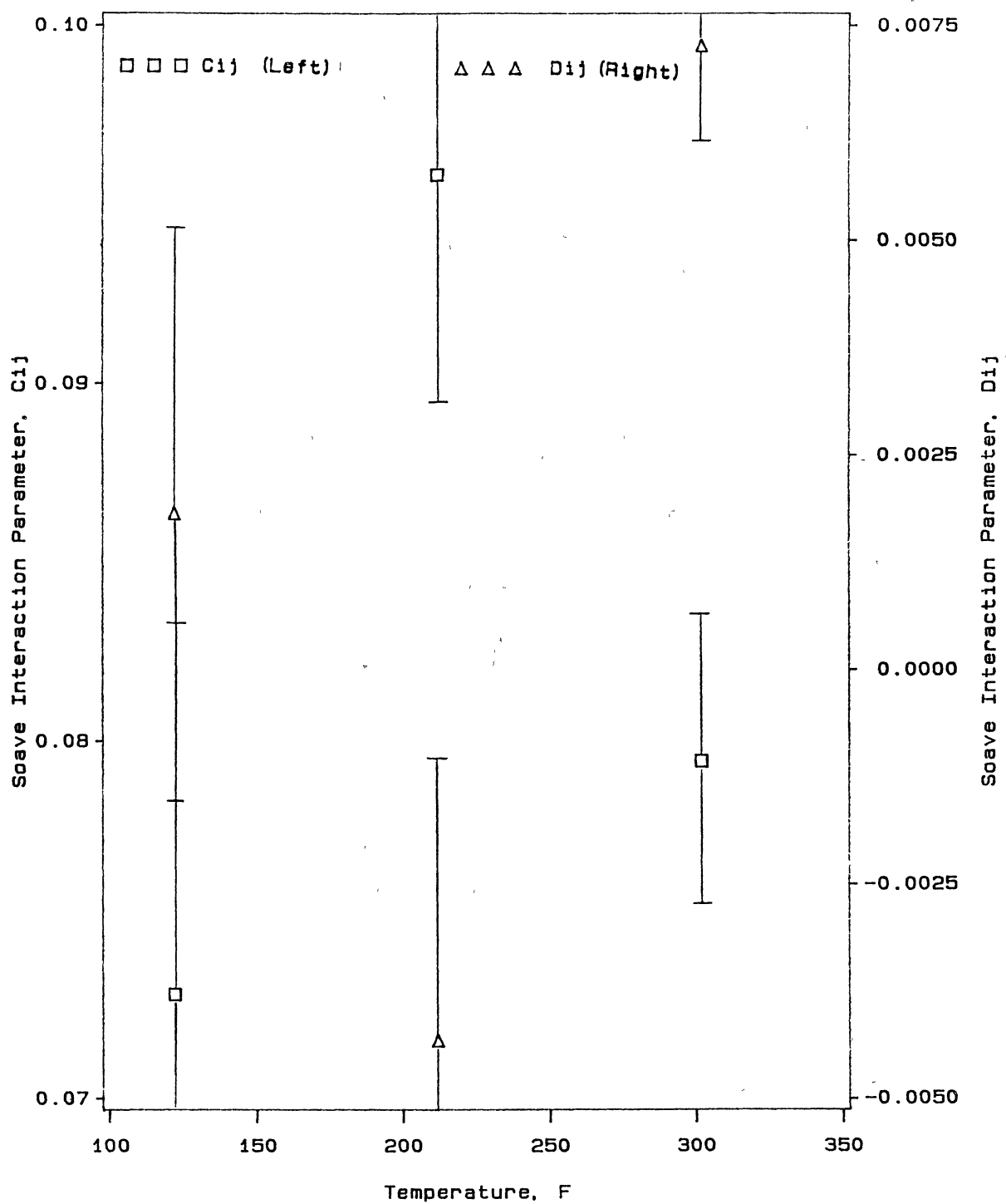
Figure 9

Soave Interaction Parameters, Cij and Dij ,for Methane + t—Decalin
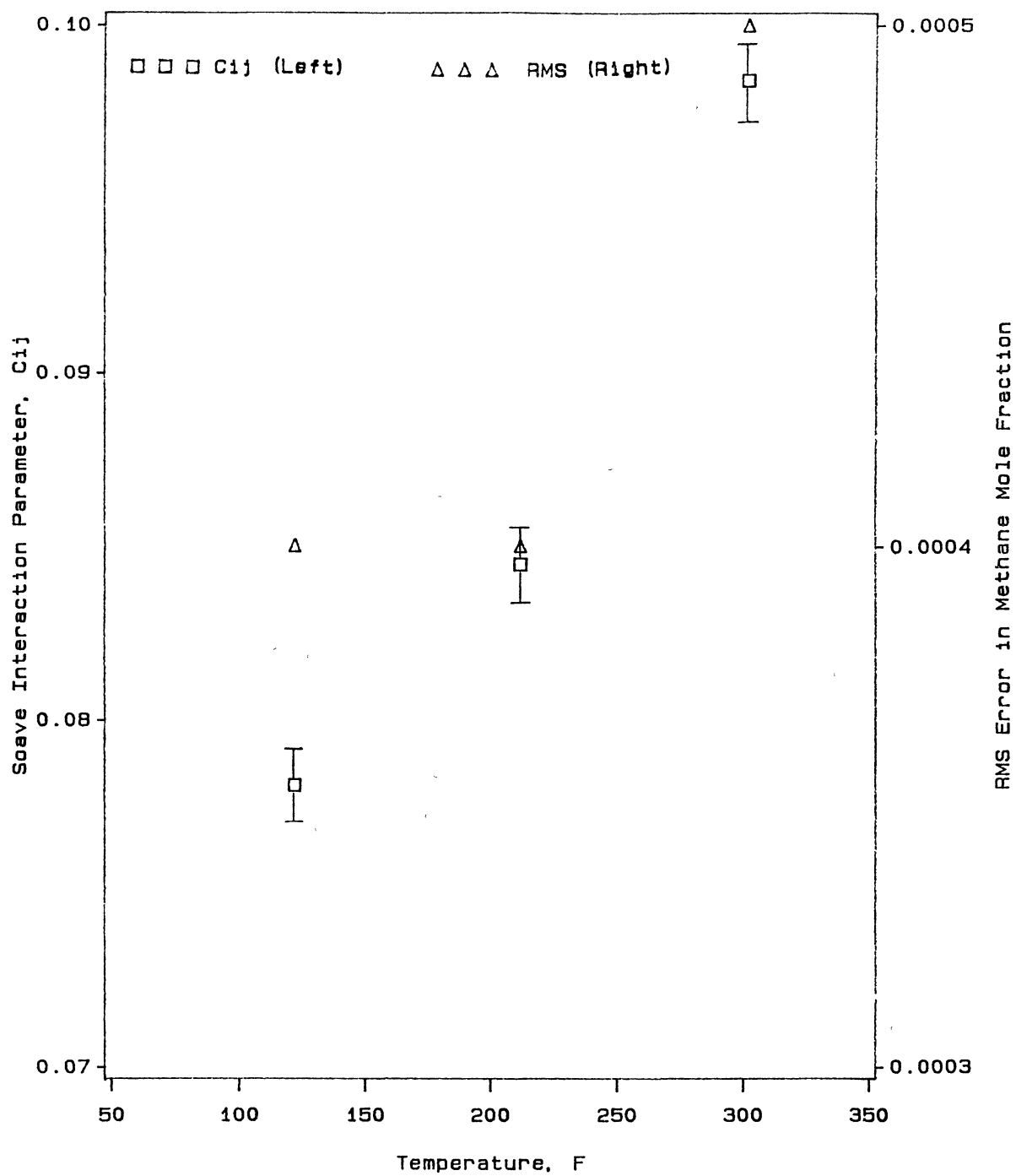
Figure 10

Soave Interaction Parameter, Cij, and Corresponding
RMS Errors for Methane + t—Decalin
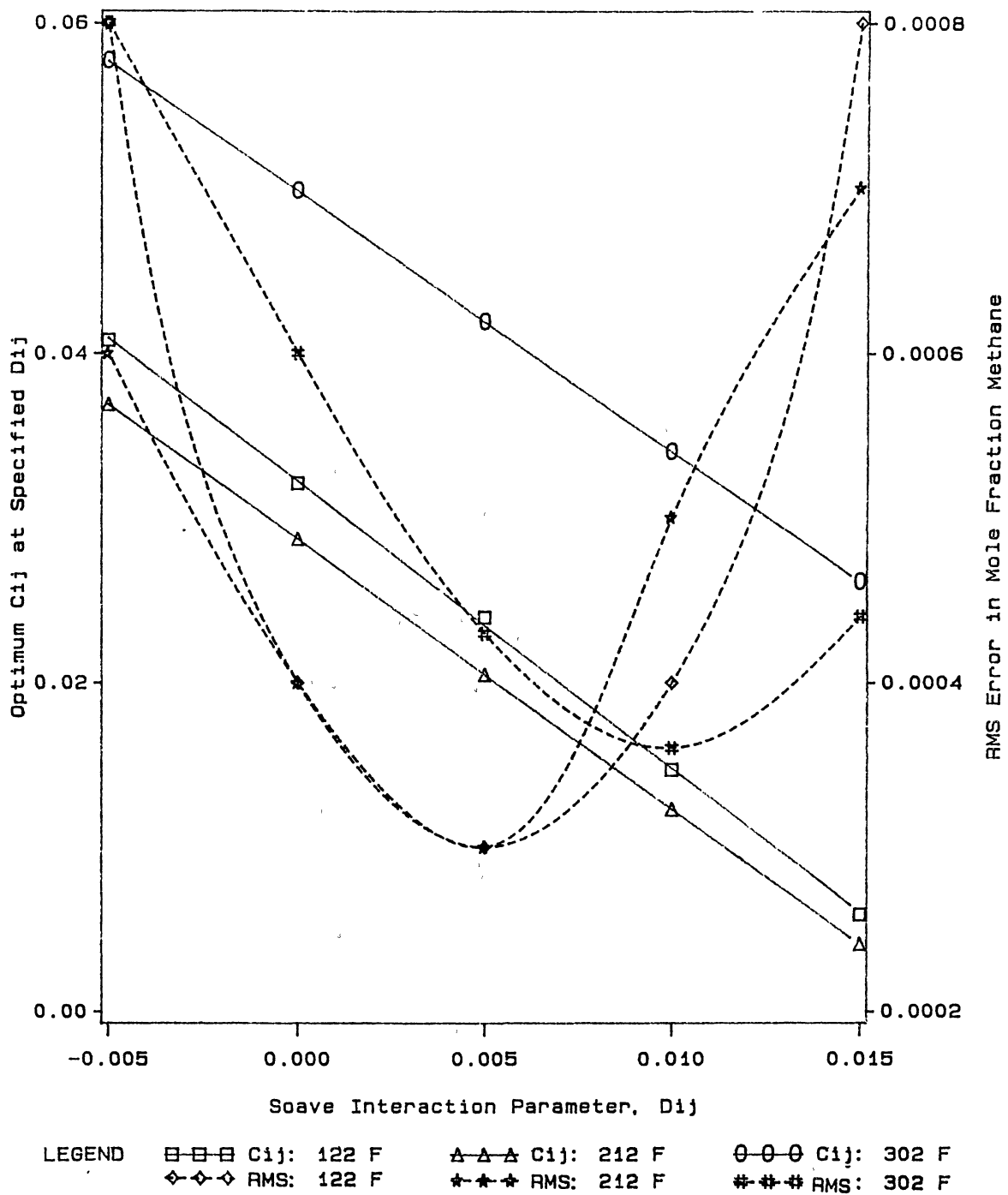
Figure 11.

Sensitivity of Optimized Cij and Corresponding RMS Errors in Mole Fraction
to Dij for Methane + Cyclohexane
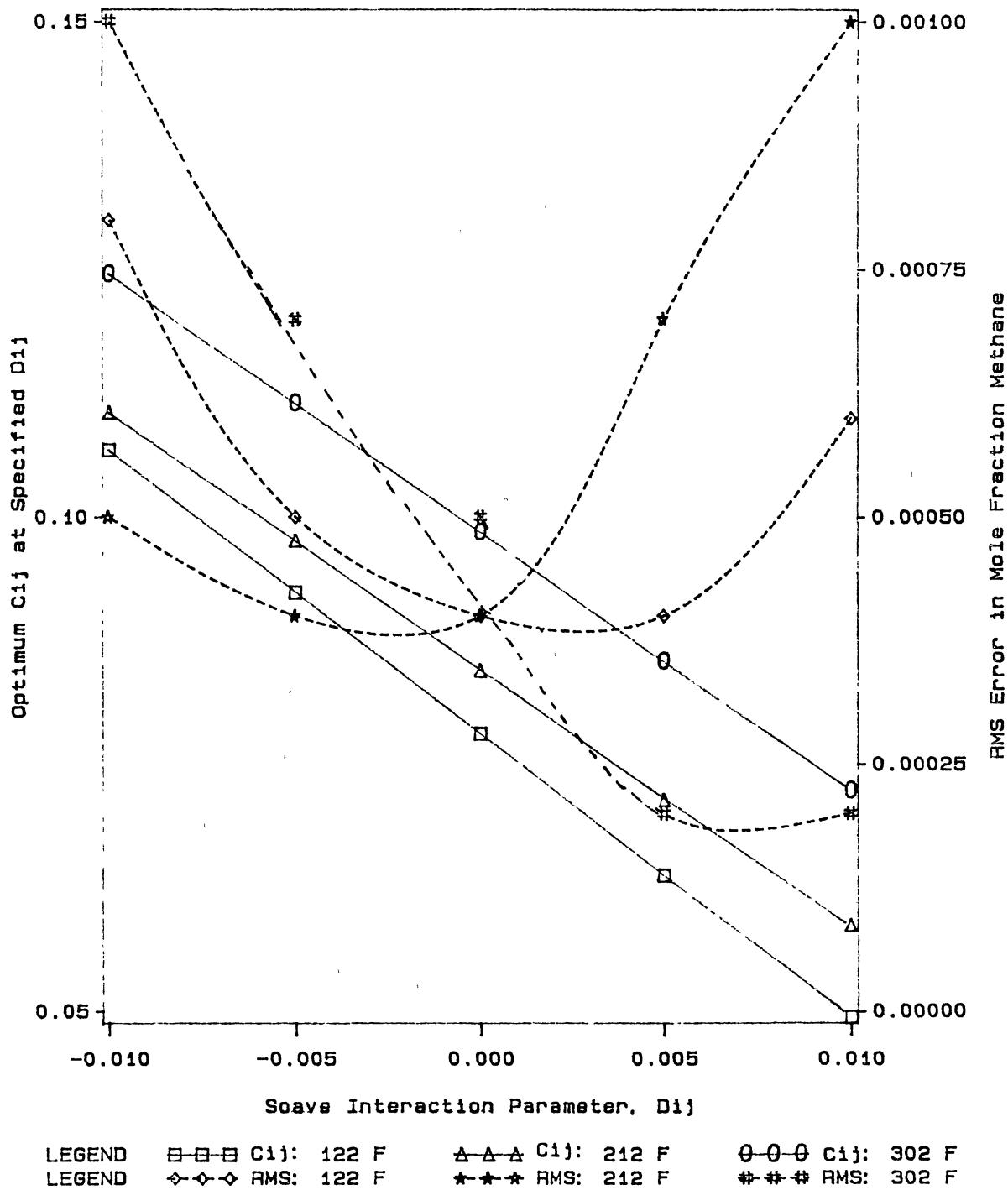
Figure 12.

Sensitivity of Optimized Cij and Corresponding RMS Errors in Mole Fraction
to Dij for Methane + t—Decalin
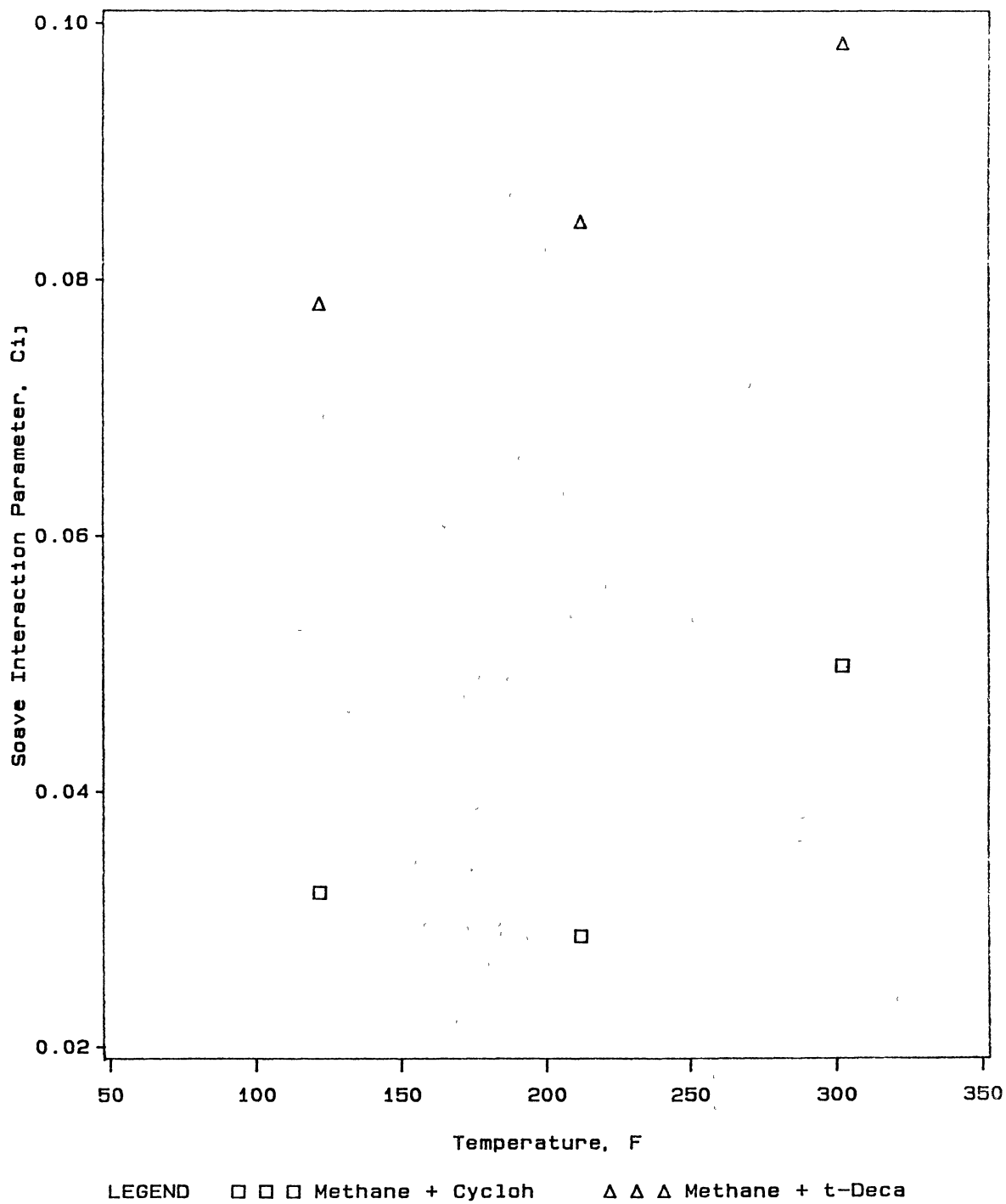
Figure 13

Soave Interaction Parameter, Cij, for Methane + Cyclohexane
and Methane + t—Decalin

CHAPTER VIII

BINARY VAPOR-LIQUID PHASE EQUILIBRIUM FOR
METHANE + AROMATIC SOLVENTS

Abstract

Binary solubility data are presented for methane in four aromatic hydrocarbons at temperatures from 323 to 433 K (122 to 320°F) and pressures to 113 bar (1640 psia). The solvents studied are benzene, naphthalene, phenanthrene and pyrene. Data for methane + benzene are in reasonable agreement with the earlier measurements of Sage. Excellent agreement is observed between our data and those of Malone for methane + phenanthrene. The new data can be described with RMS errors of 0.001 in mole fraction by the Soave-Redlich-Kwong (SRK) and Peng-Robinson (PR) equations of state when one interaction parameter is used over the complete temperature range for each of the systems studied. Henry's constants and partial molar volumes at infinite dilution are evaluated from the data using the Krichevsky-Kasarnovsky equation.

134

Introduction

The global energy situation has prompted increasing efforts to investigate alternative forms of liquid fuels such as coal derived syncrudes. Multiple phases are present in essentially all stages of feed preparation, conversion reactions, and product separation. For example, during the initial stages of coal dissolution in a coal-derived recycle solvent, many light gases are produced (e.g., CH_4, CO, CO_2, H_2S, H_2O, NH_3, and C_2-C_5) [1]. The effective design and operation of such conversion processes require accurate knowledge of the phase behavior of the fluid mixtures encountered. Studies of the solubilities of light gases in heavy hydrocarbons are also of interest in the processing of petroleum products, enhanced oil recovery and supercritcal fluid processes. Moreover, such studies are essential in the development and evaluation of solution theories.

Previously, we have reported and analyzed data on the solubility of carbon dioxide and ethane in a series of heavy hydrocarbons [2-6]. We have also recently completed an experimental study on the solubility of methane in a series of hydrocarbon solvents (paraffins, naphthenes, and aromatics). Data on methane solubilities in heavy normal paraffins and in naphthenes have been reported previously [7]. In the present work, solubility data for methane in binary systems with benzene, naphthalene, phenanthrene and pyrene are presented and correlated using the SRK [8] and PR [9] equations of state. Solubilities were measured at

temperatures from 311 to 423 K (122 to 320°F) and pressures to 113 bar (1640 psia). These data complement the available literature data and should prove useful in the development and testing of correlations describing the phase behavior of multicomponent systems involving methane.

Experimental Section

Apparatus and Procedure

The experimental apparatus used in this study is a modified version of the apparatus used by Raff [6]. A detailed description of the apparatus and the experimental procedure is given elsewhere [7].

Estimated uncertainties in experimental measurements are 0.1 K in temperature and less than 0.001 in mole fraction. The uncertainty in the measured bubble point pressure depends on the steepness of the p-x relation and is of the order of 0.35 bar (5 psia) for methane + benzene and 0.70 bar (10 psia) for the binary mixtures of methane in naphthalene, phenanthrene, and pyrene [7].

Materials

The methane had a stated purity of 99.97+ mol% and was supplied by Matheson. Benzene was supplied by J. T. Baker Chemical company and had a purity of 99.8+ mol%. Naphthalene, phenanthrene and pyrene were from Aldrich Chemical Company with quoted purities of 99+, 98+, and 99+ mol%, respectively. No further purification of the chemicals was attempted.

Results and Discussion

The experimental results appear in Tables I-IV. Differences in the lowest temperatures at which the systems were studied were dictated by the melting points of the solvents, which are solids at room temperature (except for benzene).

The experimental data are correlated using the SRK [8] and PR [9] cubic equations of state. Optimum binary interaction parameters were obtained by minimizing the sum of squares of pressure deviations from the experimental values. Detailed procedure for data reduction is given by Gasem [10]. The input parameters of the pure components (acentric factors, critical temperatures and critical pressures) required by the SRK and PR equations of state, together with the literature sources, are presented in Table V.

Figures 1 and 2 show the effects of temperature and pressure on methane solubility (liquid phase mole fraction of methane) . The solubility of methane in these aromatic hydrocarbons exhibits very weak dependence on temperature as Figure 2 reveals for the solubility of methane in naphthalene and phenanthrene.

Figure 3 shows that the Soave interaction parameter, C_{ij}, for these systems is relatively insensitive to temperature. Figure 4 shows the effect of chemical structure on the lumped Soave interaction parameter, C_{ij}, (i.e., when a single value for C_{ij} is used over the complete temperature range of each system). A linear dependence of C_{ij} on the

chemical structure is observed. However, the values of the interaction parameter, C_{ij}, are strongly influenced by the critical properties employed in the EOS prediction. For example, when the value of the acentric factor of pyrene was taken as 0.344 (as reported in Ref. 23) the optimum C_{ij} was found to be 0.41 as compared to C_{ij} of 0.15 for an acentric factor of 0.83 used in this study [24]. Nonlinear dependence of C_{ij} on chemical structure was noticed for ethane and CO_2 in the same solvents suggesting that this variation may be a result of the pure-substance parameters used in the EOS (in particular those parameters which must be estimated).

Equation-of-state representations of the solubilities for the systems under study are documented in Tables VI-IX. In general, the SRK and PR equations are capable of describing the data with RMS errors of 0.0005 in mole fraction when a single interaction parameter, C_{ij}, is used over the complete temperature range. Methane + benzene is an exception; the RMS error is 0.0013 in mole fraction. For methane solubility in benzene, improved equation-of-state predictions are realized (RMS = 0.0008) when an additional parameter, D_{ij}, is used, as indicated by results given in Table VI.

Comparisons of our results with those of various investigators appear in Figures 5-9. The comparisons are shown in terms of deviations of the solubilities from values predicted using the SRK [8] equation of state. Interaction parameters, C_{ij} or C_{ij} and D_{ij}, employed in the equation-of-

state predictions were obtained by fitting our data over the complete temperature range of the system under study. The comparisons for the methane + benzene system are shown in Figures 5 and 6.

Reasonable agreement (solubility deviations are within 0.004) is observed between our result and those of Lin, et al. [11] at 298°F (Figure 5). The best agreement observed is between the results of this work and those Sage, et al. [12] at 160 (Figure 6), where the solubility deviations are within 0.001. However, significant disagreement with Elbishlawi and Spencer [13], Legret, et al. [14], and Schoch, et al. [15] are seen in both figures.

Figures 7 and 8 show comparisons for methane + phenanthrene. These comparisons are shown in terms of both solubility deviations (Figure 7) and pressure deviations (Figure 8). Interaction parameters employed in the equation-of-state solubility prediction were obtained by fitting the data of Malone and Kobayashi [16], since their data cover a wider range of pressures than do ours. The agreement between the two data sets is excellent. The maximum pressure deviation is shown to be within 10 psia, which is within the experimental error of the measured bubble point pressure [7]. Comparable solubility differences (Figure 7) are no greater than 0.0005.

For methane + naphthalene and methane + pyrene, no previous data are available for comparisons. The ability of the SRK and PR equations of state to precisely represent

these data is illustrated by Figures 9-11. The low scatter in pressure and solubility deviations illustrate the high precision of the present data.

Krichevsky-Kasarnovsky Analysis

In the range of methane mole fractions reported in this study, the binary solubilities of methane in naphthalene, phenanthrene and pyrene are represented within 0.0002 mole fraction by the Krichevsky-Kasarnovsky (KK) equation [17] (variables are explained in the "List of Symbols"):

$$\ln(f_{CH_4}/x_{CH_4}) = \ln(H_{CH_4,P_{HC}}) + (v_{CH_4}/RT)(P-P_{HC}) \qquad (1)$$

Values of the methane fugacity, f_{CH_4}, required for the KK equation were obtained using Bender's equation of state for methane [18], since the vapor is essentially pure methane. The solubility data of methane + benzene were excluded from this analysis because of the appreciable vapor pressures of benzene at the reported temperatures.

The Henry's constants and the infinite-dilution partial molar volumes of methane regressed from solubility data of this work and other investigators, using equation 1 above, are presented in Table X and Figures 12 and 13. The standard deviation of any optimized parameters (Whenever of adequate magnitude to be shown) is shown on the figures. Henry's constants of this work agree, within 5 bars, with those of Malone [16] (Figure 12). Also, the partial molar volumes regressed from the solubility data of this work and

Malone [16] are within the reported uncertainty as Figure 13 shows. Care, however, should be exercised in attributing physical significance to these results, in particular the partial molar volumes which are known to be less accurate than the corresponding Henry's constants.

Conclusions

Data have been obtained for the solubility of methane in each of the aromatic solvents benzene, naphthalene, phenanthrene, and pyrene at temperatures from 323 to 433 K (122 to 320°F) and pressures to 112 bar (1640 psia). These data are well described by the Soave-Redlich-Kwong and Peng-Robinson equations of state and by the Krichevsky-Kasarnovsky equation. These results will be of value in establishing equation-of-state interaction parameters for light gases in heavy hydrocarbon solvents.

List of Symbols

C_{ij}, D_{ij}	interaction parameters between components i and j in mixing rules for equation of state
f_{CH_4}	fugacity of methane in the liquid (or vapor) phase
p	pressure
P_{HC}	hydrocarbon vapor pressure
H_{CH_4}, P_{HC}	Henry's constant of methane
R	universal gas constant
T	temperature
V_{CH_4}	infinite dilution partial molar volume of methane
x	liquid phase mole fraction (solubility) of methane

References

1. Hensen, B. J.; Tarrer, A. R.; Curtis, C. W.; Guin, J., Ind. Eng. Chem. Proc. Des. Dev., 21, 575-579 (1982).

2. Robinson, R. L., Jr.; Anderson, J. M.; Barrick, M. W.; Bufkin, B. A.; Ross, C. H., " Phase behavior of Coal Fluids: Data for Correlation Development," DE-FG22-86PC90523, Final Report, Department of Energy, January (1987).

3. Gasem, K. A. M.; Robinson, R. L., Jr., J. Chem. Eng. Data, 30, 53-56 (1985).

4. Anderson, J. M.; Barrick, M. W.; Robinson, R. L., Jr., J. Chem. Eng. Data, 31, 172-175 (1986).

5. Gasem, K. A. M.; Bufkin, B. A.; Raff, A. M.; Robinson, R. L., Jr., J. Chem. Eng. Data, 34, 187-191 (1989).

6. Raff, A. M., M.S. Thesis, Oklahoma state University, Stillwater, Oklahoma (1989).

7. Darwish, N. A., Ph.D. Dissertation, Oklahoma State University, Stillwater, Oklahoma (1991).

8. Soave, G., Chem. Eng. Sci., 27, 1197-1203 (1972).

9. Peng, Y. D.; Robinson, D. B., Ind. Eng. Chem. Fundam., 15, 59-64 (1976).

10. Gasem, K. A. M., Ph.D. Dissertation, Oklahoma State University, Stillwater, Oklahoma (1986).

11. Lin, H.-M.; Sebastian, H. M.; Simnick, J. J.; Chao, K. C., J. Chem. Eng. Data, 24, 146-149 (1979).

12. Sage, B. H.; Webester, D. C.; Lacey, W. N.; Ind. Eng. Chem., 28, 1045-1047 (1936).

13. Elbishlawi, M.; Spencer, J. R., Ind. Eng. Chem., 43, 1811-1815 (1951).

14. Legret, D.; Richon, D.; Renon, H., J. Chem. Eng. Data, 27, 165-169 (1982).

15. Schoch, E. P.; Hoffman, A. E.; Kasperik, A. S.; Lightfoot, J.H.; Mayfield, F. D., Ind. Eng. Chem., 32, 788-791 (1940).

16. Malone, P. V.; Kobayashi, R., Fluid Phase Equilibria, 55, 193-205 (1990).

17. Krichevsky, I. R.; Kasarnovsky, J. S., J. Am. Chem. Soc., 57, 2168-2171 (1935).

18. Sievers, U.; Schulz, S., Fluid Phase Equilibria, 5, 35-54 (1980).

19. Goodwin, R. D., "The Thermophysical Properties of Methane from 90 to 500 K at Pressures to 700 Bar", NBS Technical Note 653, 22, April (1974).

20. "Engineering Data Book", 9th Edition, Gas Processors Suppliers Associations, Tulsa, (1972).

21. Reid, R. C.; Prausnitz, J. M.; Sherwood, T. K., "The Properties of Gases and Liquids", 2nd Edition, New York: McGraw-Hill Book Company (1977).

22. API Monograph Series. Anthracene and Phenanthrene. Washington D.C.: American Petroleum Institute. Monograph No. 708, January (1979).

23. API Monograph Series. Four-Ring Condensed Aromatic Compounds. Washington D.C.: American Petroleum Institute. Monograph No. 709, March (1979).

24. Turek, E. A., Amoco Production Company, Tulsa, Oklahoma, Personal Communication (1988).

List of Tables

List of Figures

Table I

Solubility Data for Methane in Benzene

Mole Fraction Methane	Bubble Point Pressure bar	(psia)
	323.2 K (50.0°C, 122.0°F)	
0.028	14.6	(212)
0.053	28.0	(407)
0.075	39.7	(576)
0.114	61.4	(891)
0.119	64.0	(929)
0.134	72.3	(1049)
0.149	81.1	(1177)
0.167	90.9	(1318)
	373.2 K (100.0°C, 212.0°F)	
0.029	17.3	(250)
0.039	22.6	(327)
0.061	34.2	(496)
0.075	42.1	(611)
0.100	55.6	(806)
0.126	69.8	(1012)
0.152	84.8	(1230)
0.164	91.4	(1326)

Table I (Continued)

Solubility Data for Methane in Benzene

Mole Fraction Methane	Bubble Point Pressure bar	(psia)
423.2 K (150.0°C, 302.0°F)		
0.029	20.5	(297)
0.032	22.2	(321)
0.055	34.2	(496)
0.074	43.8	(636)
0.103	59.2	(859)
0.115	65.3	(946)
0.145	80.9	(1174)
0.151	84.6	(1227)

Table II

Solubility Data for Methane in Naphthalene

Mole Fraction Methane	Bubble Point Pressure bar	(psia)
373.2 K (100.0°C, 212°F)		
0.025	19.6	(284)
0.030	24.0	(349)
0.050	40.6	(590)
0.064	53.0	(769)
0.086	73.5	(1065)
0.100	86.9	(1260)
423.2 K (150.0°C, 302.0°F)		
0.024	19.4	(281)
0.031	24.8	(360)
0.045	36.4	(528)
0.060	49.3	(715)
0.075	62.5	(907)
0.100	84.8	(1229)

Table III

Solubility Data for Methane in Phenanthrene

Mole Fraction Methane	Bubble Point Pressure bar	(psia)
383.2 K (110.0°C, 230.0°F)		
0.020	20.4	(296)
0.030	31.6	(458)
0.044	48.3	(700)
0.060	67.3	(977)
0.071	81.7	(1185)
0.090	107.1	(1553)
423.2 K (150.0°C, 302.0°F)		
0.021	21.5	(312)
0.030	31.3	(454)
0.045	48.6	(705)
0.060	66.2	(960)
0.074	84.2	(1221)
0.090	104.6	(1517)

Table IV

Solubility Data for Methane in Pyrene

Mole Fraction Methane	Bubble Point Pressure bar	(psia)
433.2 K (160.0°C, 320°F)		
0.020	23.5	(341)
0.035	42.3	(614)
0.049	60.4	(875)
0.060	75.8	(1099)
0.070	89.7	(1301)
0.075	97.1	(1408)
0.086	113.0	(1639)

Table V.

Critical Properties and Acentric Factors used in the SRK and PR Equations of State

Component	Pressure (bar)	Temperature (K)	Acentric Factor	Reference
Methane	46.60	190.5	0.011	19
Benzene	48.98	561.7	0.225	20
Naphthalene	41.14	748.4	0.315	21
Phenanthrene	33.0	873.2	0.540	22
Pyrene	26.0	938.2	0.830[a]	23

[a] Ref. 24

Table VI

SRK and PR Equation-of-State Representations of Solubility of Methane in Benzene

Temperature K (°F)	Soave Parameters (P-R Parameters) C_{12}	D_{12}	Error in Mole Fraction* (Error in Pressure,bar) RMS	MAX
323.2 (122.0)	0.033 (0.036)	0.022 (0.027)	0.0002 (0.12)	0.0004 (0.23)
	0.073 (0.083)		0.0010 (0.63)	0.0017 (1.27)
373.2 (212.0)	0.026 (0.031)	0.023 (0.026)	0.0001 (0.04)	0.0001 (0.06)
	0.067 (0.074)		0.0009 (0.51)	0.0012 (0.72)
423.2 (302.0)	0.037 (0.039)	0.017 (0.019)	0.0002 (0.12)	0.0004 (0.23)
	0.067 (0.070)		0.0005 (0.26)	0.0008 (0.44)
323.2, 373.2 423.2	0.024 (0.019)	0.026 (0.035)	0.0008 (0.45)	0.0014 (0.77)
	0.071 (0.079)		0.0013 (0.74)	0.0029 (1.72)

* Errors are essentially identical for the SRK and PR EOS

Table VII

SRK and PR Equation-of-State Representations of Solubility of Methane in Naphthalene

Temperature K (°F)	Soave Parameters (P-R Parameters) C_{12}	D_{12}	Error in Mole Fraction* (Error in Pressure, bar) RMS	MAX
373.2 (212.0)	0.103	0.000	0.0002 (0.18)	0.0004 (0.30)
	(0.101)	(0.005)		
	0.104		0.0002 (0.18)	0.0003 (0.29)
	(0.117)			
423.2 (302.0)	0.073	0.009	0.0001 (0.10)	0.0002 (0.17)
	(0.077)	(0.012)		
	0.101		0.0002 (0.19)	0.0003 (0.29)
	(0.111)			
373.2, 423.2	0.093	0.003	0.0003 (0.28)	0.0007 (0.65)
	(0.087)	(0.010)		
	0.103		0.0003 (0.29)	0.0008 (0.73)
	(0.115)			

* Errors are essentially identical for the SRK and PR EOS

Table VIII

SRK and PR Equation-of-State Representations of Solubility of Methane in Phenanthrene

Temperature K (°F)	Soave Parameters (P-R Parameters) C_{12}	D_{12}	Error in Mole Fraction* (Error in Pressure,bar) RMS	MAX
383.2 (230.0)	0.131	-0.001	0.0001 (0.15)	0.0002 (0.25)
	(0.125)	(0.004)		
	0.125		0.0001 (0.15)	0.0002 (0.21)
	(0.142)			
423.2 (302.0)	0.120	0.001	0.0002 (0.21)	0.0003 (0.31)
	(0.119)	(0.005)		
	0.127		0.0002 (0.21)	0.0003 (0.34)
	(0.142)			
383.2, 423.2	0.126	-0.000	0.0002 (0.30)	0.0005 (0.59)
	(0.123)	(0.004)		
	0.126		0.0002 (0.30)	0.0005 (0.59)
	(0.142)			

* Errors are essentially identical for the SRK and PR EOS

Table IX

SRK and PR Equation-of-State Representations of
Solubility of Methane in Pyrene

Temperature K ($^{\circ}$F)	Soave Parameters (P-R Parameters)		Error in Mole Fraction	
	C_{12}	D_{12}	RMS	MAX
433.2 (320.0)	0.124	0.006	0.0001	0.0002
	(0.126)	(0.009)		
	0.159		0.0002	0.0004
	(0.180)			

Table X

Henry's Constants and Infinite-Dilution Partial Molar
Volumes for Methane in Aromatic Hydrocarbons

Temp. K	Ref.	Henry's Const. bar	Partial Mol. Vol. cm^3/g-mole	RMS Error in Mole Fraction
		Naphthalene		
373.2	This Work	770 ($\pm$4)*	338 ($\pm$50)*	0.0005
423.2	This Work	780 ($\pm$2)	350 ($\pm$25)	0.0001
		Phenanthrene		
383.2	This Work	1006 ($\pm$4)	495 ($\pm$30)	0.0001
423.2	This Work	1013 ($\pm$3)	530 ($\pm$25)	0.0002
398.2	16	1019 ($\pm$2)	480 ($\pm$5)	0.0002
423.2	16	1019 ($\pm$4)	490 ($\pm$15)	0.0003
448.2	16	1014 ($\pm$2)	514 ($\pm$10)	0.0002
		Pyrene		
433.2	This Work	1152 ($\pm$4)	510 ($\pm$25)	0.0003

* Standard deviation of estimated parameters
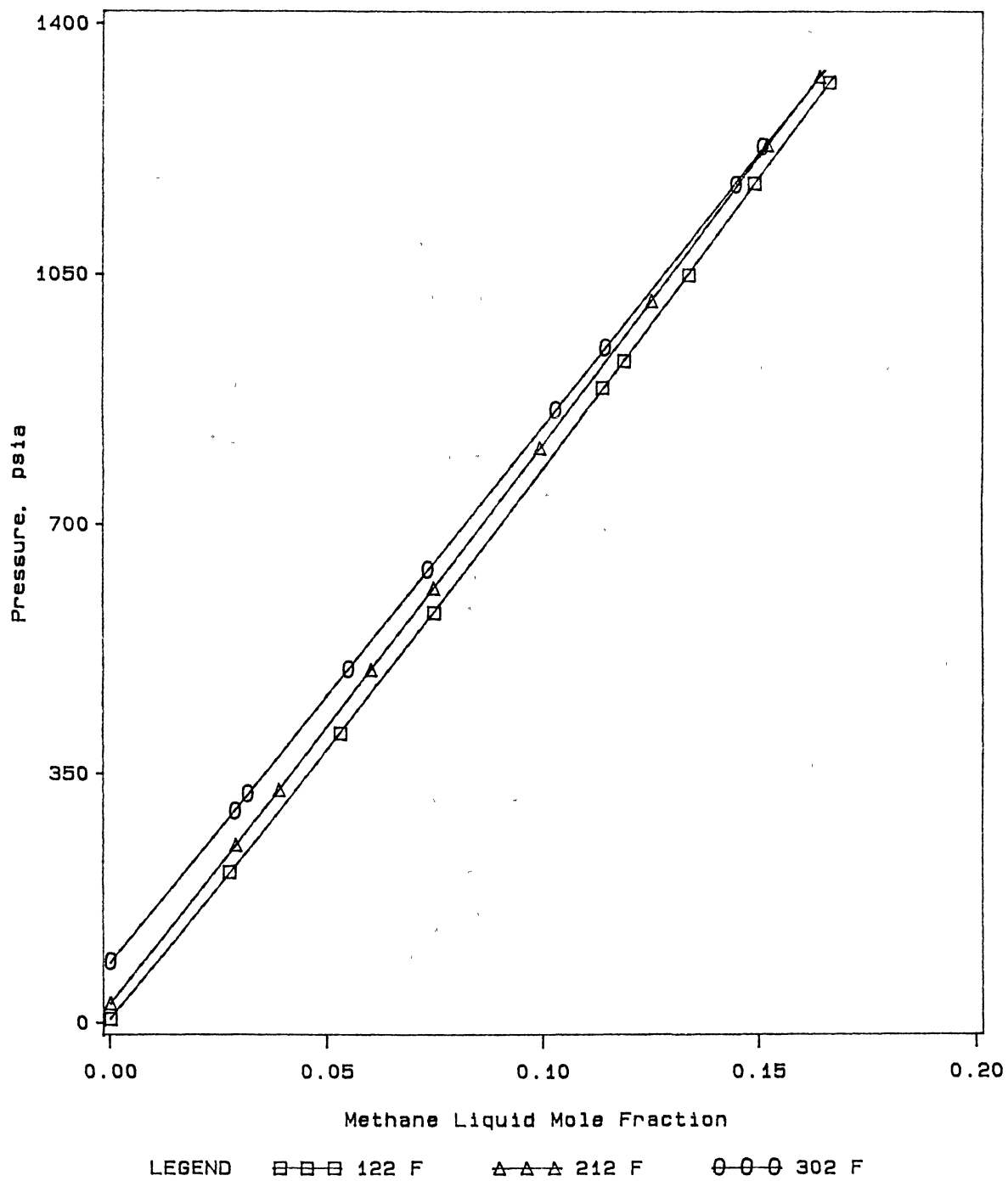
Figure 1

Bubble Point Pressure Data for Methane + Benzene
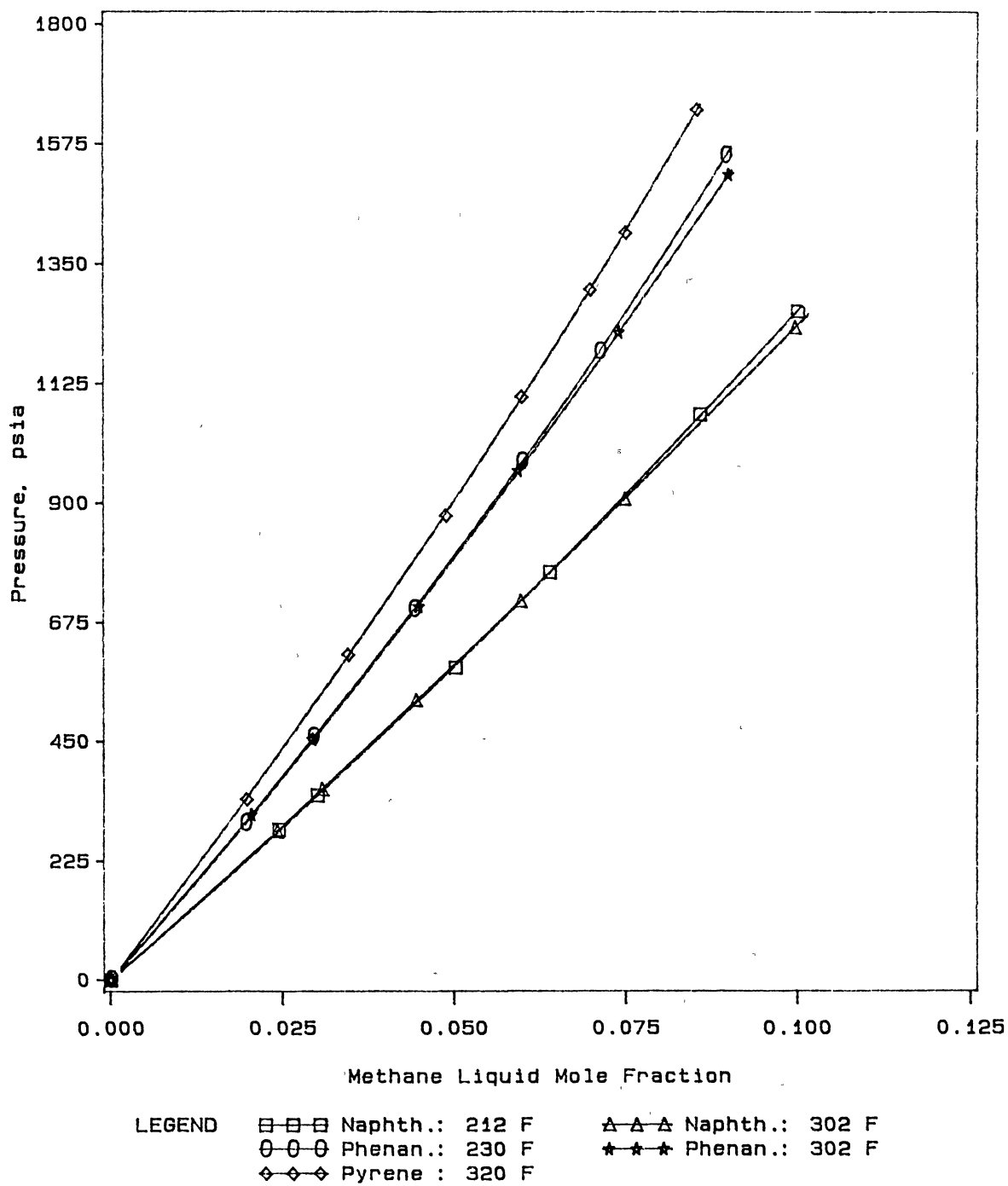
Figure 2

Bubble Point Pressure Data for Methane + Aromatic Hydrocarbons
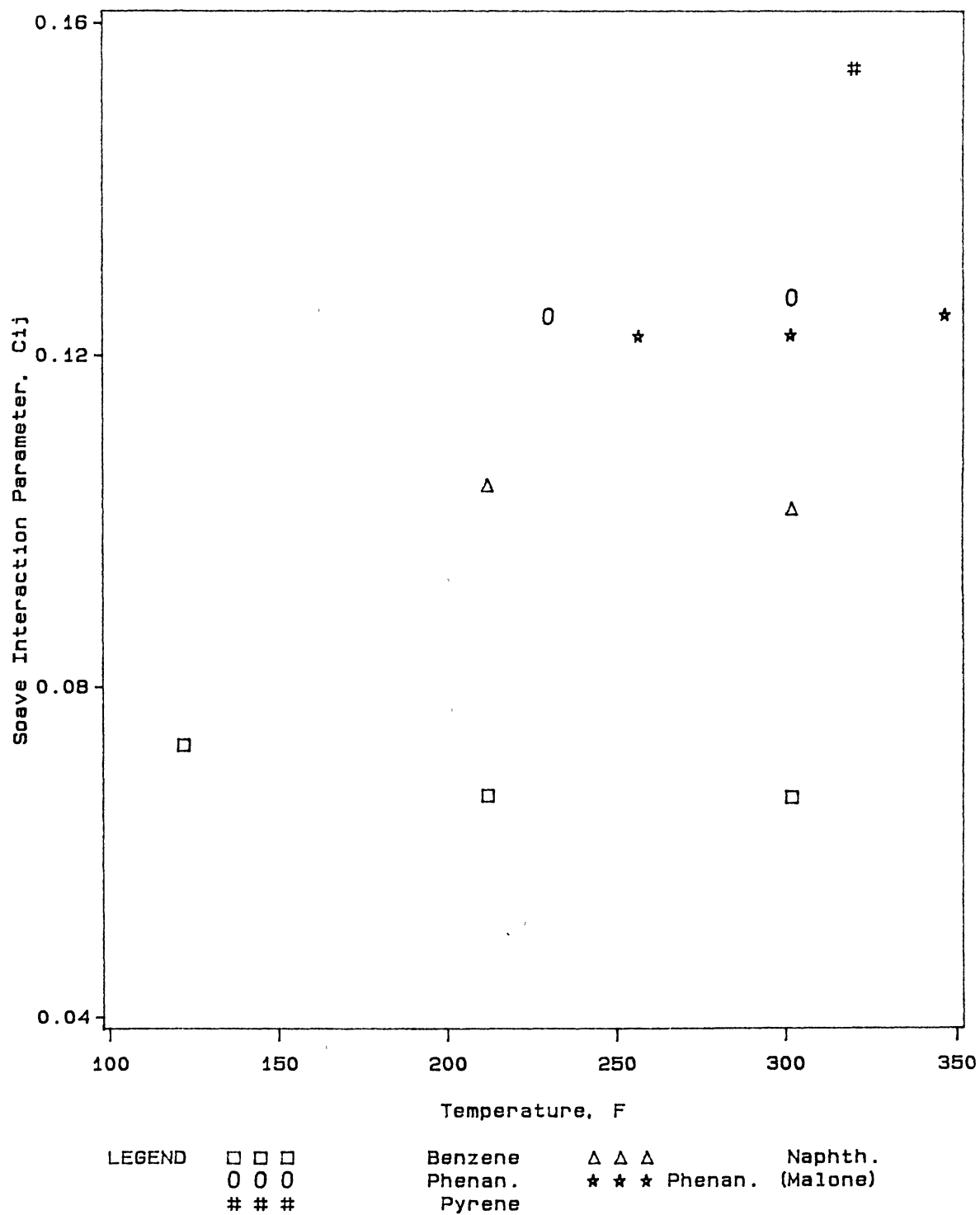
Figure 3

Soave Interaction Parameter, Cij(T), for Methane + Aromatic Hydrocarbons
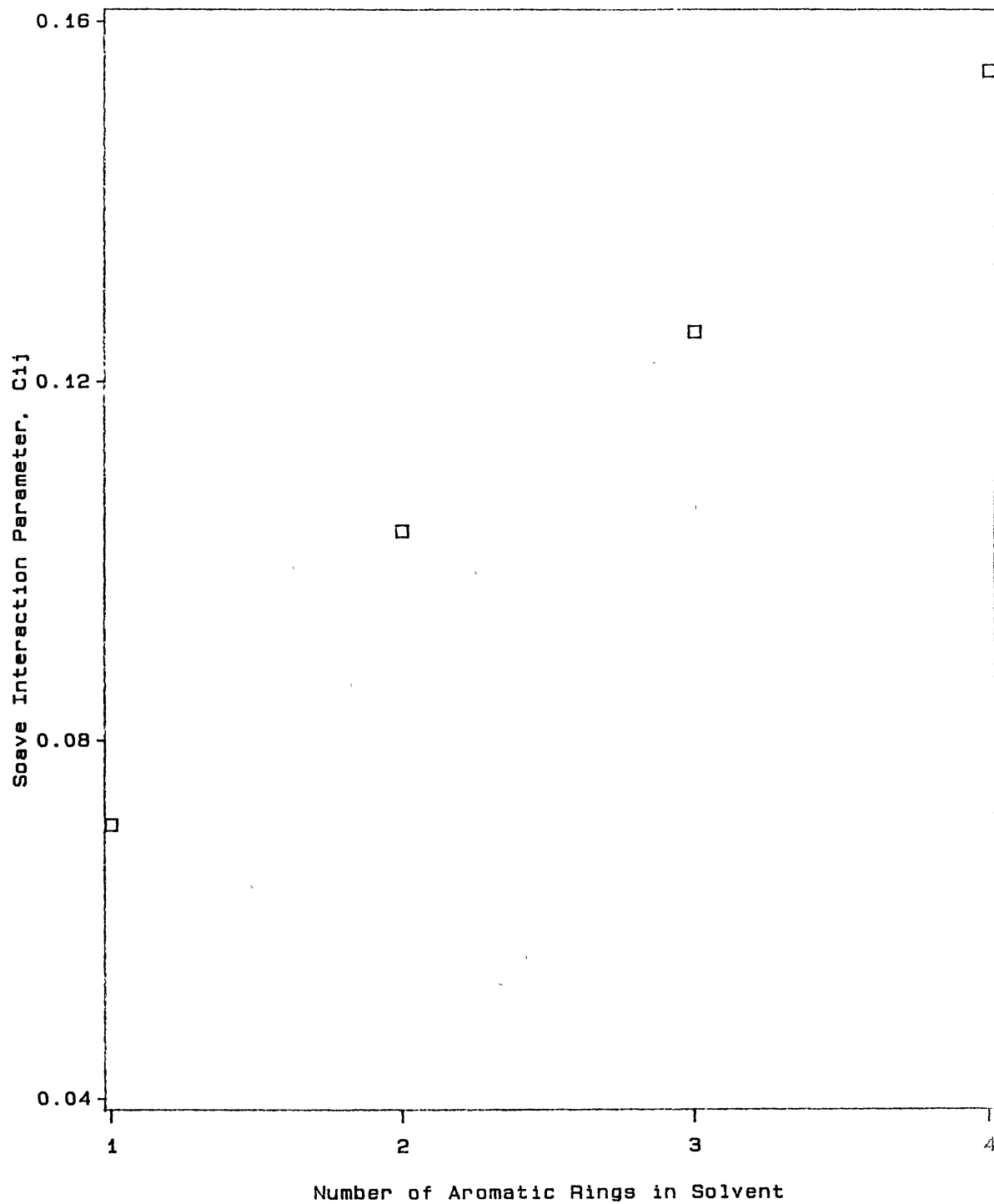
Figure 4

Soave Interaction Parameter, Cij, for Methane + Aromatic Hydrocarbons
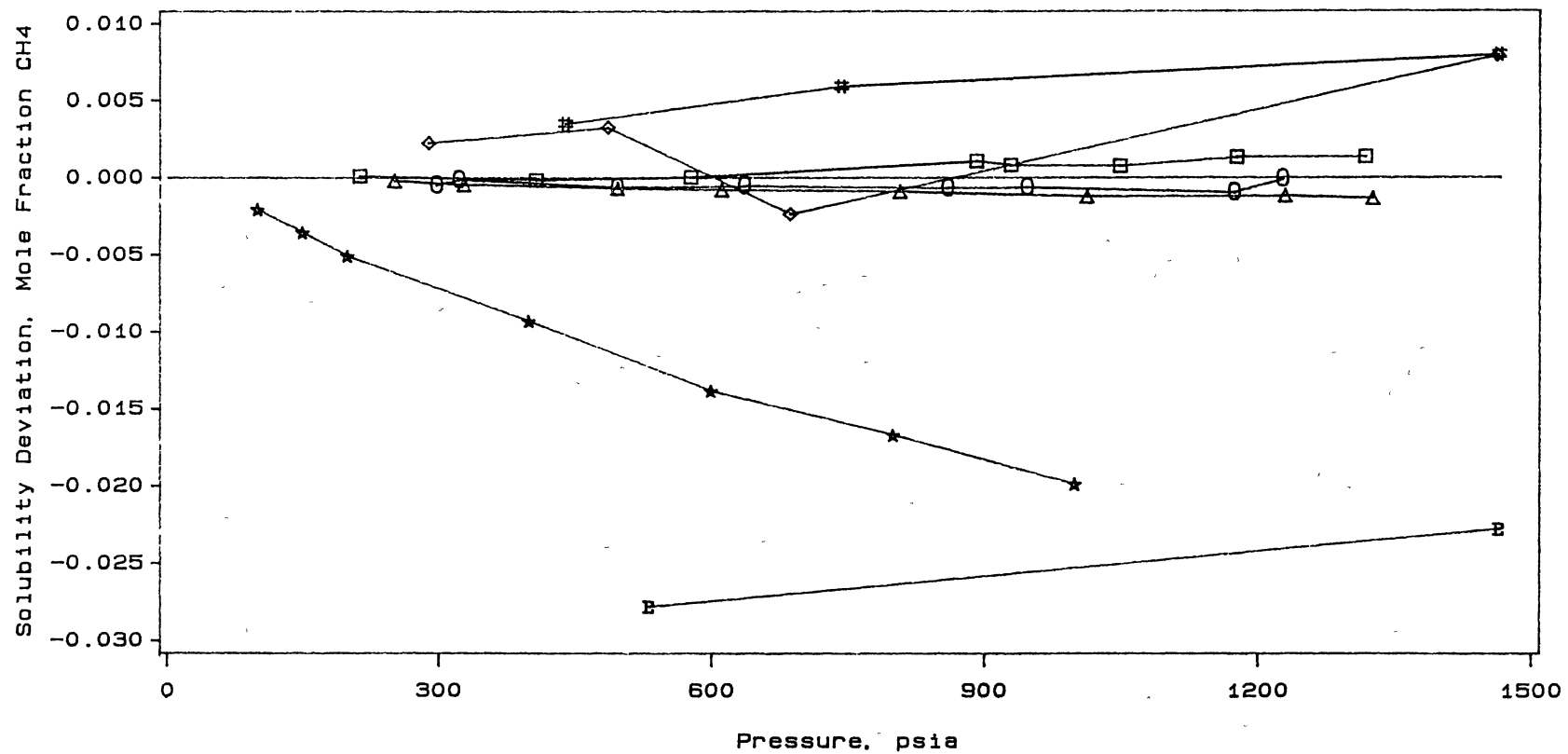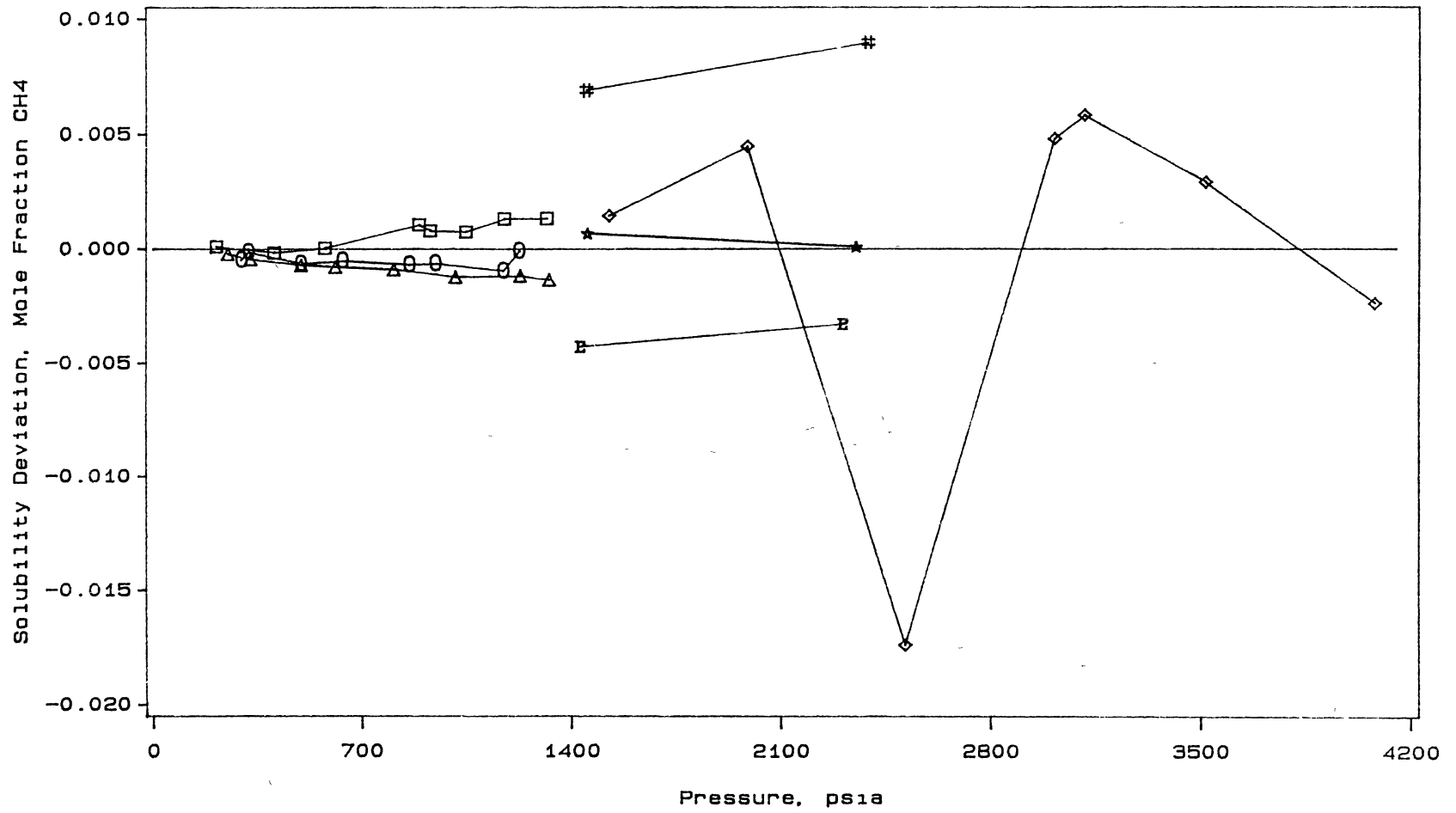
Figure 5.

Comparison of Methane Solubilities in Benzene (a)

Figure 6
Comparison of Methane Solubilities in Benzene (b)
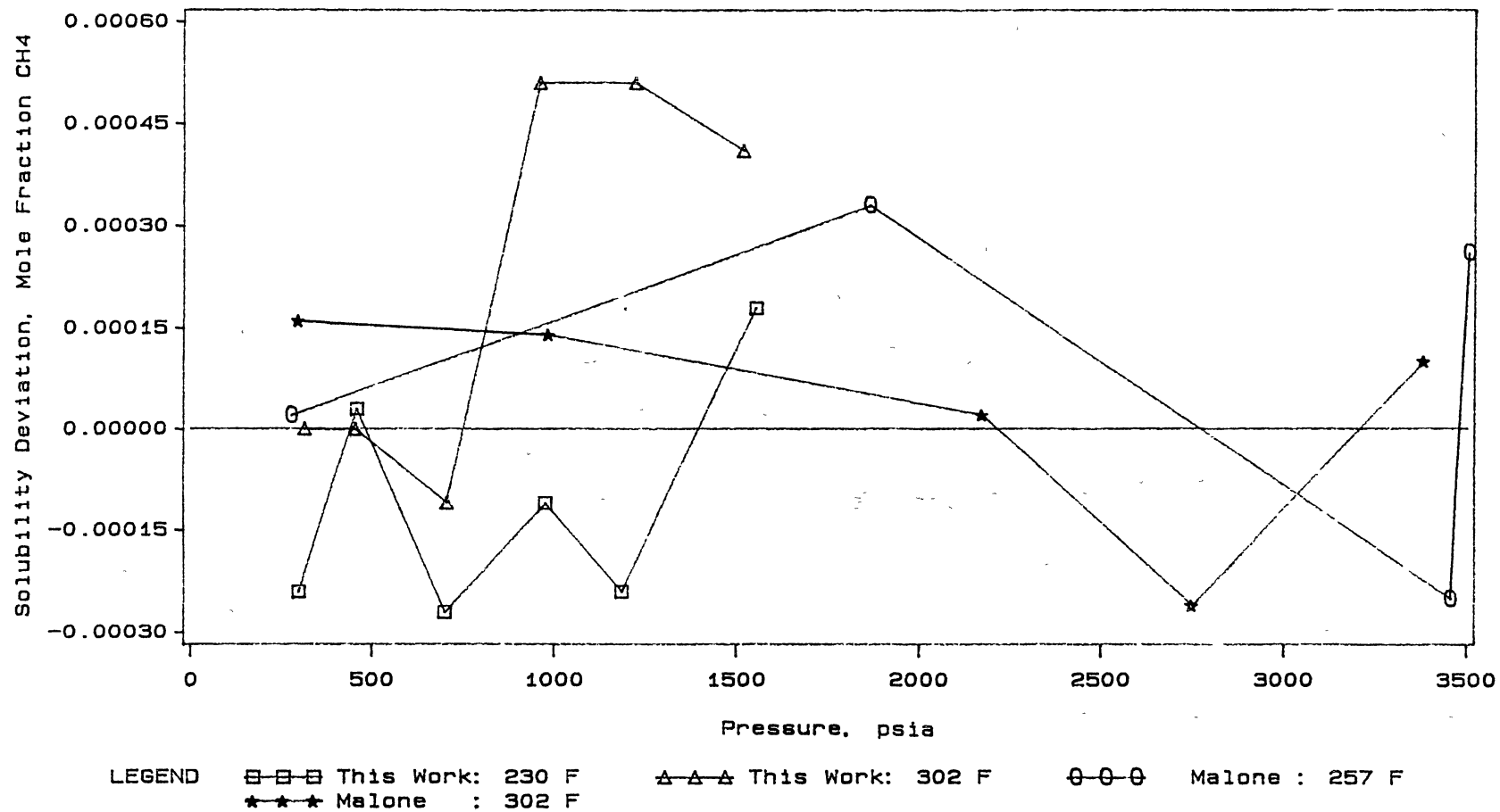
Figure 7

Comparison of Methane Solubilities in Phenanthrene
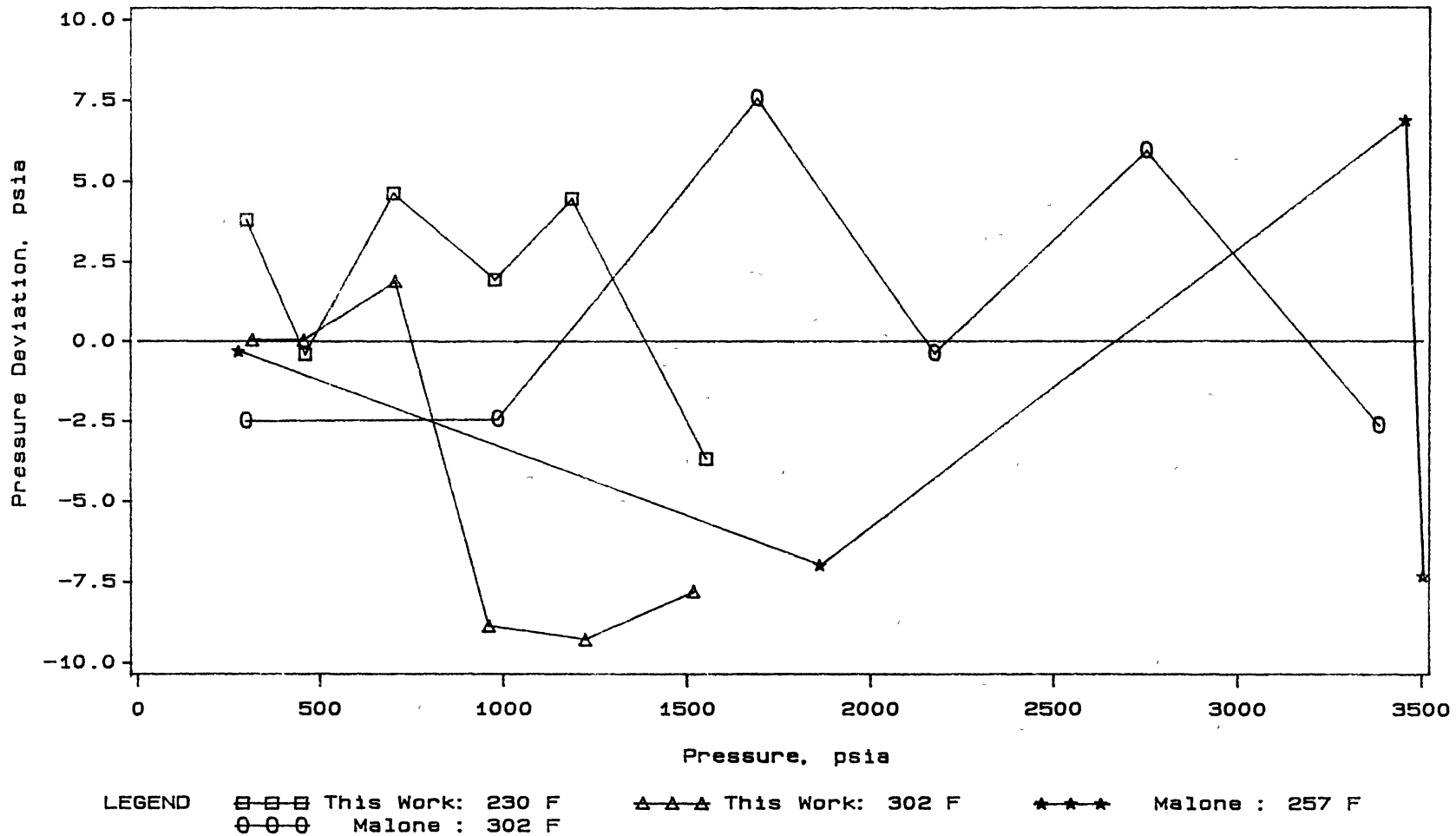
Figure 8

Prediction of Bubble Point Pressures of Methane in Phenanthrene Using the SRK Equation of State
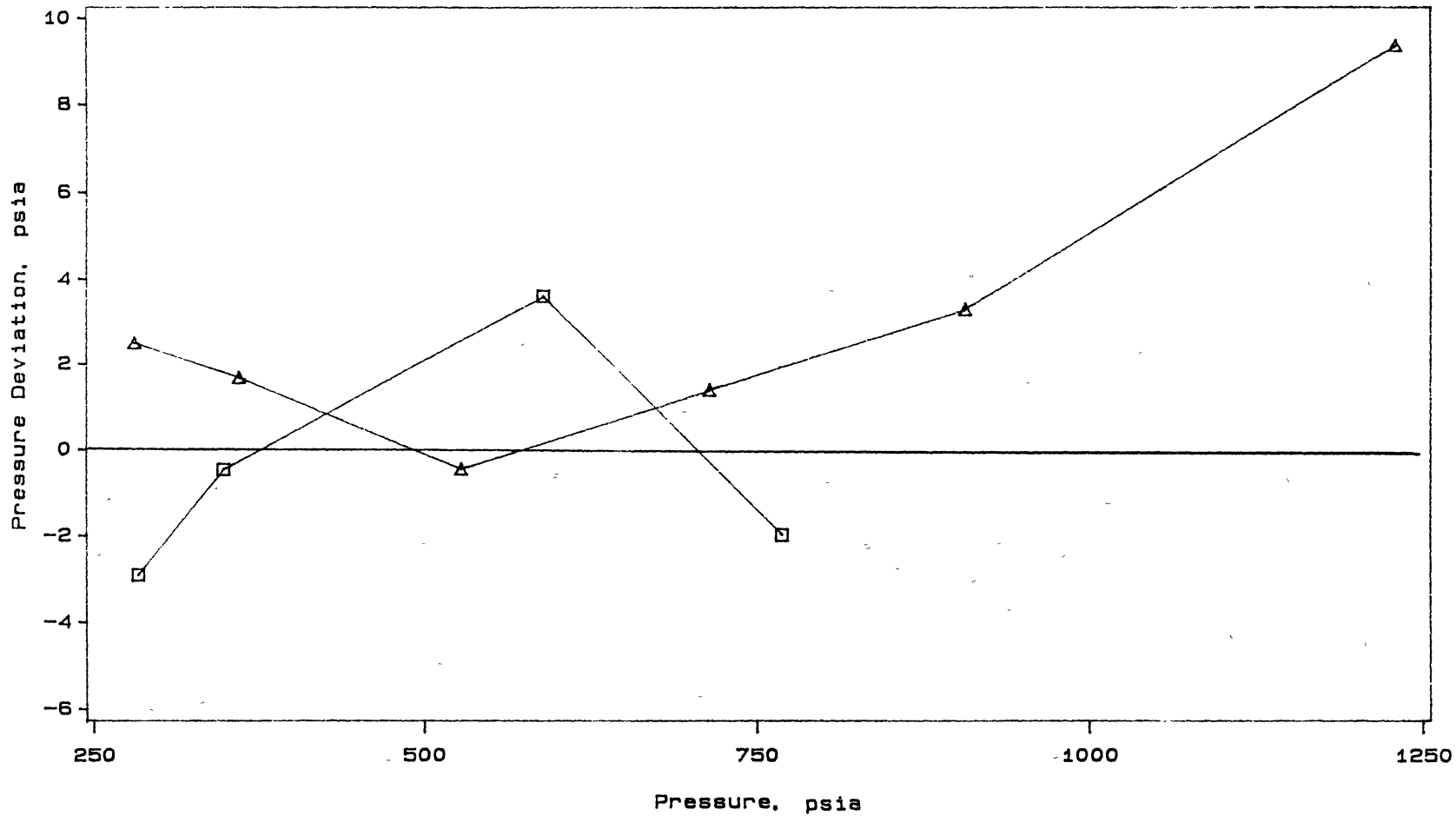
Figure 9

Prediction of Bubble Point Pressures of Methane in Naphthalene Using the SRK Equation of State
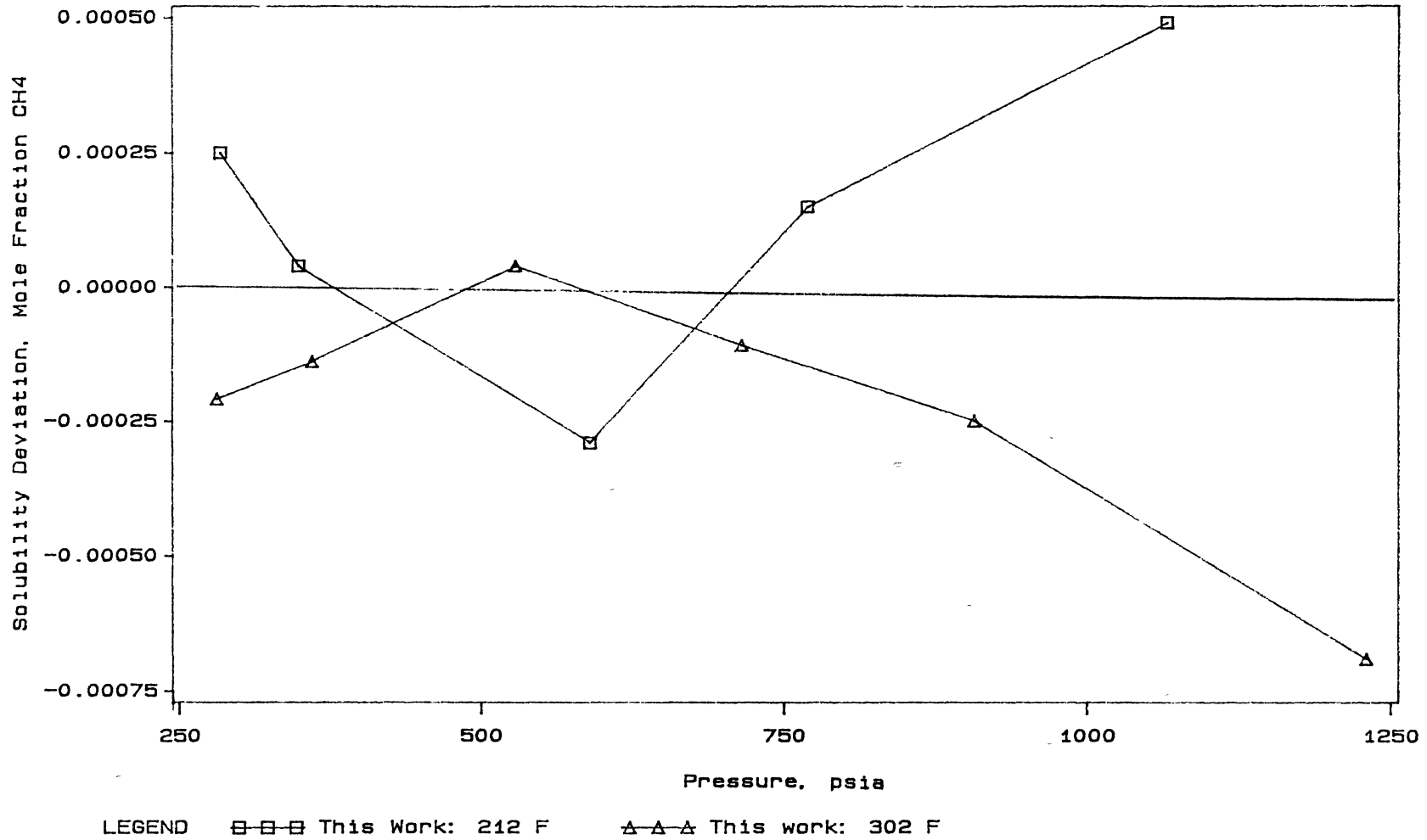
Figure 10

Prediction of Methane Solubilities in Naphthalene Using the SRK Equation of State
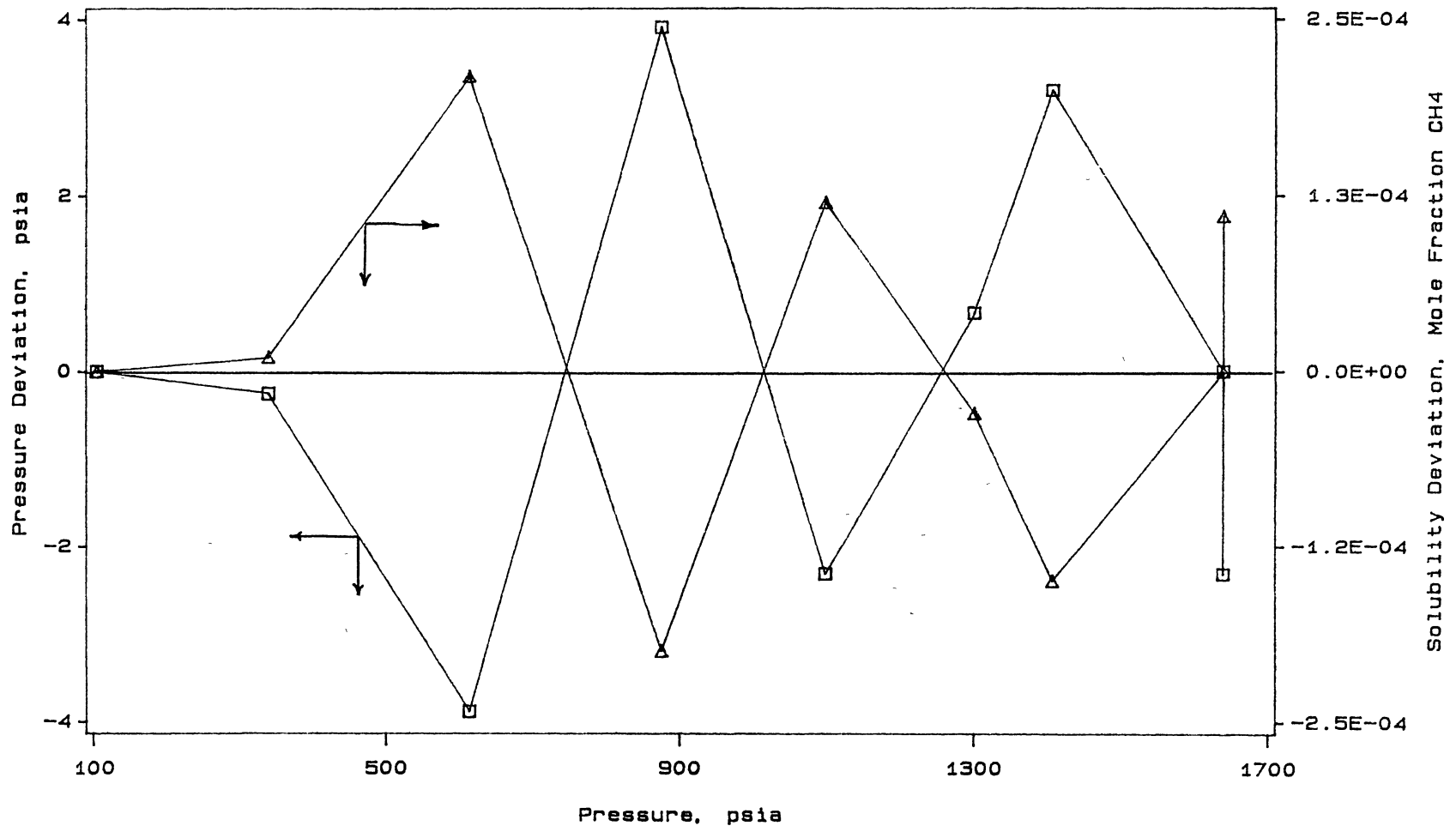
Figure 11

Prediction of Bubble Point Pressures and Solubilities of Methane in Pyrene Using the SRK Equation of State
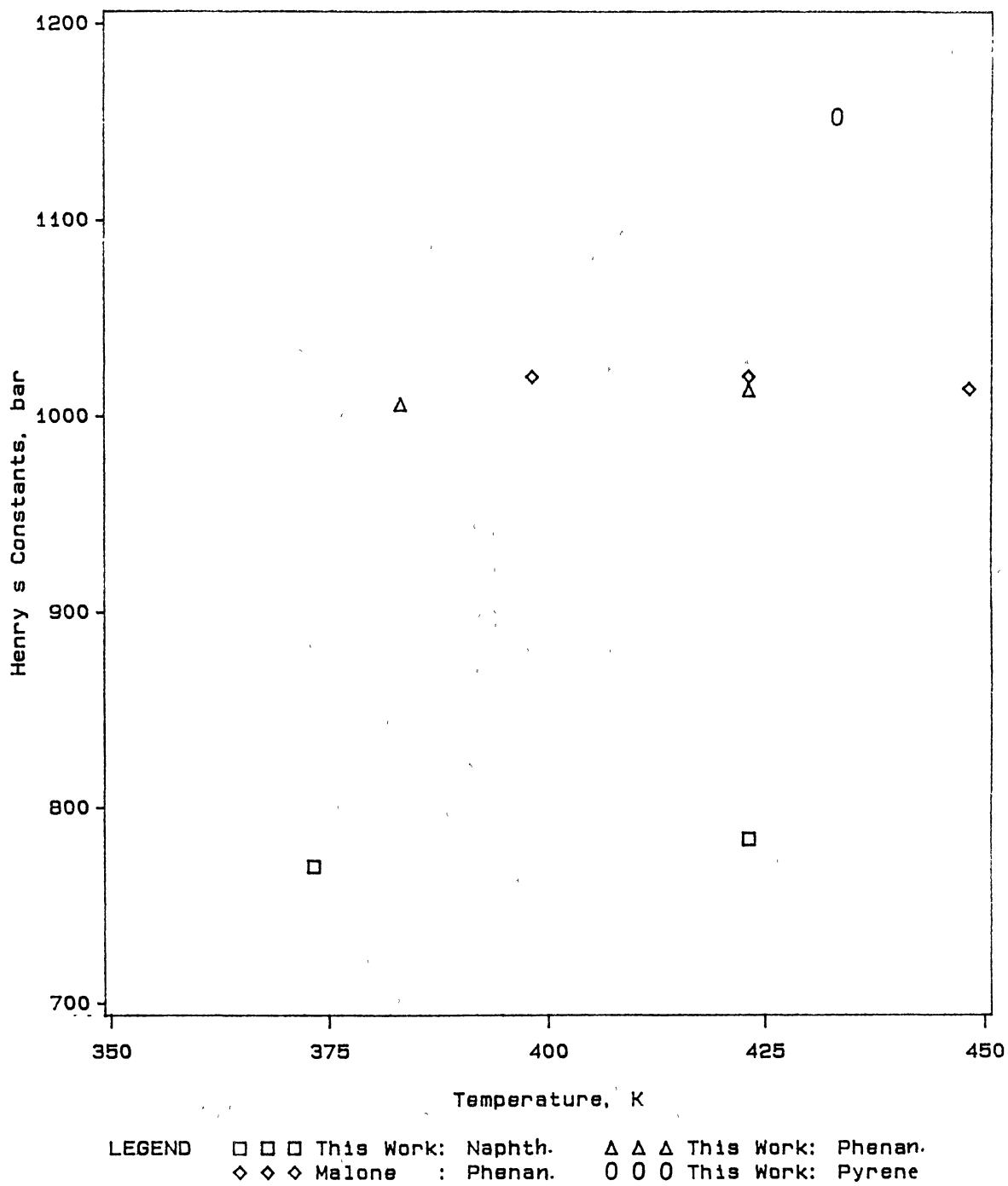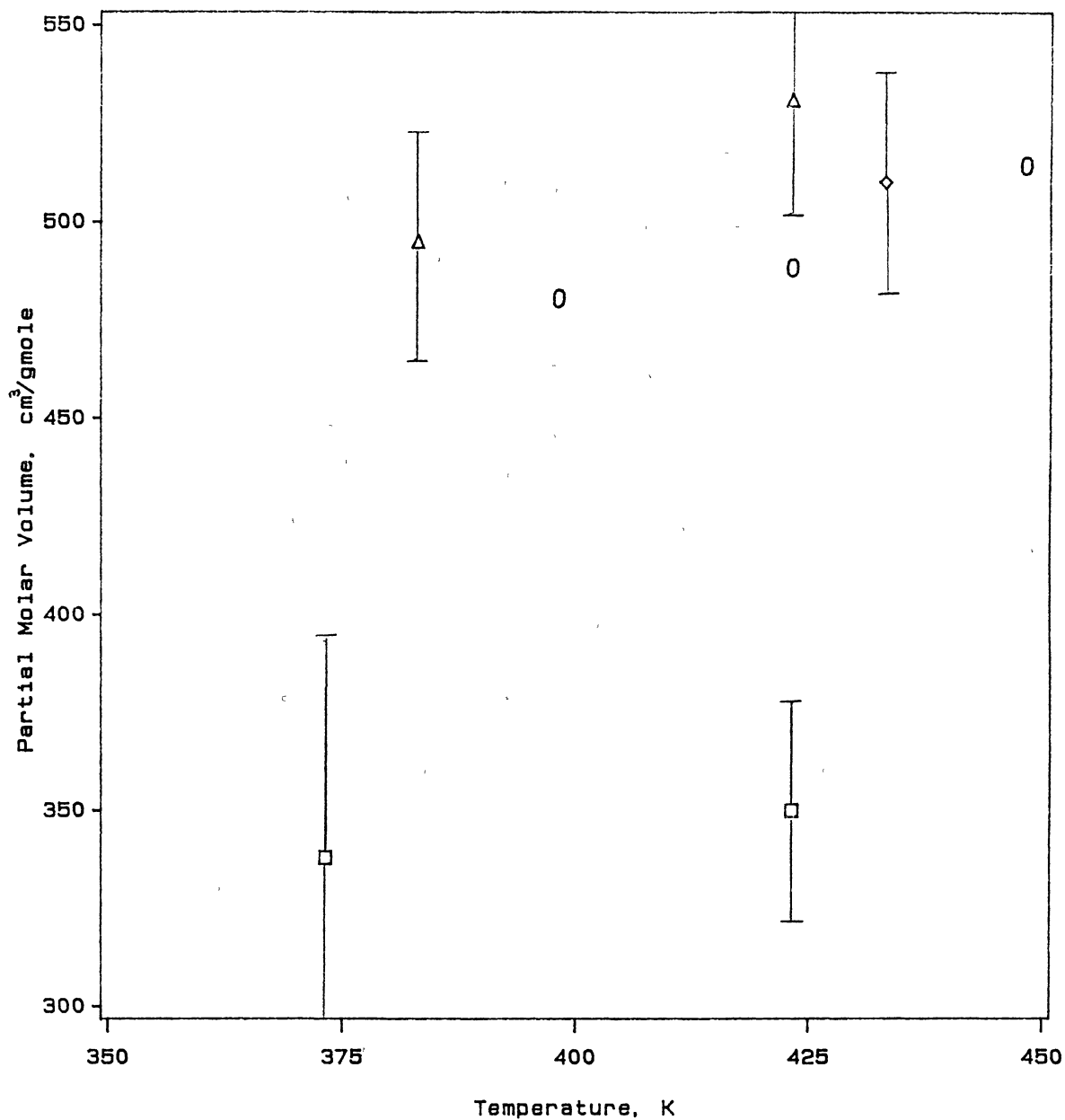
Figure 12

Comparison of Henry's Constants of Methane in Aromatic Hydrocarbons

Figure 13

Comparison of Infinite—Dilution Partial Molar Volumes
of Methane in Aromatic Hydrocarbons

CHAPTER IX

CORRELATION OF METHANE SOLUBILITIES IN NORMAL

PARAFFINIC AND AROMATIC SOLVENTS

Abstract

The ability of the Soave-Redlich-Kowng (SRK) and Peng-Robinson (PR) equations of state (EOS) to represent the phase behavior of binary mixtures of methane + n-paraffins and methane + aromatics has been evaluated. In this evaluation, our experimental data on the solubility of methane in five heavy n-paraffins ($n-C_{10}$, $n-C_{20}$, $n-C_{28}$, $n-C_{36}$ and $n-C_{44}$) and four aromatics (benzene, naphthalene, phenanthrene, and pyrene), together with data from the literature, are used. Optimum interaction parameters are presented for each system considered for a variety of cases ranging from using a single interaction parameter, C_{ij}, to represent the full database to the most detailed case of employing two interaction parameters, C_{ij} and D_{ij}, for each isotherm in each specific system.

Based on methane + n-paraffins data base, a new correlation for the covolume parameter, b, in the SRK and PR EOS has been developed to account for molecular size and temperature effects. By employing a single value of the interaction

parameter, c_{ij}, the SRK and PR EOS, using the new correlation for b, predict the bubble point pressures of methane + n-paraffins extending from C_3 to $n-C_{44}$ (n-tetratetracontane) with a root mean square error, RMSE, of 1.2 bar and absolute average deviation, AAD, of 0.80 bar. Other cases of generalization of the SRK and PR EOS parameters are also presented for methane +n-paraffins and methane + aromatics. For methane + naphthenes no generalization is made because of the lack of sufficient data.

Introduction

For process design and optimization calculations, phase behavior is most conveniently described in terms of closed-form analytic models. Essentially all state-of-the-art models (including equations of state (EOS) and activity coefficient models) for phase behavior contain one [1,2], two [3] or three [4] interaction parameters to account for unlike molecular pair interactions. These "empirical" interaction parameters have a dramatic effect on the predicted properties of mixtures and are thus required for accurate predictions.

In most instances, successful modelling of the behavior of complex multicomponent mixtures requires accurate information on the pure compounds and on the binary interactions that exist between the different molecular species. Experimental measurements made on systematically chosen binary mixtures can be used to evaluate interaction parameters and, more importantly, furnish the basis for

generalization of the parameters to allow interpolation (and
perhaps extrapolation) to other solvents in the same
homologous series. Such generalizations are particularly
important [5,6,7] since complete studies of all possible
solute/solvent pairs are obviously infeasible.

Toward this end, we have previously reported and
analyzed data on the solubility of carbon dioxide, ethane and
methane in a series of hydrocarbons [5-9]. The purpose of
the present work is to evaluate the ability of the SRK [1]
and PR [2] equations of state to represent the phase behavior
of binary systems containing methane. Accordingly, our
solubility data for methane + hydrocarbons [9], together with
data from the literature, have been used to provide optimum
interaction parameters for the SRK and PR equations of state
and to present generalized correlations for such parameters.

Data Bases Used

Methane + n-Paraffins

Binary mixture data for methane + heavy n-paraffins
acquired at Oklahoma State University [9], together with
literature data for solvents of lower carbon number, were
used in this study. Table I presents the database, together
with the literature sources, covering n-paraffins from C_3 to
n-C_{44}. All data were used as isothermal P-x measurements,
i.e., the bubble point pressure as a function of solute
liquid mole fraction, x_1 (or, alternatively, the solubility

of the solute as a function of pressure). The temperature range covered extends from 100°F to about 400°F and pressures to 100 bar. No internal consistency tests were attempted to screen the database; instead, however, pressure prediction using the SRK EOS, employing two interaction parameters (C_{ij} and D_{ij}), per isotherm was compiled and experimental data points having a deviation of 2.5 times the RMSE or more were considered as outliers and deleted from the data base.

Methane + Aromatics

Binary solubility data for methane in aromatics which were acquired at Oklahoma State University [9], complemented with literature data on methane solubilities in aromatics, constitute the second database (shown in Table II) used in this study. This database was used in the evaluation of the SRK optimum interaction parameters. The temperature range covered for these systems extends from 100°F to 450°F and pressures to 100 bar. Outlier experimental data points were deleted as mentioned above.

The pure fluid properties used in this work are given in Table III.

SRK and PR Equations of State

Two equations of state used widely in industry are the Soave-Redlich-Kwong (SRK) [1] and Peng-Robinson (PR) [2] equations, which are explicit in pressure and cubic in volume. Correlation of binary phase behavior data of methane

+ hydrocarbons (n-paraffins and aromatics) was carried out
in terms of these two EOS. A modified version of SRK and PR
EOS is proposed for the purpose of correlation of phase
behavior data of heavy solvents.

The SRK equation of state is

$$P = \frac{RT}{V-b} - \frac{a(T)}{V(V+b)} \tag{1}$$

where

$$a(T) = a_c \cdot \alpha(T) \tag{2}$$

$$b = 0.08664 \ RT_c/P_c \tag{3}$$

and

$$a_c = 0.42748 \ R^2 T_c^2/P_c \tag{4}$$

$$\alpha(T)^{1/2} = 1 + k(1 - T_r^{1/2}) \tag{5}$$

$$k = 0.480 + 1.574 \ w - 0.176 \ w^2 \tag{6}$$

The PR equation of state is of similar form [2]

$$P = \frac{RT}{V-b} - \frac{a(T)}{V(V+b) + b(V-b)} \tag{7}$$

where a(T) and b are given as

$$a(T) = a_c \cdot \alpha(T) \tag{8}$$

$$b = 0.0778 \ RT_c/P_c \tag{9}$$

where

$$a_c = 0.45724 \ R^2 T_c^2/P_c \tag{10}$$

$$\alpha(T)^{1/2} = 1 + k(1 - T_r^{1/2}) \tag{11}$$

$$k = 0.37464 + 1.54226 \ w - 0.26992 \ w^2 \tag{12}$$

To apply the SRK or PR equations of state to mixtures, the values of a and b can be determined using the mixing rules

$$a_m = \Sigma \ \Sigma \ z_i z_j (1 - C_{ij})(a_i a_j)^{1/2} \tag{13}$$

$$b_m = 0.5 \ \Sigma \ \Sigma \ z_i z_j (1 + D_{ij})(b_i + b_j) \tag{14}$$

One of our objectives in this work was to present generalized values or expressions for the interaction parameter, C_{ij}, in Eq. 13 for both SRK and PR EOS. Also, generalization was carried out for a modified version of SRK and PR EOS.

The modification of SRK and PR EOS proposed in this study involves the covolume parameter "b" appearing in Eqs. 3 and 9 above. This modification is purely empirical and introduced solely for convenience in representing a whole body of data. The covolume parameter "b" is treated here as temperature and acentric factor dependent (in a parallel fashion to the definition of a(T) in Eq. 8) as follows:

$$b(T) = b_c . \beta(T) \tag{15}$$

$$\beta(T)^{1/2} = 1 + m(1 - T_r^{1/2}) \tag{16}$$

$$m = B_0 + B_1 w + B_2 w^2 \tag{17}$$

$$b_c = (\text{constant}) \ RT_c/P_c \tag{18}$$

This modification was found to represent the data of methane + n-paraffins better than incorporating the effects of temperature and molecular size in C_{ij} even if more adjustable

constants were used in the C_{ij} correlation. The coefficients in Eq. 17 are determined in this work by utilizing binary solubility data and they are specific to the database from which they are derived.

Data Reduction Procedure

Since much of the available data is in T-P-x form (no vapor phase measurements), only the measured properties T, P, and x were used in the data reduction procedure. If uncertainties in the temperature measurements are assumed to be negligible, the following weighted-least-square objective function, SS, is appropriate for the evaluation of EOS parameters:

$$SS = \Sigma[(P_{icalc} - P_{iexp})/\sigma_{Pi}]^2 \qquad (19)$$

where P_{exp} is the experimental bubble point pressure, P_{calc} is the calculated bubble point pressure, i denotes the particular data point, n is the total number of data points and

$$(\sigma_P)^2 = (\epsilon_P)^2 + (\partial P/\partial x)^2 (\sigma_x)^2 \qquad (20)$$

To calculate the overall uncertainty in a given bubble point pressure, σ_{Pi}, an estimate for the uncertainty in the pressure measurements, ϵ_{Pi}, and in the mixture mole fraction, σ_{xi}, are required in Eq. 20. Although such estimates are available for our data [9], adequate information is not available for all data sets used, so an equal weight was

assigned to each data point, i.e. $\sigma_{Pi} = 1$. A Marquart [10] non-linear regression procedure was used in the calculations. Details regarding the data reduction procedure are presented elsewhere [11].

Model Evaluation

Seven different models were examined in this study. These are presented in Table IV where a systematic progression in complexity of the models is evident. These evaluations were performed using the SRK EOS; however, the conclusions drawn here apply equally well to the PR EOS where an equivalence of the phase behavior predictions from the two equations has been observed [9,12,13]. The generalization of the EOS parameters, (discussed later), was performed for both the SRK and PR EOS.

Table V presents a summary of results for the cases described in Table IV, where definitions of the statistical quantities used to evaluate the results are given in the list of symbols. The overall model statistics are given for the bubble point pressure predictions for the seven cases, for both methane + n-paraffins and methane + aromatics. Also, given in Table V is the RMSE in the predicted mole fraction when the interaction parameters are set at their optimum values for each evaluation case.

To initiate the evaluation the raw ability of SRK EOS (Case 1 in Table IV; $C_{ij} = D_{ij} = 0$) was assessed. Whereas reasonable representation was obtained for ethane +

n-paraffins (RMSE = 1.4 bar and %AAD =5) [14], methane +

n-paraffins exhibit significantly larger deviations for the

binary systems considered (RMSE = 6.0 bar, and %AAD = 10.5)

as Table V shows. The inadequacy of the "raw" SRK prediction

is also obvious from the 0.022 RMSE in mole fraction. For

methane + aromatic solvents the SRK EOS with no interaction

parameters predicts bubble point pressures poorly (RMSE =

14.3 bar and %AAD = 20.8). This illustrates that application

of the SRK (or PR) EOS to predict phase behavior of methane +

hydrocarbons could lead to significant errors when no

interaction parameters are used.

Case 2 in model evaluation (Tables IV and V) addresses

the improvements realized when a single interaction parameter

(applied to all binary systems) is considered. The results

of this case indicate marginal improvement in the predictive

ability of the SRK EOS over those of case 1 for methane + n-

paraffins (RMSE = 5.6 bar and %AAD = 8.8). For methane +

aromatics, however, the improvement is substantial relative

to the results of case 1 as signified by more than 60%

reduction in RMSE in pressure and solubility prediction (RMSE

= 5.3 bar and %AAD = 6.9).

Significant improvement in the predictive ability of the

SRK EOS is achieved when two interaction parameters, C_{ij} and

D_{ij}, are applied to all binary systems (Case 3 in Tables IV

and V). More than 50% reduction in pressure and solubility

RMSE, relative to the results of Case 2, is obtained

for both methane + n-paraffinic and methane + aromatic

solvents.

The use of a separate interaction parameter, C_{ij}, for each binary system (Case 4 in Tables IV and V) is the common industrial practice, and it definitely improves the results. Results of Table V indicate an RMSE of 1.5 bar and %AAD of 2.7 for methane + n-paraffins versus an RMSE of 0.6 bar and %AAD of 0.9 for methane + aromatic solvents.

The results of methane + n-paraffins in this case (Case 4) are typical of cubic EOS representation using a single system specific interaction parameter [13,16]. Using two (optimum) interaction parameters, C_{ij} and D_{ij}, for each binary system (Case 5) seems to be unnecessary since the improvement, relative to the results of Case 4, is small as shown in Table V (RMSE = 1.3 bar for methane + n-paraffins and 0.5 bar for methane + aromatics).

The improvements achieved when the temperature dependence of C_{ij} is considered (i.e. when a single C_{ij} is fitted to each isotherm) is shown in Case 6 (Table IV and V). A pronounced improvement in the SRK (or PR) EOS prediction is obtained for methane + n-paraffins (RMSE = 0.7 bar and %AAD = 1.5). For methane + aromatic solvents, however, the interaction parameter, C_{ij}, shows a weak dependence on temperature as evident from Table V. This weak temperature dependency of C_{ij} was also observed in ethane binaries [14].

Case 7 of model evaluation represents the most detailed case where two parameters, Cij and Dij, are fitted to each isotherm. The prediction capability of the SRK (or PR) is

fully utilized in this case where the best possible representation of the data is achieved. However, in view of the adequacy of prediction obtained in Case 6 for methane + n-paraffins and Case 4 for methane + aromatics, using two parameters for each isotherm seems unnecessary.

Tables VI and VII present the optimum interaction parameters, C_{ij} and D_{ij}, for the SRK EOS for the various cases outlined in Table IV. The average expected uncertainty in the reported interaction parameters (standard deviation of the optimized parameters) varies from one case to another and from one set of data to another depending on the precision of the respective data set, sensitivity of the SRK prediction to the optimized parameter(s), and the degree of correlation between the optimized parameters. In general, however, the estimated uncertainty ranges from 0.0005 to 0.005 for C_{ij} and from 0.0003 to 0.002 for D_{ij}.

Generalization of Interaction Parameters (C_{ij})

Four different generalization procedures (explained in Table VIII) are examined in this study. The generalizations were carried out employing both the SRK and PR EOS. The data base of methane + n-paraffins used in the generalization of parameters is the same data base employed in the evaluation cases considered previously. For methane + aromatics, however only data of this work (Table II) are considered here because the available literature data are not well described by our model.

Table IX presents a summary of results for the cases described in Table VIII, where overall model statistics are given for the bubble point pressure predictions for both methane + n- paraffins and methane + aromatics.

Case 1 (same as Case 2 in Tables IV and V) is presented here as the simplest generalization procedure where a single interaction parameter is used to represent the whole set of binary systems for each data set. The results of this case, although apparently not good, represent a substantial improvement over those of using no interaction parameter (Case 1 Table V). The optimum interaction parameter, C_{ij}, for methane + n-paraffins in this case of generalization is 0.0195 for the SRK and 0.0226 for the PR EOS and that for methane + aromatics is 0.0965 for the SRK EOS and 0.1076 for the PR EOS.

In the second case of generalization we treat C_{ij} as a second order polynomial in acentric factor. The leading term of this polynomial is set equal to C_{ij}^s, the optimum overall value of C_{ij} (keeping "b" as given originally in the SRK and PR EOS, i.e., Eqs. 3 and 9) that fits the binary solubility data of methane + low molecular weight solvents (liquid solvents at room temperature) and thus one value of C_{ij}^s is obtained for each data base. The fixed values of C_{ij}^s used in this case are 0.0371 for methane + n-paraffins and 0.0700 for methane + aromatic hydrocarbons. The results of this case (shown in Table IX) represent substantial improvements over those of Case 1 above (RMSE = 1.9 and 1.5 and %AAD = 3.3

and 2.2 for n-paraffins and aromatics, respectively.

In the third case of generalization (Table IX), we use the interaction parameter C_{ij}^s, (defined above), to represent its own data base and simultaneously treat "b", the covolume parameter in the SRK and PR EOS, as temperature and acentric factor dependent employing a similar analytical functionality as that of a(T) (see Eqs. 11 and 16). Figure 1 shows the effects of reduced temperature and molecular size on the optimum covolume parameter, b, when a common value of the interaction parameter ($C_{ij} = C_{ij}^s$) was applied to each solvent of the n-paraffins database. This functionality of b was also found convenient to represent liquid densities [40]. Results of this case of generalization show pronounced improvement over those of Cases 1 and 2 above for both methane + n-paraffins (RMSE = 1.2, and %AAD = 2.4) and methane + aromatics (RMSE = 0.6, and %AAD = 1.1). coefficients of the generalized "m" polynomial (Eq. 17) are represented in Table X.

The last case of generalization is a combination of cases 2 and 3 above. The same correlation obtained in Case 3 above for the covolume parameter, b, is employed here while the interaction parameter, C_{ij}, is correlated as in Case 2. The regressed coefficients, therefor, are A_1 and A_2 (since A_0 = C_{ij}^s). Results of this case show no improvement over those of Case 3 (RMSE = 1.2 and 0.6 and %AAD = 2.5 and 1.1 for n-paraffins and aromatics, respectively).

Inferior results relative to those obtained in Case 3

above were obtained from other cases of generalization; For example polynomial correlation of C_{ij} in terms of acentric factor and temperature requires more adjustable parameters to give results similar to those of Case 3. Also, no improvement (relative to Case 3) was obtained by regressing the leading term of C_{ij} polynomial in Case 4.

Discussion

The results obtained for model evaluation reveal an increase in accuracy which parallels the complexity of the models employed. For SRK EOS, a gradual decrease in the RMSE in bubble point pressures for methane + n-paraffins, from 6.0 to 0.3 bar, is obtained in going from Case 1 (Cij = Dij = 0) to Case 7 (Cij(T); Dij(T)). Similarly, for methane + aromatics the pressure RMSE is reduced from 14.3 to 0.2 bar. Such results when expressed as "normalized RMSE", with respect to the best case (Case 7), NRMSE, show a twenty two-fold and a eighty four-fold reduction in the observed error deviation for methane + n-paraffins and methane + aromatics, respectively (see Table V).

Regarding generalization of SRK and PR EOS interaction parameter, C_{ij}, the simplest and most direct procedure is to use a single interaction parameter to represent the whole set of binaries of the same homologous series. This case of generalization (Case 1 in Table VIII), however, is not capable of representing the phase behavior of n-paraffins and aromatics involving methane as evident from Table IX.

Generalization Case 2 represents a compromise between simplicity and accuracy where bubble point pressures are predicted within 2 bars using a simple polynomial (second order in acentric factor) for C_{ij}.

Case 3 represents a working strategy of generalization regarding accuracy and simplicity where four parameters are needed to predict bubble point pressures within 1.2 bar. The developed correlations for the covolume parameter, b, (one for n-paraffins and another for aromatics) are purely empirical and are not recommended for uses other than those presented in this work.

Figure 2 presents the error profile for the first three cases of generalization considered (since Case 4 gave similar results to those of Case 3) illustrating molecular size effects on the quality of the prediction. Case 1 is shown to work well below $n-C_{20}$ after which the RMSE in the predicted bubble point pressures increases linearly with the carbon number untill it reaches about 17 bar for $n-C_{44}$ (Figure 2). Results of Case 2 represent substantial improvements over those of Case 1 where the pressures are predicted with an RMSE less than 4 bar for the whole range of carbon numbers. The best results are obtained from Case 3 where the RMSE in the predicted pressures is below 2 bar.

Conclusions

Our experimental data on the solubility of methane in five heavy n-paraffins (n-C_{10}, n-C_{20}, n-C_{28}, n-C_{36} and n-C_{44}), and four aromatics (benzene, naphthalene, phenanthrene, and pyrene), together with data from the literature, were evaluated using SRK and PR EOS. Reasonable representation of methane + n-paraffins, extending from C_3 to n-C_{44}, and methane + aromatics (RMSE within 1.4 bar for the bubble point pressures) requires an interaction parameter for each binary system. For better accuracy (RMSE within 0.5 bar) an interaction parameter for each isotherm is needed.

Simple generalized correlations for the optimum interaction parameter, C_{ij}, in SRK and PR EOS were developed. With the generalized parameter EOS, the bubble point pressure could be predicted with an RMSE of 1.2 and 0.6 bar for methane + n-paraffins and methane + aromatics, respectively.

List of Symbols

AAD	absolute average deviation, $\sqrt{\Sigma\|Dev\|/n}$.
%AAD	percentage absolute average deviation.
$A_0 \ldots A_3$	correlation constants for C_{ij}.
a(T)	energy parameter in the SRK and PR EOS.
BIAS	bias in predictions, $(\Sigma Dev)/n$.
$B_0 \ldots B_2$	correlation constants for m in Eq. 17.
C_{ij}, D_{ij}	binary interaction parameters in the SRK and PR EOS.
C_{ij}°	overall binary interaction parameter
C_{ij}^{s}	overall binary interaction parameter for low molecular weight solvents
k, m	parameters dependent on w for SRK and PR EOS.
n	number of data points.
P	pressure.
R	universal gas constant.
RMSE	Root Mean Square Error, $[\sqrt{\Sigma}\ (Dev)^2/n]^2$.
SS	objective function (defined by Eq. 19).
T	temperature.
x	mole fraction.
w	acentric factor.
V	molar volume.

Greek letters

α	temperature dependent parameter in Eqs. 5 and 11.
β	temperature dependent parameter in Eq. 16.
σ	uncertainty in a measured or calculated property.
ϵ	prime (instrumental) error.

Subscripts

c	critical state.
calc	calculated.
exp	experimental.
i	component "i" in a mixture.
m	mixture.
P	pressure.
r	reduced property.

References

1. Soave, G., Chem. Eng. Sci., 27, 1197-1203 (1972).

2. Peng, Y. D.; Robinson, D. B., Ind. Eng. Chem. Fundam., 15, 59-64 (1976).

3. Turek, E. A.; Metcalfe, R. S.; Yarborough, L.; Robinson, R. L., Jr, J. Soc. Petrol. Eng., 24, 308-324 (1984).

4. Assadipour, H.; Hajela, V., "New Mixing Rules for Parameters of a three-Parameter Equation of State", Paper presented at AIChE Meeting, New Orleans, April 6-10 (1986).

5. Robinson, R. L., Jr.; Anderson, J. M.; Barrick, M. W.; Bufkin, B. A.; Ross, C. H., " Phase behavior of Coal Fluids: Data for Correlation Development," DE-FG22-86PC90523, Final Report, Department of Energy, January (1987).

6. Gasem, K. A. M.; Robinson, R. L., Jr., J. Chem. Eng. Data, 30, 53-56 (1985).

7. Anderson, J. M.; Barrick, M. W.; Robinson, R. L., Jr. J. Chem. Eng. Data, 31, 172-175 (1986).

8. Gasem, K. A. M.; Bufkin, B. A.; Raff, A. M.; Robinson, R. L., Jr., J. Chem. Eng. Data, 34, 187-191 (1989).

9. Darwish, N. A., Ph.D. Dissertation, Oklahoma State University, Stillwater, Oklahoma (1991).

10. Jackson, L. W., M.S. Report, Oklahoma State University, Stillwater, Oklahoma (1978).

11. Gasem, K. A. M., Ph.D. Dissertation, Oklahoma State University, Stillwater, Oklahoma (1986).

12. Robinson, R. L., Jr.; Gasem, K. A. M.; Raff, A. M.; Qin, Y., " Phase behavior of Coal Fluids: Data for Correlation Development" ,DE-FG22-86PC90523-12, progress Report, Department of Energy, January (1988).

13. Gasem, K. A. M.; Robinson, R. L., Jr., "Predictions of CO_2 solubility in heavy normal paraffins using generalized-parameter cubic equation of state" Paper presented at National AIChE Meeting, Houston, TX (1985).

14. Gasem, K. A. M.; Robinson, R. L., Jr., Fluid Phase Equilibria, 58, 13-33 (1990).

15. Raff, A. M., M.S. Thesis, Oklahoma State University, Stillwater, Oklahoma (1989).

16. Oellrich, L.; Plocker, U.; Prausnitz, J. M., Int. Chem. Eng., 21, 1-16 (1981).

17. Reamer, H. H; Sage, B. H.; Lacey, W. N., Ind. Eng. Chem., 42, 534-539 (1950).

18. Wiese, H. C.; Jacobs, J.; and Sage, B. H., J. Chem. Eng. Data, 15, 82-92 (1970).

19. Roberts, L. R.; Wang, R. H.; Azarnoosh, A.; McKetta, J. J., J. Chem. Eng. Data, 7, 484-485 (1962).

20. Kohn, J. P.; Bradish, W. F., J. Chem. Eng. Data, 9, 5-8 (1964).

21. Joosub, S.; Kohn, J. P., J. Chem. Eng. Data, 7, 3-7 (1962).

22. Reamer, H. H.; Sage, B. H.; Lacey, W. N., Chem. Eng. Data Series, 1, 29-42 (1956).

23. Shipman, L. L.; Kohn, J. P., J. Chem. Eng. Data, 11, 176-180 (1966).

24. Reamer, H. H.; Olds, R. H.; Sage, B. H.; Lacey, W. N., Ind. Eng. Chem., 34, 1526-1531 (1942).

25. Lin, H.; Sebastian, H. B.; Chao, K. C., J. Chem. Eng. Data, 25, 252-254 (1980).

26. Huang, S. H.; Lin, H.; Chao, K. C., J. Chem. Eng. Data, 33, 145-147 (1988).

27. Huang, S. H.; Lin, H.; Chao, K. C., J. Chem. Eng. Data, 33, 143-145 (1988).

28. Tsai, F.; Huang, S. H.; Lin, H.; Chao, K. C., J. Chem. Eng. Data, 32, 467-469 (1987).

29. Lin, H.; Sebastian, H. M.; Siminick, J. J.; Chao, K. C., J. Chem. Eng. Data, 24, 146-149 (1979).

30. Ng, H. J.; Sam, S. S.; Robinson, D. B., J. Chem. Eng. Data, 27, 119-122 (1982).

31. O'Reilly, W. F.; Blumer, T. E.; Luks, K. D.; ohn, J. J., Chem. Eng. Data, 21, 220-222 (1976).

32. Sebastian, H. M.; Siminick, J.; Lin, H.; Chao, K. C. J., Chem. Eng. Data, 24, 149-152 (1979).

33. Goodwin, R. D., "Thermophysical Properties of Methane from 90 to 500 K at Pressures to 700 Bar", NBS Technical Note 653, 22, April (1974).

34. Ely, H. F., NBS Technical Notes, 1039 (1981).

35. Ross, C. H., M.S. Report, Oklahoma State University, Stillwater, Oklahoma, (1985).

36. Ambrose, D., "Vapor-Liquid Critical Properties", National Physical Laboratory, Teddington, Middlesex TW11 OLW, UK (1980).

37. Reid, R. C.; Prausnitz, J. M.; Sherwood, T. K., The Properties of Gases and Liquids. 2nd Edition, New York: McGraw-Hill Book Co., (1977).

38. API Monograph Series, "Anthracene and Phenanthrene", Washington, D.C.: American Petroleum Institute. Monograph No. 708, January (1979).

39. API Monograph Series, "Four-Ring Condensed Aromatic Compounds", Washington, D.C.: American Petroleum Institute. Monograph No. 709, March (1979).

40. Moshfeghian, M.; Shariat, A.; Maddox, R. N., Chem. Eng. Comm., 73, 205-215 (1988).

List of Tables

Table I

Experimental Data for Methane + n-Paraffins
Used in This Study

Paraffin Carbon Number, CN	Temperature Range, °F	Methane Mole Fraction Range, x_{CH_4}	Ref.	Number of Points
3	100 - 190	0.03 - 0.49	17	62
4	160 - 220	0.03 - 0.39	18,19	9
6	122 - 302	0.01 - 0.39	21	37
7	100 - 340	0.10 - 0.40	22	12
8	77 - 302	0.02 - 0.29	20	28
9	122 - 302	0.03 - 0.31	23	39
10	100 - 400	0.01 - 0.32	This Work, 24	53
16	372	0.08 - 0.32	25	4
20	122 - 392	0.04 - 0.25	This Work, 26	19
28	212 - 392	0.05 - 0.30	This Work, 27	18
36	212 - 392	0.05 - 0.30	This Work, 28	19
44	212 - 302	0.05 - 0.25	This Work	15

Table II

Experimental Data for Methane + Aromatics Used in This Study

Solvent	Temperature Range,°F	Methane Mole Fraction Range, x_{CH_4}	Ref.	Number of Points
Benzene	122 - 302	0.03 - 0.17	This Work	22
Naphthalene	212 - 302	0.02 - 0.10	This Work	12
Phenanthrene	230 - 302	0.02 - 0.09	This Work	12
Toluene	300 - 442	0.02 - 0.20	29	7
m-Xylene	100 - 400	0.04 - 0.22	30	7
n-Butylbenzene	158 - 212	0.02 - 0.14	31	12
Diphenylmeth-ane	373	0.03 - 0.15	32	4
Pyrene	320	0.02 - 0.09	This Work	7

Table III

Fluid Critical Properties Used in SRK EOS Predictions

Component	Critical Temp.,°F	Critical Press., psia	Acentric Factor	Reference
.... n-Paraffins				
C_1	-116.67	667.08	0.0113	33
C_3	206.01	615.97	0.1542	34
n-C_4	305.62	550.59	0.2004	34
n-C_6	454.53	439.18	0.2978	34
n-C_7	512.58	396.75	0.3499	34
n-C_8	564.21	362.26	0.3995	34
n-C_9	610.54	331.78	0.4450	34
n-C_{10}	651.92	304.10	0.4885	34
n-C_{16}	837.32	199.51	0.7311	34
n-C_{20}	927.23	162.01	0.8791	35
n-C_{28}	1029.65	95.87	1.1617	35
n-C_{36}	1095.50	62.08	1.4228	35
n-C_{44}	1136.20	42.06	1.6664	35
.... Aromatics				
Benzene	552.22	710.40	0.2120	36
Naphthalene	887.45	587.84	0.3028	37
Phenanthrene	1112.09	478.63	0.5400	38
Pyrene	1229.10	377.10	0.8300[a]	39
Toluene	605.55	595.19	0.2630	36
m-Xylene	651.02	512.74	0.3250	36
n-Butylbenzene	729.14	418.69	0.3930	36
Diphenylmeth-ane	926.60	414.43	0.4420	36

[a] Turek, E. A., Amoco Production Company, Tulsa, Oklahoma, Personal Communication (1988).

Table IV

Specific Cases for Interaction Parameters
Used in the EOS Model Evaluation

Case	Description
1 $C_{ij} = 0$ $D_{ij} = 0$	The 'raw' ability of the EOS, using one-fluid mixing rules with no interaction parameters; permits prediction from pure-component data.
2 C_{ij}	A single value of C_{ij} is used for application to all binary systems.
3 C_{ij}, D_{ij}	Two interaction parameters are determined for application to all binary systems.
4 C_{ij}	A separate value of C_{ij} is determined for each binary system, independent of temperature; this is the most commonly used EOS representation in the literature.
5 C_{ij}, D_{ij}	Two interaction parameters are determined for application to each binary systems, independent of temperature.
6 $C_{ij}(T)$	A separate value of C_{ij} is determined for each binary system at each temperature; this case permits C_{ij} to be temperature dependent.
7 $C_{ij}(T)$ $D_{ij}(T)$	A separate pair of parameters is determined for each binary system at each temperature.

Table V

Summary of Results for Model Evaluation for Methane +
Hydrocarbons Using the SRK EOS

| Case Number | Bubble Point Pressure | | | | NRMSE [a] | RMSE [b] in Mole Fraction |
	RMSE (bar)	BIAS (bar)	AAD (bar)	%AAD		
.... Methane + n-Paraffins						
1	5.95	-1.86	4.37	10.53	22.0	0.022
2	5.56	0.51	3.29	8.76	20.6	0.019
3	2.62	-0.24	1.89	4.67	9.7	0.010
4	1.46	0.02	1.00	2.72	5.4	0.006
5	1.29	-0.11	0.91	2.49	4.8	0.005
6	0.68	0.09	0.49	1.54	2.5	0.003
7	0.27	-0.04	0.17	0.55	1.0	0.002
.... Methane + Aromatic Hydrocarbons						
1	14.27	-11.33	11.33	20.83	83.9	0.022
2	5.34	-0.18	3.90	6.93	31.4	0.007
3	1.84	0.14	1.21	2.75	10.8	0.004
4	0.57	-0.08	0.40	0.93	3.4	0.0011
5	0.49	-0.01	0.34	0.79	2.9	0.0009
6	0.42	-0.10	0.31	0.77	2.5	0.0008
7	0.17	-0.001	0.14	0.37	1.0	0.0003

[a] NRMSE = RMSE/(RMSE, Case 7)
[b] Solubility is calculated from SRK EOS using the optimum
interaction parameter(s) (Tables VI and VII) for each case.

Table VI

SRK EOS Optimum Interaction Parameters
for Methane + n-Paraffins

Component T(°F)	Case Number (See Table IV)[a]					
	4	5		6	7	
	C_{ij}	C_{ij}	D_{ij}	C_{ij}	C_{ij}	D_{ij}
C_3	0.032	0.035	0.002			
100.0				0.028	0.028	0.000
130.0				0.039	0.039	0.000
160.0				0.066	0.066	0.002
190.0				0.056	0.056	0.000
$n-C_4$	0.048	0.048	-0.001			
160.0				0.044	0.047	-0.006
220.0				0.056	0.047	0.028
$n-C_6$	0.032	0.032	0.000			
122.0				0.043	0.045	-0.001
167.0				0.037	0.042	0.004
212.0				0.029	0.029	0.001
302.0				0.030	0.038	-0.007
$n-C_7$	0.028	0.025	0.002			
100.0				0.025	0.029	-0.003
160.0				0.026	0.044	-0.011
220.0				0.034	0.044	-0.006
280.0				0.052	0.074	-0.012
$n-C_8$	0.043	0.018	0.012			
77.0				0.038	0.042	-0.002
167.0				0.040	-0.001	0.020
212.0				0.047	-0.025	0.035
302.0				0.066	0.007	-0.030
$n-C_9$	0.043	0.064	-0.011			
122.0				0.042	0.060	-0.009
167.0				0.042	0.083	-0.021
212.0				0.048	0.032	0.008
302.0				0.041	0.100	-0.029
$n-C_{10}$	0.036	0.068	-0.014			
100.0				0.033	0.052	-0.009
160.0				0.028	0.045	-0.006
220.0				0.031	0.054	-0.010
280.0				0.036	0.069	-0.015
340.0				0.057	0.061	-0.002
400.0				0.067	0.084	-0.007

Table VI (Continued)

SRK EOS Optimum Interaction Parameters
for Methane + n-Paraffins

Component	T($^\circ$F)			Case Number (See Table IV)[a]		
	4 C_{ij}	5 C_{ij}	D_{ij}	6 C_{ij}	7 C_{ij}	D_{ij}
n-C$_{16}$	0.025	0.094	-0.021			
372.7				0.025	0.094	-0.021
n-C$_{20}$	0.009	0.070	-0.012			
122.0				0.021	0.070	-0.009
212.0				0.002	0.080	-0.016
392.0				-0.034	0.058	-0.017
n-C$_{28}$	-0.072	0.005	-0.011			
212.0				-0.043	0.059	-0.014
302.0				-0.087	0.004	-0.014
392.0				-0.133	-0.044	-0.012
n-C$_{36}$	-0.128	0.049	-0.023			
212.0				-0.095	0.019	-0.014
302.0				-0.135	0.008	-0.019
392.0				-0.241	-0.064	-0.020
n-C$_{44}$	-0.199	-0.084	-0.0121			
212.0				-0.160	-0.031	-0.013
302.0				-0.237	-0.083	-0.016

[a] Case 1: $C_{ij} = D_{ij} = 0$
  Case 2: $C_{ij} = 0.020 \pm 0.003$
  Case 3: $C_{ij} = 0.069 \pm 0.002$ and $D_{ij} = -0.021 \pm 0.001$

Table VII

SRK EOS Optimum Interaction Parameters for
Methane + Aromatic Hydrocarbons

Component T(°F)	Case Number (See Table IV)[a]					
	4	5		6	7	
	C_{ij}	C_{ij}	D_{ij}	C_{ij}	C_{ij}	D_{ij}
Benzene	0.069	0.025	0.025			
122.0				0.071	0.032	0.022
212.0				0.065	0.025	0.023
302.0				0.066	0.044	0.013
Naphthalene						
	0.100	0.089	0.004			
212.0				0.101	0.099	0.001
302.0				0.099	0.071	0.009
Phenanthrene						
	0.122	0.120	0.001			
230.0				0.121	0.123	−0.001
302.0				0.123	0.115	0.002
Toluene	0.101	0.088	0.007			
300.7				0.093	0.079	0.006
372.0				0.105	0.009	0.055
m-Xylene	0.054	0.066	−0.006			
250.7				0.048	0.064	−0.008
400.0				0.063	−0.007	0.036
n-Butylbenzene						
	0.061	0.049	0.004			
158.0				0.060	0.063	−0.001
212.0				0.061	0.026	0.012
Diphenylmethane						
	0.119	0.092	0.008			
372.7				0.119	0.092	0.008
Pyrene	0.155	0.117	0.006			
320.0				0.155	0.117	0.006

[a] Case 1: $C_{ij} = D_{ij} = 0$
Case 2: $C_{ij} = 0.093 \pm 0.004$
Case 3: $C_{ij} = 0.032 \pm 0.003$ and $D_{ij} = 0.0192 \pm 0.0008$

Table VIII

Specific Cases for Generalization of Interaction
Parameter, Cij, in SRK and PR EOS.

Case	Description
1 $C_{ij} = C_{ij}^{\circ}$	A single value of C_{ij} is determined for application to all binary systems (same as Case 2 in Table IV)
2 $C_{ij} = f(w)$	C_{ij} is correlated in terms of acentric factor of the solvent via a second order polynomial. The leading term of this polynomial is the optimum interaction parameter for low molecular weight solvents (C_{ij}^{s}). The parameters optimized in this case are A_1 and A_2 below. $$C_{ij} = A_0 + A_1*w + A_2*w^2$$ where $A_0 = C_{ij}^{s}$
3 $C_{ij} = C_{ij}^{s}$ $b = g(T_r, w)$	C_{ij} is set to a prescribed value, C_{ij}^{s}, (the optimum for low molecular weight solvents) while β is considered as a function of reduced temperature and acentric factor. The parameters optimized in this case are B_0, B_1 and B_2. $$C_{ij} = A_0 = C_{ij}^{s}$$ $$b(T_r;w) = b_c\beta(T_r;w)$$ $$\beta(T_r)^{1/2} = 1 + m(1-T_r^{1/2})$$ $$m = B_0 + B_1*w + B_2*w^2$$
4 $C_{ij} = f(w)$ $b = g(T_r, w)$	This case is a combination of cases 2 and 3 above. The correlation found in Case 3 for $b(T_r;w)$ is used in combination with a second order polynomial for C_{ij} as in Case 2 above. The parameters optimized in this case are A_1 and A_2. $$C_{ij} = A_0 + A_1 w + A_2 w^2 \quad ; \quad (A_0 = C_{ij}^{s})$$ $$\beta(T_r)^{1/2} = 1 + m(1-T_r^{1/2})$$ $$m = B_0 + B_1*w + B_2*w^2$$

Table IX

Summary of Results for Model Generalization of Methane +
Hydrocarbons Using the SRK and PR EOS

| Case No. | Bubble Point Pressure | | | %AAD SRK(PR) | RMSE [a] in Mole Fraction |
	RMSE, bar SRK(PR)	BIAS, bar SRK(PR)	AAD, bar SRK(PR)		
.... Methane + n-Paraffins					
1	5.56(5.59)	0.52(0.64)	3.29(3.22)	8.76(8.60)	0.0190
2	1.89(1.84)	0.13(0.17)	1.29(1.26)	3.26(3.14)	0.0078
3	1.24(1.27)	-0.05(0.02)	0.95(0.93)	2.44(2.35)	0.0050
4	1.24(1.27)	-0.02(-0.06)	0.96(0.94)	2.47(2.38)	0.0049
.... Methane + Aromatic Hydrocarbons					
1	6.05(7.67)	-0.49(-0.77)	4.50(5.76)	7.10(9.17)	0.0070
2	1.46(1.76)	-0.31(-0.34)	1.16(1.42)	2.17(2.60)	0.0016
3	0.63(0.70)	-0.19(-0.25)	0.47(0.52)	1.10(1.25)	0.0011
4	0.62(0.69)	-0.20(-0.23)	0.47(0.52)	1.09(1.25)	0.0011

[a] Solubility is calculated from SRK EOS using the generalized
interaction parameter(s) (Table VIII) for each case.

Table X

Coefficients of C_{ij} and m Generalized Polynomials
for Different Cases of Generalizations
$$\beta(Tr)^{1/2} = 1 + m(1-Tr^{1/2})$$
$$m = B_0 + B_1*w + B_2*w^2$$
$$C_{ij} = A_0 + A_1 w + A_2 w^2$$

Coef.	Case Number (See Table VIII)		
	2 SRK (PR)	3 SRK (PR)	4 SRK (PR)

.... Methane + n-Paraffins ....

Coef.	2 SRK (PR)		3 SRK (PR)		4 SRK (PR)	
A_0	0.0371	(0.0371)	0.0371	(0.0371)	0.0371	(0.0371)
A_1	0.0646	(0.0632)	–		-0.0007	(-0.0001)
A_2	-0.1487	(-0.1405)	–		0.0022	(0.0015)
B_0	–		0.0946	(0.0644)	0.0946	(0.0644)
B_1	–		-0.4129	(-0.3333)	-0.4129	(-0.3333)
B_2	–		0.4258	(0.3922)	0.4258	(0.3922)

.... Methane + Aromatics ....

Coef.	2 SRK (PR)		3 SRK (PR)		4 SRK (PR)	
A_0	0.0700	(0.0700)	0.0700	(0.0700)	0.0700	(0.0700)
A_1	0.3570	(0.4008)	–		0.4E-4	(0.0009)
A_2	-0.2131	(-0.2347)	–		-0.6E-5	(-0.0012)
B_0	–		-0.1650	(-0.2019)	-0.1650	(-0.2019)
B_1	–		0.1282	(0.1334)	0.1282	(0.1334)
B_2	–		-0.1518	(-0.1788)	-0.1518	(-0.1788)
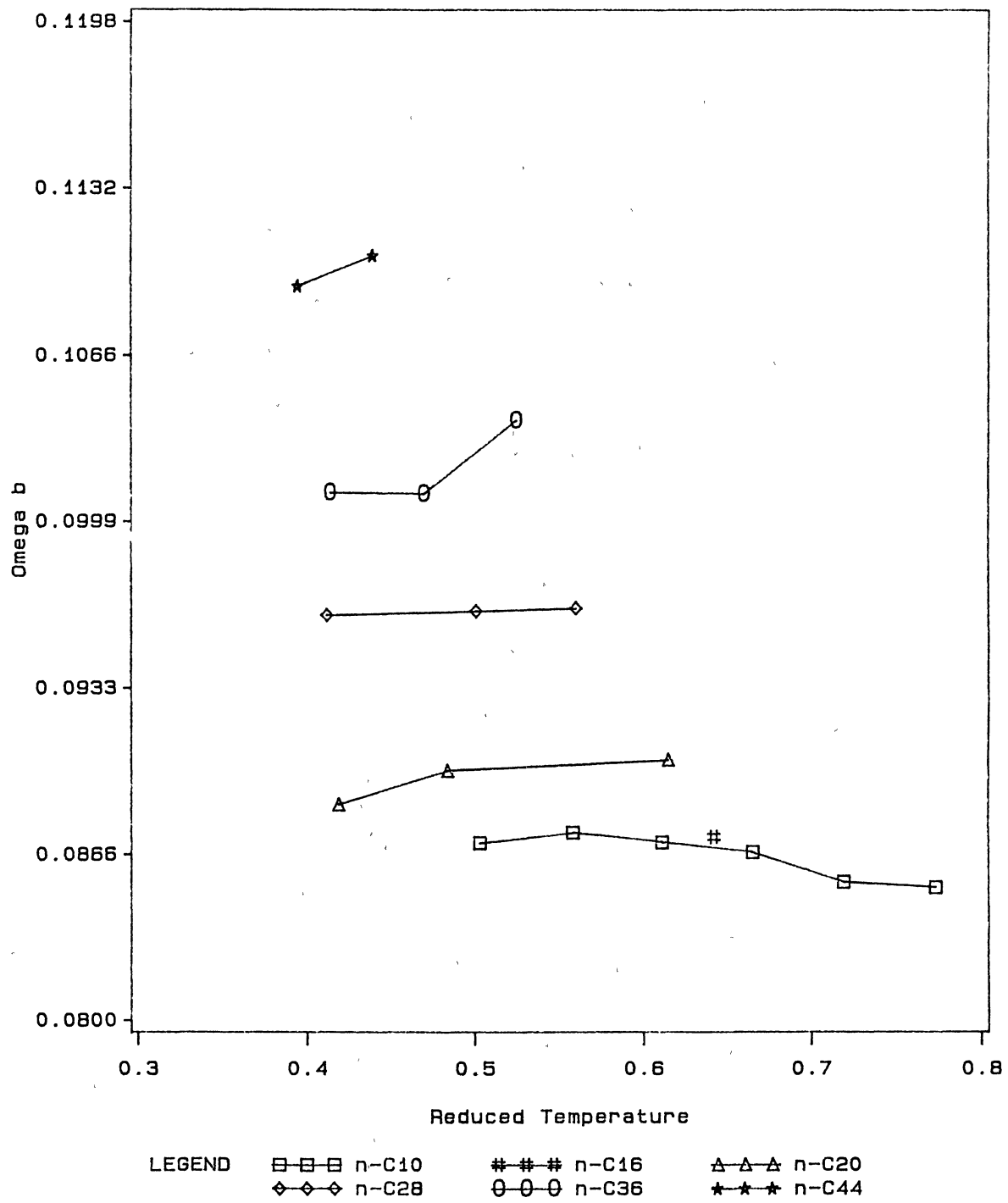
Figure 1

Effects of Reduced Temperature and Solvent Molecular Size on the Optimized

Beta Parameter in the SRK EOS
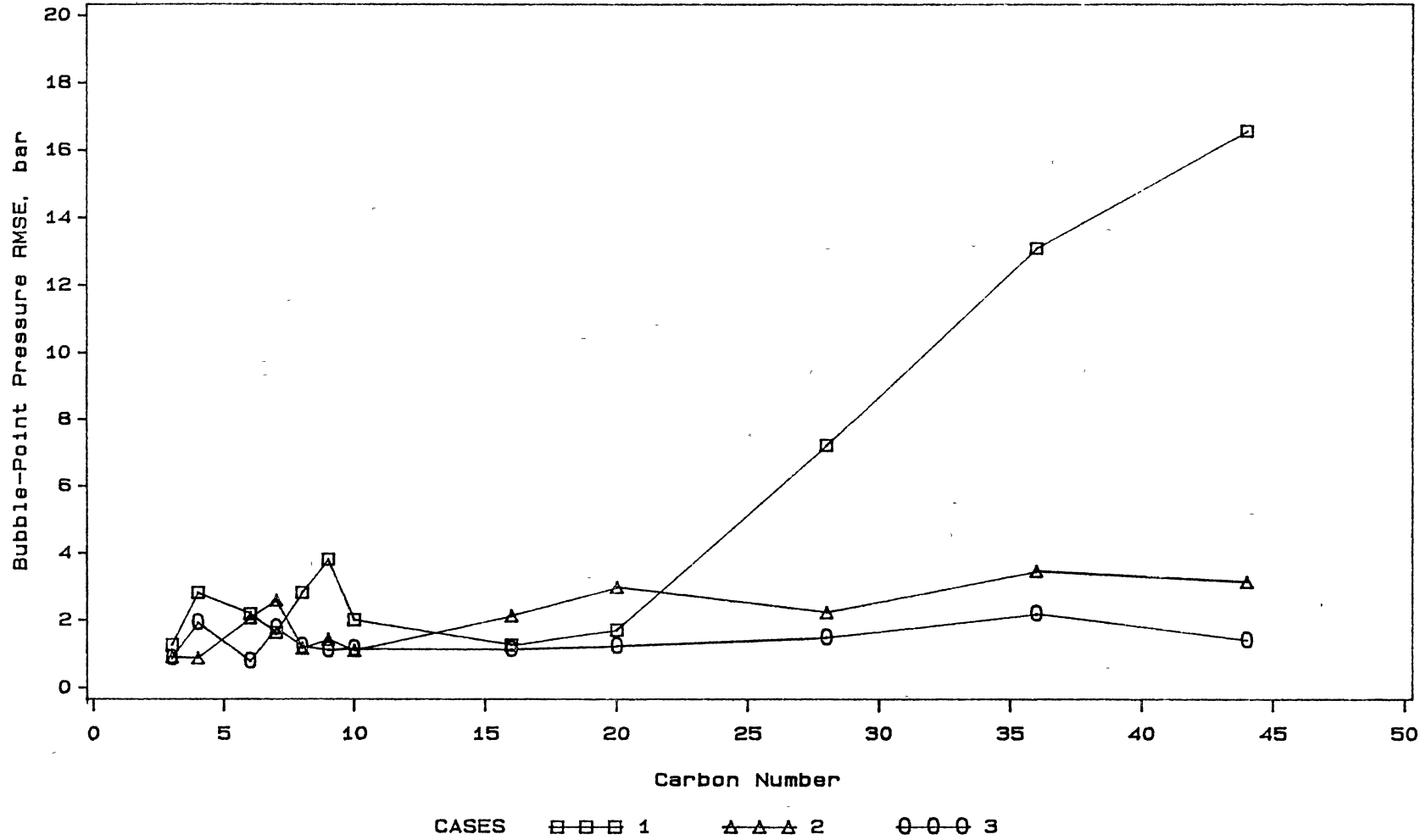
Figure 2.

Molecular Size Effects on Generalized—Parameter SRK EOS Prediction for Methane + n—Paraffins

CHAPTER X

CONCLUSIONS AND RECOMMENDATIONS

Conclusions

1. An experimental apparatus was modified for the measurement of bubble point pressures for binary mixtures of methane in paraffinic ($n-C_{10}$, $n-C_{20}$, $n-C_{28}$, $n-C_{36}$ and $n-C_{44}$), naphthenic (cyclohexane, and trans-decalin), and aromatic (benzene, naphthalene, phenanthrene, and pyrene) solvents at temperatures from 311 to 433 K and pressures to 113 bar. The modifications resulted in a number of improvements including: improved mixing, reduced dead volume, and improved procedures for cleaning and degassing. The apparatus works well; the short equilibration time indicates good mixing and low dead volume in the cell. Reconstruction of the apparatus has also simplified the necessary maintenance.

2. Comparisons of data generated by the apparatus on test systems for which data are available in the literature are very favorable. The bubble point pressure measurements are believed to have an imprecision of no more than 0.4 bar for methane + n-paraffins and methane + naphthenes, and 0.9 bar for methane + aromatics. Instrumental and internal consistency tests performed on the data indicate a high degree of experimental consistency.

3. Data obtained in this study and data found in the literature for binary mixtures of methane in paraffinic, naphthenic, and aromatic solvents were analyzed using the Soave-Redlich-Kwong (SRK) and Peng-Robinson (PR) equations of state (EOS). Interaction parameters for the SRK and PR EOS, based on the new data, were obtained. The SRK and PR EOS, with a single interaction parameter, C_{ij}, for each binary system, were found to represent the acquired binary data for methane + naphthenic and methane + aromatic solvents within 0.002 mole fraction. The EOS prediction capability was improved further by employing a second interaction parameter, D_{ij}. For methane + n-paraffins, the SRK and PR EOS require two interaction parameters, C_{ij} and D_{ij}, for each isotherm to predict the experimental solubility data within 0.002. The optimized interaction parameter, C_{ij}, (setting $D_{ij} = 0.0$) tends to assume higher values at higher temperatures and higher molecular weight of the solvent.

4. The data (new data and data available in the literature) were analyzed using the Krichevsky-Kasarnovsky (KK) equation to provide estimates for the Henry's constants and the infinite-dilution partial molar volumes of methane in solvents having insignificant vapor pressures at the experimental temperatures (and to test the internal consistency of the data). Solubility predictions with average errors less than 0.001 in mole fraction were obtained by employing the KK equation. While the Henry's constants obtained from the KK analyses are believed accurate within a

few percent, the partial molar volumes may not be as accurate (uncertainty may reach 60% of the regressed volume).

5. Generalized expressions for the binary interaction parameter C_{ij}, have been developed in terms of the solvent acentric factor and temperature. Both temperature-dependent and temperature-independent generalized expressions are obtained for the interaction parameters. The quality of the predictions obtained using such correlations is dependent on the complexity of the generalization scheme employed.

Recommendations

1. Regarding the experimental apparatus, it is recommended that all "HIP" valves and connections be replaced by "Autoclave" valves since the latter have been found to be more durable and need less maintenance. The old cell holder inside the oven needs to be removed to provide more working space for the rocking cell. This will also provide more room for a better pivoting assembly of the equilibrium cell.

2. Further studies should be conducted on methane + naphthenic solvents with higher molecular weights (e.g., cyclopentane, tetralin) as well as on methane + mixed solvents containing both sufficient naphthenic and aromatic components which are typical constituents of coal fluids. Systems involving mixed solvents will simulate more realistically methane/hydrocarbons interactions encountered in the actual coal liquefaction processes. Similar experimental studies involving other solutes encountered in

coal liquefaction processes (e.g., nitrogen, carbon monoxide,
etc...) are needed to complement the existing data base on
CO_2, ethane, and methane systems.

3. The generalization procedure, employed in this study
for the SRK and PR EOS, is recommended to be applied in a
parallel fashion for some semi-empirical EOS (e.g., the
simplified perturbed hard chain equation of state) so that
the performance of different groups of equations of state
could be compared and the relative merits of one equation
over the other could be explored.

LITERATURE CITED**

1. Wichterle, I; Linek, J.; Hala, E., Vapor-Liquid Equilibrium Data Bibliography, Elsevier, New York (1973, 1976, 1979, 1982, 1985).

2. Ohe, S., Vapor-Liquid Equilibrium Data at High Pressure, Elsevier, Japan (1990).

3. Mohindra, S., M.S. Thesis, University of Oklahoma, Norman, Oklahoma (1987).

4. Fornari, P. E.; Alessi, P.; Kiki, I., Fluid Phase Equilibria, 57, 1-33 (1990).

5. Hala, E.; Pick, J.; Fried, V.; Vilim, O., Vapor-Liquid Equilibrium, Pergamon Press (1967).

6. Malone, P. V.; Kobayashi, R., Fluid Phase Equilibria, 55, 193-205 (1990).

7. Eubank, P. T.; Hall, K. R., 2nd Int. Conference on Phase Equilibria and Fluid Properties in Chemical Industry, Dechema, Frankfurt, Part II, 675 (1980).

8. Richon, D.; Renon, H., Fluid Phase Equilibria, 14, 235-243 (1983).

9. Gomez-Nieto, I.; Thodos, M., Chem. Eng. Sci., 33, 189-195 (1978).

10. Radosz, M., Supercritical Fluid Technology, Elsevier, Amsterdam, 179 (1985).

11. Simnick, J. J.; Lawson, C. C.; Lin, H.-M.; Chao, K. C., AIChE J., 23, 469-476 (1977).

12. Al-Sahhaf, T. A.; Kidnay, A. J.; Sloan, E. D., Ind. Eng. Chem. Fundam., 22, 372-380 (1983).

13. Kim, C. H.; Vimalchand, P.; Donohue, M. D., Fluid Phase Equilibria, 31, 299-311 (1986).

** References of chapters VI, VII, VIII, and IX are not included here. Each of these chapters has its own references.

14. Parrish, W. R.; Sitton, D. M., J. Chem. Eng. Data, 27, 303-306 (1982).

15. Occhiogrosso, R.; Igel, J. T.; McHugh, M. A., Fluid Phase Equilibria, 26, 165-179 (1986).

16. Huang, S. S.; Leu, A. D.; Ng, H. J.; Robinson, D. B., Fluid Phase Equilibria, 19, 21-32 (1985).

17. Malanowski, S., Fluid Phase Equilibria, 9, 311-311 (1982).

18. Gasem, K. A. M., Ph.D. Dissertation, Oklahoma State University, Stillwater, OK (1986).

19. Raff, A. M., M.S. Thesis, Oklahoma State University, Stillwater, OK (1989).

20. Lin, H.-M.; Sebastian, H. M.; Simnick, J. J.; Chao, K. C., J. Chem. Eng. Data, 24, 146-149 (1979).

21. Beaudoin, J. M.; Kohn, J. P., J. Chem. Eng. Data, 12, 189-191 (1967).

22. Reamer H. H.; Olds, R. H.; Sage, B. H.; Lacey, W. N., Ind. Eng. Chem., 34, 1526-31 (1942).

23. Lavender, H. M.; Sage, B. H.; Lacey, W. N., The Oil and Gas Journal, 46-49, July (1940).

24. Huang, S. H.; Lin, H.-M.; Chao, K. C., J. Chem. Eng. Data, 33, 145-147 (1988).

25. Huang, S. H.; Lin, H.-M.; Chao, K. C., J. Chem. Eng. Data, 33, 143-145 (1988).

26. Tsai, F.-N.; Huang, S. H.; Lin, H.-M.; Chao, K. C., J. Chem. Eng. Data, 32, 467-469 (1987).

27. Schoch, E. D.; Hoffmann, A. E.; Mayfield, F. D., Ind. Eng. Chem., 32, 1351-1353 (1940).

28. Sage, B. H.; Webester, D. C.; Lacey, W. N., Ind. Eng. Chem., 28, 1045-1047 (1936).

29. Reamer, H. H; Sage, B. H.; Lacey, W. N., Ind. Eng. Chem. (Chemical and Engineering Data Series), 3, 240-245 (1958).

30. Lin, H.-M.; Sebastian, H. M.; Simnick, J. J.; Chao, K. C., J. Chem. Eng. Data, 24, 146-149 (1979).

31. Schoch, E. P.; Hoffman, A. E.; Kasperik, A. S.; Lightfoot, J. H.; Mayfield, F. D., Ind. Eng. Chem. 32, 788-791 (1940).

32. Sage, B. H.; Webester, D. C.; Lacey, W. N., Ind. Eng. Chem., 28, 1045-1047 (1936).

33. Elbishlawi, M.; Spencer, J. R., Ind. Eng. Chem. 43, 1811-1815 (1951).

34. Legret, D.; Richon, D.; Renon, H., J. Chem. Eng. Data, 27, 165-169 (1982).

35. Malone, P.V.; Kobayashi, R., Fluid Phase Equilibria, 55, 193-205 (1990).

36. Van Ness, H. C.; Abbott, M. M., "Classical Thermodynamics of Nonelectrolyte Solutions with Applications to Phase Equilibria", McGraw-Hill, New York (1982).

37. Prausnitz, J. M., "Molecular Thermodynamics of Fluid Phase Equilibria", Prentice-Hall, Englewood Cliffs, N.J. (1969).

38. Prausnitz, J. M.; Anderson, T.; Grens, E.; Eckert, C.; Hsieh, R.; O'Connel, J. P., "Computer Calculations for Multicomponent Vapor-Liquid and Liquid-Liquid Equilibria", Prentice-Hall, Englewood Cliffs, N.J. (1980).

39. Chao, K. C.; Robinson, R. L., Jr., (Editors), "Equations of State in Engineering and Research", American Chemical Society, Washington, DC (1979).

40. Chao, K. C.; Robinson, R. L., Jr., (Editors), "Equations of State, Theories and Applications", American Chemical Society, Washington, DC (1986).

41. Chao, K. C.; Greenkorn, R. A., "Thermodynamics of Fluids", Dekker, New York (1975).

42. Walas, S. M., " Phase Equilibria in Chemical Engineering", Butterworth Publishers, Southestone, M.A. (1985).

43. Soave, G., Chem. Eng. Sci. 27, 1197-1203 (1972).

44. Peng, Y. D.; Robinson, D. B., Ind. Eng. Chem. Fundam. 15, 59-64 (1976).

45. Turek, E. A.; Metcalf, R. S.; Yarborough, L.; Robinson, R. L., Jr., Soc. Pet. Eng. J., June, 308-324 (1984).

46. Barrick, M. W., M.S. Thesis, Oklahoma State University, Stillwater, Oklahoma (1985).

47. Anderson, J. M., M.S. Thesis, Oklahoma State University, Stillwater, Oklahoma (1985).

48. Buffkin, B. A., M.S. Thesis, Oklahoma State University, Stillwater, Oklahoma (1986).

49. Ross, C. H., M.S. Report, Oklahoma State University, Stillwater, Oklahoma (1987).

50. Aim, K., Fluid Phase Equilibria 2, 119-129 (1978).

51. Robinson, R. L., Jr., Personal Communication, Oklahoma State University, Stillwater, Oklahoma (1989).

52. Kobotake, Y.; Heldebrand, J. H., J. Phys. Chem., 65, 331-336 (1961).

53. Sievers, U.; Schulz, S., Fluid Phase Equilibria, 5, 35-54 (1980).

54. Schamp, H. W., Jr.; Mason, E. A.; Richardson, A. C.; Altman, A., The Physics of Fluids, 1, 329-337 (1958).

55. Goodwin, R. D., "The Thermophysical Properties of Methane From 90 to 500 K at Pressures to 700 Bars", NBS Technical Note 653, 22 (1974).

56. Old, R. H.; Reamer, H. H.; Sage, B. H.; Lacey, W. N., Ind. Eng. Chem., 35, 922-924 (1943).

57. Neindre, B. L.; Vodar B., (Editors); " Experimental Thermodynamics", Vol. II, Butterworths, London (1975).

58. Wolberg, J. R., "Prediction Analysis", D. Van Nostrand Company, Inc., Princeton, New Jersey (1967).

59. Gupta, M. K.; Li, Y. H.; Hulsey, B. J.; Robinson, R. L., Jr., J. Chem. Eng. Data, 27, 55-60 (1982).
     a) Bubble point pressure measurements;
     b) Phase composition measurements.

60. Goodwin, R. D.; Haynes W. M., "Thermophusical Properties of Propane from 85 to 700 K at Pressures to 70 MPa", Nat. Bur. Stand. Monog., 170 (1980).

61. ASHRAE Handbook 1981 Fundamentals, American Society of Heating, Refrigerating, and Air-Conditioning Engineers, Inc., Atlanta, Ga. (1981).

62. Ambrose, D.; Counsell, F. D.; Davenport, A. J., J. Chem. Thermody., 2, 283-291 (1970).

63. "Lange's Handbook of Chemistry", 12th Edition, Dean, J. D., (Editor), McGraw-Hill Book Company, New York, (1979).

64. Flory, P. J.; Orwoll, R. A.; Vrij, A., J. Am. Chem. Soc., 86, 3507-3515 (1964).

65. API Research Project 44, Selected Values of Properties of Hydrocarbons and Related Compounds. Thermodynamic Research Center, Texas A&M College, College Station, Texas, October (1972).

66. Gurevich, B. S.; Bednov, V. M., "Temperature Variation of the Density and Viscosity of Aromatic Substances.", Russian Journal of Physical Chemistry, 46, 1532-1534 (1972).

APPENDIXES

APPENDIX A

ANALYSIS OF EXPERIMENTAL ERRORS

Experimental measurements usually are vulnerable to two kinds of experimental errors: systematic and random. Systematic errors are attributed to an inherent bias in the procedure used which results in a consistent deviation of the measured variables from their true values. Systematic errors, therefore, affect directly the accuracy of the experiment. Random errors, on the other hand, are assumed to result from unavoidable small disturbances of the experimental conditions and thus have a direct influence on the precision of the experiment. Precision in this context refers to the reproducibility of the observable under "identical" experimental conditions.

Systematic Errors

Systematic errors arise from many sources including [57]: bias in the experimental and/or computational procedures, inherent assumptions in processing the data, uncertainties in ancillary input data taken from other works, possible sensitivity or resolution in the measurements and many other causes. When an indication of systematic error exists, it is imperative to identify and eliminate the cause.

213

Experience is an important factor in dealing with systematic errors; however, systematic procedures are needed to test regularly for the presence of such errors. Toward this end, three test procedures were employed to guard against probable systematic errors as follow:

Instrumental Consistency Tests

These tests include: frequent calibration of pressure gauges against a dead weight tester as described previously in Chapter IV, frequent calibration of temperature measuring elements by conducting water ice-point and boiling-point tests, and calibration of the volumetric screw pumps (the gas pump and the hydrocarbon injection pump) against each other.

External Reproducibility Tests

The objective of these tests is to verify directly the accuracy of the experimental procedure by comparing the results obtained using the present apparatus with those of other investigators at the same (or similar) experimental conditions. Toward this end, two kinds of reproducibility tests (on systems for which literature data are abundant) were conducted: vapor pressure measurements of selected pure materials, and bubble point pressure measurements for selected binary systems.

Representative vapor pressure measurements of pure propane, ammonia, benzene and cyclohexane are given in Table A-1, along with the reported literature values. The measured

vapor pressures of this work and the reported literature values agree within 1 psia over the whole pressure range (maximum estimated uncertainty in our vapor pressure measurements is 0.5 psia). The slight differences exhibited may be attributed to differences in the purity of the materials used in the different investigations.

Bubble point pressure measurements were conducted on two test binary systems: CO_2 + benzene and CO_2 + n-hexatriacontane (n-C_{36}). The choice of CO_2 + benzene was dictated mainly by the abundance of literature data on this system, whereas the second system (CO_2 + n-C_{36}), (besides the available literature data) was chosen as a test system because it is typical of most of the solvents encountered in this study, (i.e., solid at room temperature). Data on these two test systems are presented in Table A-2. Comparisons of our results for these two test systems with those reported by various investigators, are shown in Figures A-1 and A-2. The comparisons are shown in terms of deviations of the solubilities from values predicted using the Soave-Redlich-Kwong (SRK) [43] equation of state (EOS). For CO_2 + n-C_{36} system, interaction parameters employed in the EOS prediction were obtained by minimizing the sum of squares of pressure deviation from the experimental values of this work, whereas for CO_2 + benzene system interaction parameters used in the EOS prediction are those fitting Gupta's data [59] because of the wider pressure range covered. Detailed procedure for data reduction is given by Gasem [18]. The quality of our

data for both systems are the same as those of other investigators [18,19,26,47,59] as revealed by Figures A-1, A-2, and A-3.

Self-Consistency Test

The objective here is to check for the consistency of the data collected on the same apparatus at different experimental conditions. In such tests, the pressure-to-mole fraction ratio, $(P-P^o)/x_{CH_4}$, is plotted against CH_4 mole fraction, therefore, any inherent pressure errors are magnified by the reciprocal of the mole fraction, which, combined with the fact that plots of P/x against x are often nearly linear, facilitates identification of erroneous runs. Another reason this test works so well is that the $(P-P^o)/x_{CH_4}$ values cover a range less than P. The amount of scatter in such a plot is indicative of the precision of the data analyzed, and the quality of variation of $(P-P^o)/x_{CH_4}$ with x_{CH_4} among different isotherms is a reflection on the accuracy of the data obtained. A typical $(P-P^o)/x_{CH_4}$ plot appears in Figure A-3.

Random Errors

Random errors result from small unavoidable disturbances of the experimental conditions about their true values. This gives rise to the concept of uncertainty in each measurable variable. Uncertainty here, which could be expressed in a number of different ways [57], designates an interval around

the measured value of the variable which accommodates the true value of that variable. Due to their random nature, random errors lend themselves to statistical analysis. In general, for any observable "Y" that depends on the measured, independent variables X_1, X_2,...,X_n according to the functional relation:

$$Y = f(X_1, X_2,...,X_n)$$ (A-1)

the expected variance $(\sigma^2 Y)$ is given by [58]:

$$(\sigma_Y)^2 = (\partial Y/\partial X_1)^2(\sigma X_1)^2 + (\partial Y/\partial X_2)^2(\sigma_{X2})^2 +...+$$
$$(\partial Y/\partial X_n)^2(\sigma_{Xn})^2$$ (A-2)

where $(\sigma X_1)^2$, $(\sigma_{X2})^2$, ..., $(\sigma_{Xn})^2$ are the variances in the input measured variables X_1, X_2,...,X_n. If the variable "Y" is also measurable, the instrumental error "ϵ_Y" must be included into Equation A-2 to give equation A-3 below [18]:

$$(\sigma_Y)^2 = (\partial Y/\partial X_1)^2(\sigma X_1)^2 + (\partial Y/\partial X_2)^2(\sigma_{X2})^2 +...+$$
$$(\partial Y/\partial X_n)^2(\sigma_{Xn})^2 + (\epsilon_Y)^2$$ (A-3)

Expected Uncertainty in Mole Fraction

Mole fraction is a computed variable defined as:

$$x_i = n_i/(\Sigma n_i)$$ (A-4)

where x_i and n_i are the mole fraction and number of moles of species "i", respectively, and the sum is over all species present in the mixture. For a binary mixture this becomes:

$$x_1 = n_1 / (n_1 + n_2) \qquad \qquad (A-5)$$

substituting for n_1 and n_2 in terms of molar density and injected volumes for the solute (1) and the solvent (2) we get:

$$x_1 = \frac{\Sigma(\rho_{1i} v_{1i})}{\Sigma(\rho_{1i} v_{1i}) + \rho_2 v_2} \qquad \qquad (A-6)$$

where the sum now is over the number of gas injections which produces the mole fraction x_1. For an average of three injections of the gas done under the same conditions of temperature and pressure and one injection of the solvent, equation A-6 above becomes :

$$x_1 = \frac{\rho_1 \Sigma v_{1i}}{\rho_1 \Sigma v_{1i} + \rho_2 v_2} \qquad \qquad (A-7)$$

The uncertainty in x_1 of equation A-7 in the light of equation A-2, after simple manipulations and arrangements becomes:

$$(\sigma_{x1})^2 = x_1^2 (1-x_1)^2 [(\sigma \rho_1 / \rho_1)^2 + (\sigma \rho_2 / \rho_2)^2 + (\sigma v_2 / v_2)^2 + \Sigma(\sigma v_{1i} / \Sigma v_{1i})^2] \qquad (A-8)$$

To give an estimate of the uncertainty of methane mole fraction in each of the different solvents considered in this study, as Equation A-8 suggests, one needs to assume, for a certain mole fraction (x_1), values for: $(\sigma \rho_1 / \rho_1)$, $(\sigma \rho_2 / \rho_2)$, $(\sigma v_2 / v_2)$ and (σv_{1i}). Conservative assumptions are made for these as follows:

$(\sigma\rho_1/\rho_1) = 0.0015$ (Relative uncertainty in methane density)

$(\sigma\rho_2/\rho_2) = 0.0015$ (Relative uncertainty in solvent density)

$(\sigma v_2/v_2) = 0.0013$ (Relative uncertainty in solvent volume,

assuming an uncertainty of 0.0075 cc in

hydrocarbon injection pump, and 6 cc of

solvent injection)

$(\sigma v_{1i}) = 0.0075$ cc (Uncertainty in gas injection pump)

To give an estimate of the last term $(\Sigma(\sigma v_{1i}/\Sigma v_{1i})$, one needs

the total amount of gas (Σv_{1i}) that produces methane mole

fraction of (x_1). The total volume of gas required to give

a certain mole fraction of methane at a certain temperature

is easily calculated from Equation A-7. These data are shown

in Table A-3 along with the computed uncertainty in mole

fraction (σx_1) from Equation A-8.

Expected Uncertainty in Bubble Point Pressure

Bubble point pressure of a given binary mixture depends

on the composition and temperature of the mixture. So, in the

light of Equation A-3, the uncertainty in pressure (σ_P) is

given by:

$$(\sigma_P)^2 = (\epsilon_P)^2 + (\partial P/\partial x_1)^2 (\sigma x_1)^2 + (\partial P/\partial T)^2 (\sigma_T)^2 \qquad (A-9)$$

Where ϵ_P is the instrumental error in pressure measurement,

σx_1 is the uncertainty in methane mole fraction and σ_T is the

uncertainty in temperature measurement. Typical conservative

values for ϵ_P and σ_T are 0.5 psia and 0.1°C respectively.

However, there is still one source of variability that

affects bubble point pressure measurement which is not accounted for by Equation A-9, that is uncertainty attributed to the procedure used in determining the bubble point pressure. To quantify this uncertainty, repeated bubble point pressure measurements were made on each of several fluid mixtures at fixed temperature and composition. This was done by repeating the pressure-volume transvers several times and comparing the pressures at which the break occurred. The procedural uncertainty was found to depend on the pressure level of the mixture as shown in Table A-4. This dependency could be expressed as follows:

$$\epsilon_P = 0.004 \; P \quad (psia) \tag{A-10}$$

Equation A-10 includes both the prime and the procedural error but not the propagated error due to uncertainty in mole fraction. To account for such a contribution Equations A-9 and A-10 are combined to give the expected error in the bubble point pressure as follows:

$$\sigma_P = [(0.004 \; P)^2 + (\partial P/\partial x_1)^2 (\sigma_{x_1})^2]^{1/2} \tag{A-11}$$

The temperature contribution to the uncertainty of pressure, being of the order of 0.1 psia, has been neglected.

To estimate the uncertainty in pressure from Equation A-11, one needs values of the rate of change of pressure with respect to mole fraction ($\partial P/\partial x_1$) at the same mole fraction levels at which values of σ_{x_1} were estimated. This was achieved by employing a third order polynomial fit of P-x

data at the specified isotherm of each system. The slopes thus obtained are presented in Table A-5. Substituting into Equation A-11 for $(\partial P/\partial x_1)$ from Table A-5, σ_{x_1} from Table A-3 and P that corresponds to x_1 for each system, we get the final uncertainty estimates for bubble point pressures appearing in Table A-5.

Table A-1

Vapor Pressure Measurements

Material	Temperature (°F)	Vapor Pressure, psia		Ref. No.
		Experimental	Literature	
Propane	122.0	249.2	249.4	60
Ammonia	116.3	270.0	271.5	61
Ammonia	125.3	308.3	309.3	61
Ammonia	161.3	500.6	501.1	61
Benzene	302.0	85.0	84.9	62
Cyclohexane	196.5	20.7	20.0	63
Cyclohexane	267.4	54.2	53.5	63

Table A-2

Solubility Data for Carbon Dioxide + Benzene and Carbon Dioxide + n-Hexatriacontane

Mole Fraction Carbon Dioxide	Bubble Point Pressure bar	(psia)
CO_2 + Benzene at 313.2 K (40.0°C, 104.0°F)		
0.099	12.6	(183)
0.207	24.8	(359)
0.267	30.8	(446)
0.364	39.6	(574)
CO_2 + n-Hexatriacontane at 373.2 K (100.0°C, 212.0°F)		
0.067	6.3	(91)
0.144	12.9	(187)
0.255	25.6	(372)
0.336	37.2	(539)
0.445	56.4	(818)

Table A-3

Typical Volumes of Methane Injected to Yield the Average Mole
Fraction of the Corresponding Isotherm, Along with the
Uncertainty in Mole Fraction as Computed
from Equation (A-8)

Solvent	Temp. ($^\circ$F)	Vol.(V), cc	$\sigma V/V$	σ_{x1} (Eq. A-8)
n-Decane	220	2.8	0.0027	0.0007
n-Eicosane	212	1.5	0.0050	0.0012
n-Octacosane	212	1.2	0.0061	0.0014
n-Hexatriacon-tane	212	1.3	0.0058	0.0013
n-Tetratetra-contane	212	0.9	0.0081	0.0018
Benzene	212	6.5	0.0012	0.0004
Cyclohexane	212	5.3	0.0014	0.0005
t-Decalin	212	3.8	0.0020	0.0005
Naphthalene	212	2.3	0.0033	0.0004
Phenanthrene	230	1.8	0.0041	0.0005
Pyrene	320	1.7	0.0044	0.0006

Table A-4

Reproducibility of the Bubble Point Determination

Pressure Range (psia)	Reproducibility (psia)
0- 250	0.6
250- 500	1.7
500- 750	2.7
750- 1000	3.5
1000-1600	5.0

Table A-5

Uncertainty in Bubble Point Pressure of Methane Binary
Systems Estimated at the Average Composition of the
Corresponding Isotherm

| Solvent	Temp., °F	$(\partial P/\partial x_1)$, psia	σ_{x_1}	σ_P, psia (Eq. A-11)
n-Decane	220	4.8×10^3	0.0007	4
n-Eicosane	212	3.9×10^3	0.0012	5
n-Octacosane	212	3.4×10^3	0.0014	5
n-Hexatriacon-tane	212	3.1×10^3	0.0013	4
n-Tratetra-contane	212	2.6×10^3	0.0018	5
Benzene	212	8.0×10^3	0.0004	5
Cyclohexane	212	5.7×10^3	0.0005	4
t-Decalin	212	6.8×10^3	0.0005	5
Naphthalene	212	1.3×10^4	0.0004	7
Phenanthrene	230	1.7×10^4	0.0005	10
Pyrene	320	2.0×10^4	0.0006	13
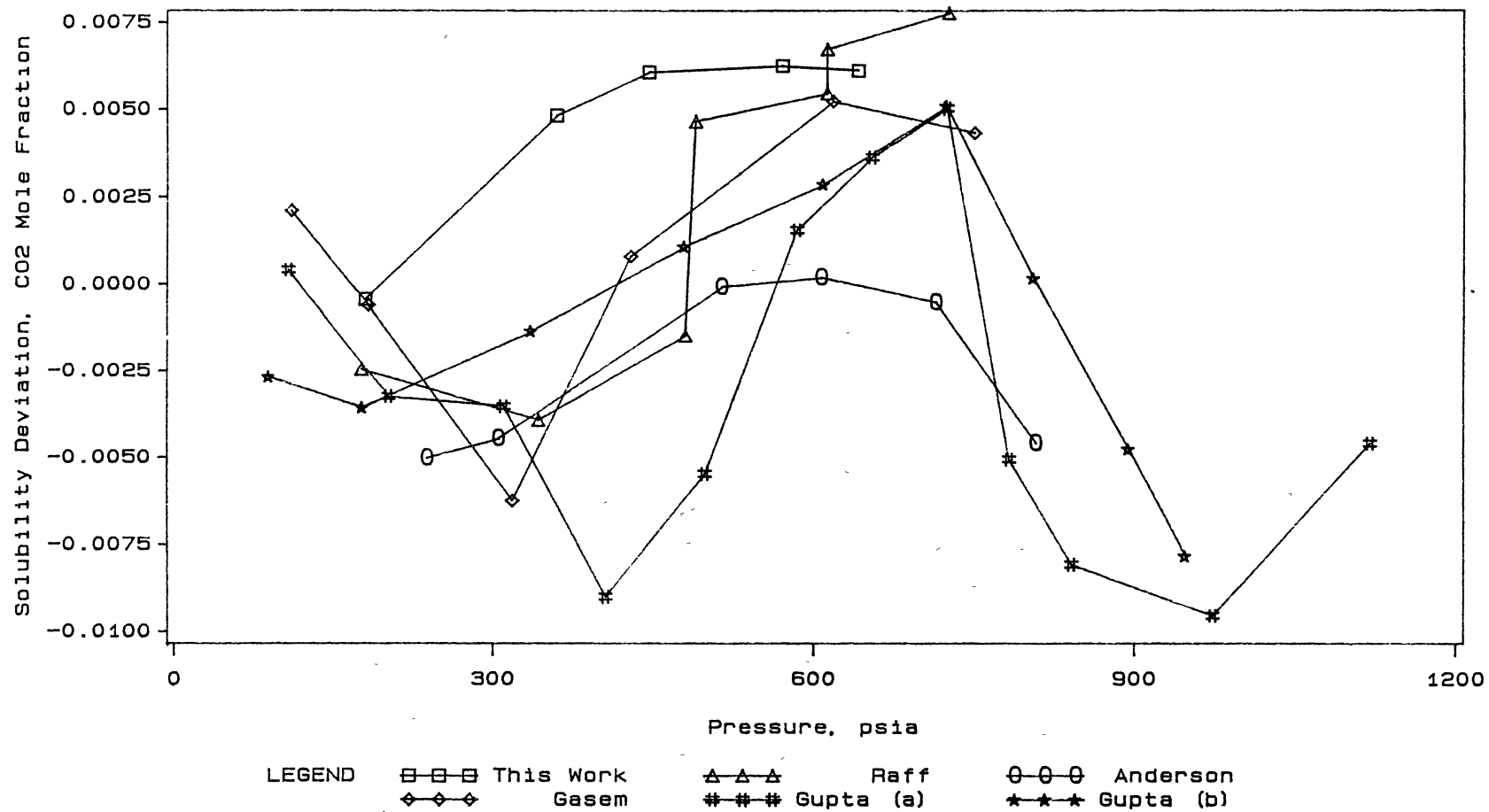
Figure A—1

Comparison of Carbon Dioxide Solubilities in Benzene at 104 F
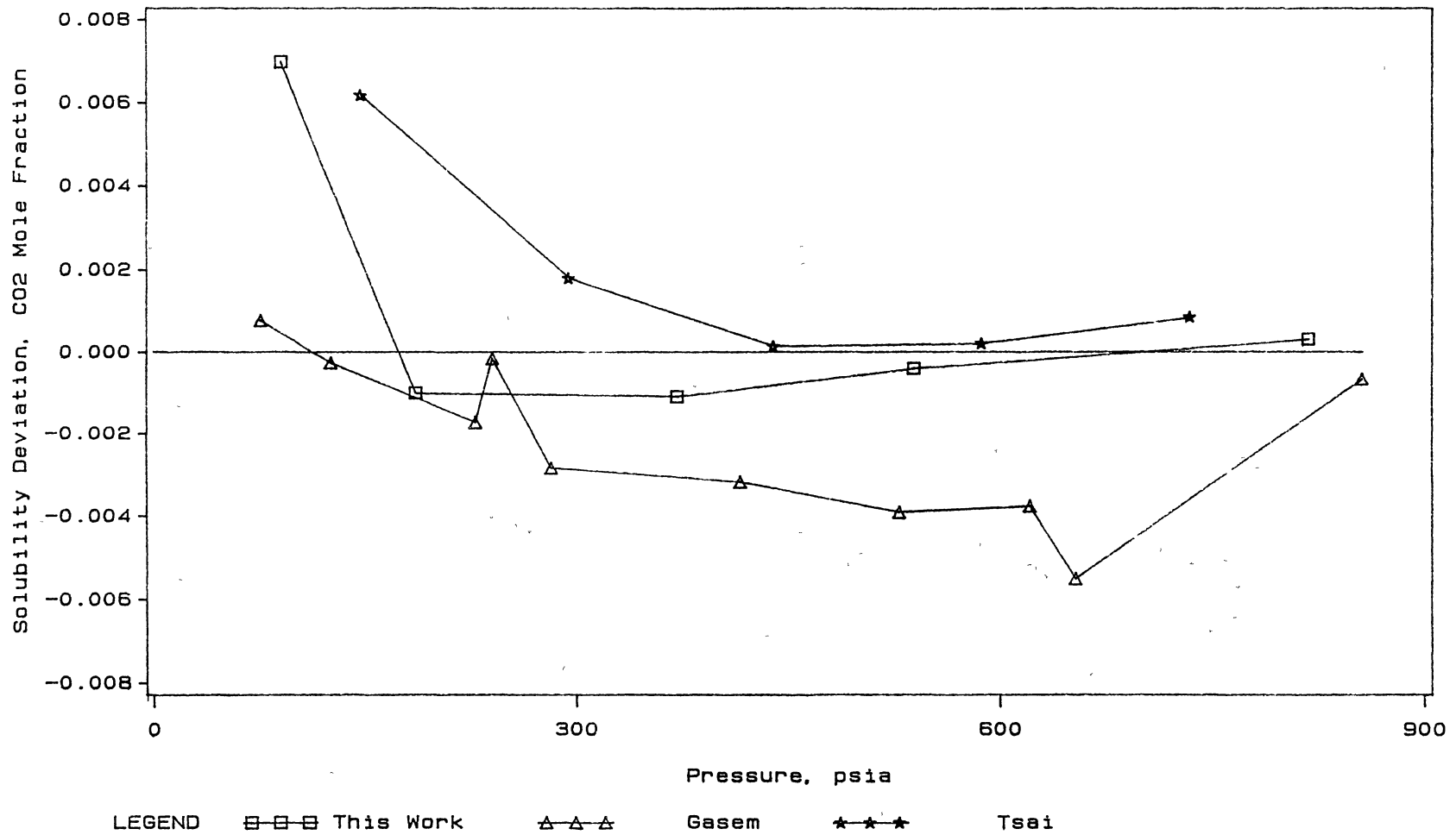
Figure A—2

Comparison of Carbon Dioxide Solubilities in n—Hexatriacontane at 212 F
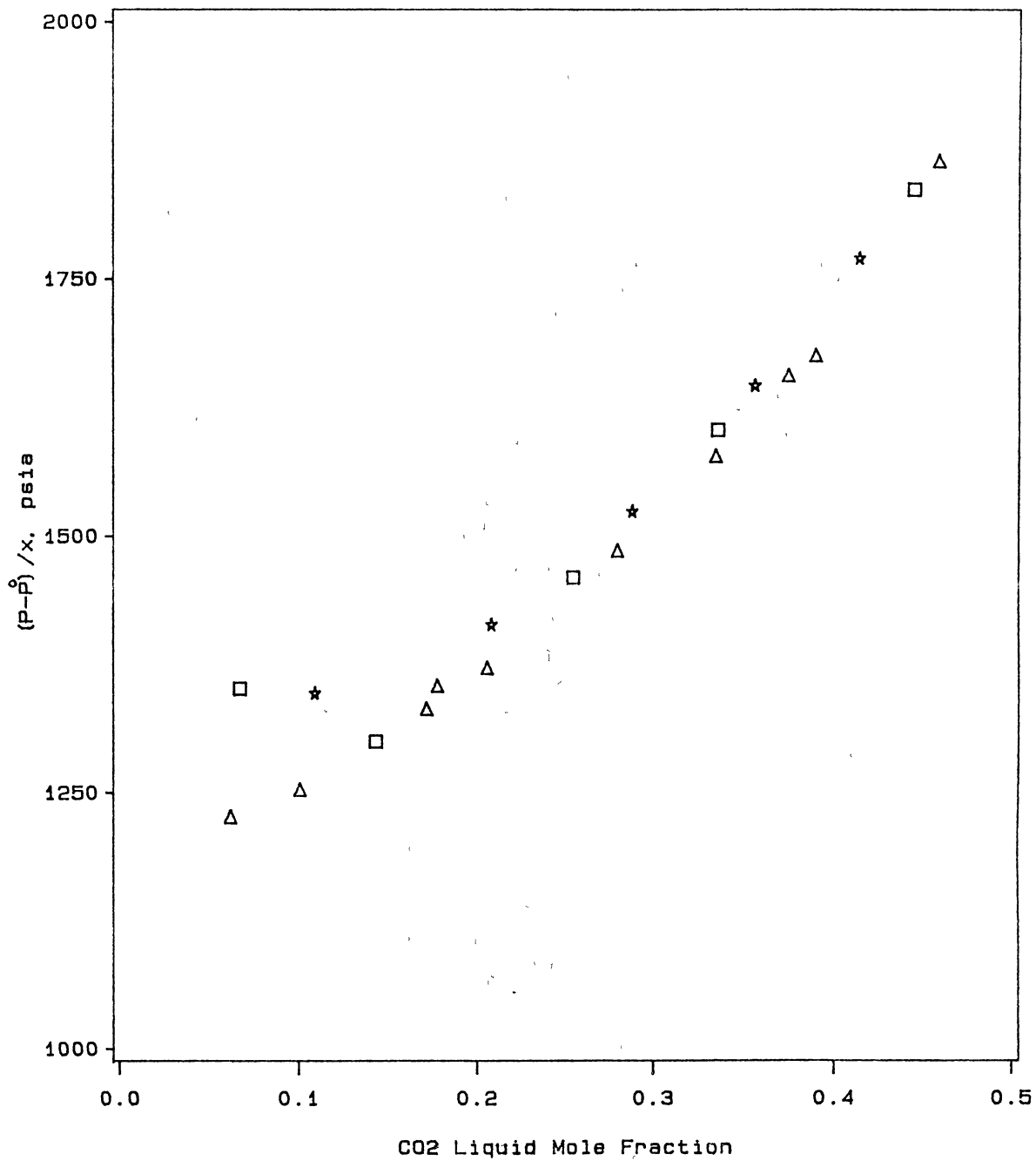
Figure A—3

Bubble Point Pressure Data for Carbon Dioxide + n—Hexatriacontane at 212 F

APPENDIX B

Table B-1

DENSITIES OF SOLVENTS USED IN THIS STUDY

Solvent	Temperature (°F)	Density (g/cc)	Reference
$n-C_{10}$	100	0.7167	64
	160	0.6908	64
	220	0.6669	64
	280	0.6407	64
$n-C_{20}$	122	0.7693	64
	212	0.7347	64
	302	0.704	64
$n-C_{28}$	167	0.7716	64
	212	0.7555	64
	302	0.7235	64
$n-C_{36}$	212	0.7666	64
	302	0.7357	64
$n-C_{44}$	212	0.776	64
	302	0.745	64
Cyclohexane	122	0.7362	65
	212	0.6956	65
	302	0.6474	65
t-Decalin	122	0.8450	65
	212	0.8124	65
	302	0.7865	65
Benzene	122	0.8469	65
	212	0.7907	65
	302	0.7295	65
Naphthalene	212	0.9628	66
	302	0.9219	66
Phenanthrene	230	1.0613	66
	302	1.0326	66
Pyrene	320	1.1065	46

229

APPENDIX C

UNCERTAINTY IN METHANE DENSITY

The methane density, as well as the uncertainty in the gas density, depends on the temperature and pressure of the gas. In this study all of methane gas injections were done at 50°C leaving us with the freedom to choose the injection pressure in the gas pump. A pressure range (if any) over which the uncertainty of gas density is high should be avoided since this uncertainty will reflect itself in the uncertainty of the calculated mole fractions. This appendix presents the necessary calculations for such an analyses.

The uncertainty in density of methane, as given by error propagation formula, is

$$\sigma \rho_{CH_4} = [(\partial \rho_{CH_4}/\partial P)^2 (\sigma_P)^2 + (\partial \rho_{CH_4}/\partial T)^2 (\sigma_T)^2]^{1/2} \qquad (C-1)$$

where

$\sigma \rho_{CH_4}$ is the uncertainty in methane density

σ_P is the uncertainty in pressure

σ_T is the uncertainty in temperature

The partial derivatives and the density are calculated from Bender's equation of state for methane :

$$P = RT\rho + B\rho^2 + C\rho^3 + D\rho^4 + E\rho^5 + F\rho^6 + $$
$$(G\rho^3 + H\rho^5)\exp(-a_{20}\rho^2) \qquad (C-2)$$

where P and T are pressure and temperature, ρ is the density and R the universal gas constant. B, C, D, E, F, G, and H are functions of temperature [see ref. 20 in Chapter VI].

From Eq. C-2 we get by direct differentiating:

$$(\partial P/\partial \rho)_T = RT + 2B\rho + 3C\rho^2 + 4D\rho^3 + 5E\rho^4 + 6F\rho^5 +$$
$$(3G\rho^2 + 5H\rho^4)\exp(-a_{20}\rho^2) +$$
$$(G + H\rho^2)\rho^3\exp(-a_{20}\rho^2)(-2a_{20}\rho) \qquad (C-3)$$

$$(\partial P/\partial T)_\rho = R\rho + B^P\rho^2 + C^P\rho^3 + D^P\rho^4 + E^P\rho^5 + F^P\rho^6 +$$
$$(G^P + H^P\rho^2)\exp(-a_{20}\rho^2)\rho^3 \qquad (C-4)$$

noting that the "P" indicates differentiating with respect to temperature and that

$$(\partial \rho/\partial P)_T = 1/(\partial P/\partial \rho)_T$$
$$(\partial \rho/\partial T)_P = -(\partial P/\partial T)_\rho (\partial \rho/\partial P)_T$$

and substituting into Eq. C-1 we get an expression for the uncertainty in density which could be calculated for each selected pressure. The uncertainty in methane density is calculated at 50°C, as described above, for pressures to 1500 psia and the profile obtained is shown in Figure C-1.
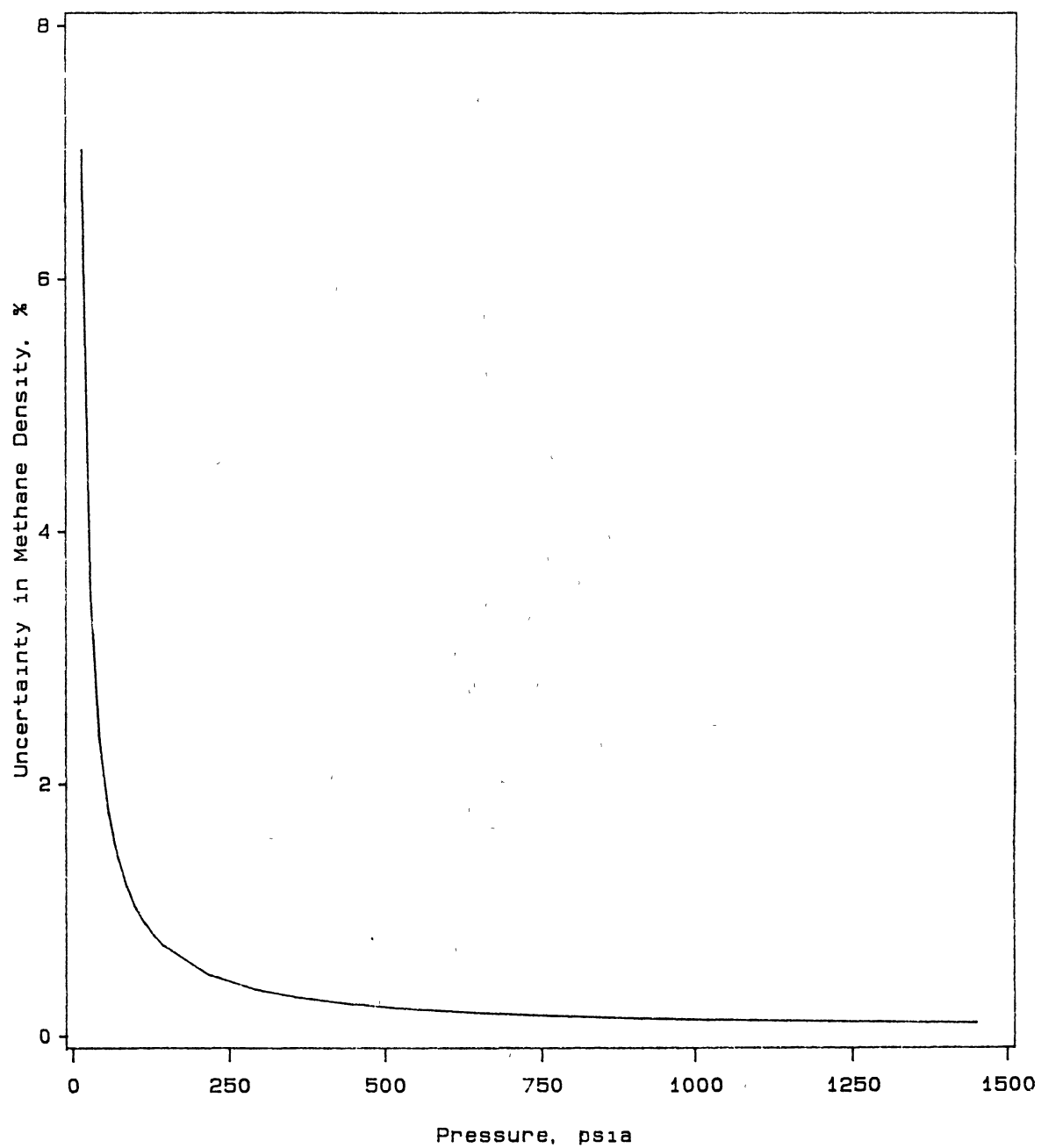
Figure C—1

Percentage Uncertainty in Methane Density at 50°C

APPENDIX D

PRESSURE CORRECTIONS

Pressures indicated by the pressure transducers, PT1 and PT2 (see Figure D-1) must be corrected for mercury head in the lines and for drift effects which could be accounted for by frequent calibration of the pressure transducers. Calibration of PT1 is usually done using a dead-weight gauge. PT2 is then calibrated against PT1. The result of a calibration procedure (details are given in Chapter V) is a table containing corrections for the observed pressures of PT1 (shown in Table D-1) and a calibration sheet presenting the correspondence between the pressure readings conveyed by PT1 and PT2.

Pressures indicated by PT1

To find the true pressure corresponding to the observed one indicated by PT1, the proper correction, coming from the correction table (Table D-1) is merely added to the observed pressure.

True Bubble Point

The true bubble point pressure of the binary mixture in the equilibrium cell (EC) is found as follows:

233

1. The observed bubble point pressure is read from a plot of pressure versus injected volume.

2. The observed pressure is corrected by adding the corresponding correction obtained from the correction table.

3. The mercury head from equilibrium cell (EC) to PT1, which is 53.3 cm Hg (10.3 psia) as shown in Figure D-1, is subtracted from the result of step 2 above.

True Gas Pressure

Calibration of pressure transducer PT2 is usually done by cross calibration with PT1 through a gas-mercury interface (GMI). To find the true pressure in the gas pump (GP) the following action is taken:

1. The observed gas pressure is taken from the PT2 readout.

2. From the calibration sheet interpolate to find the corresponding pressure of PT1.

3. The mercury head in the gas-mercury interface is subtracted from pressure value of step 2 above.

4. The pressure thus obtained is corrected by adding the corresponding correction from the correction table.
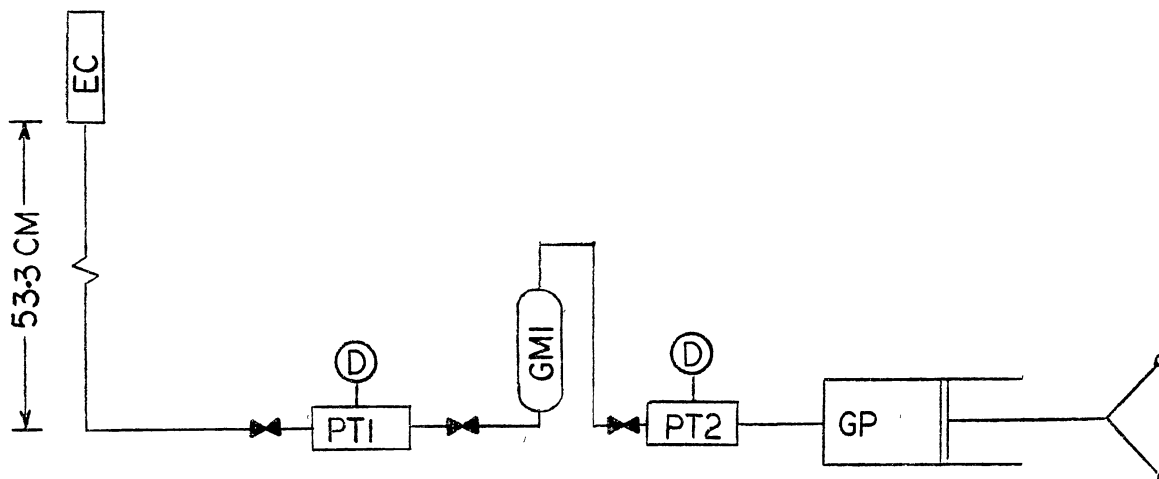
D   : Digital Readout   GP : Gas Pump
EC : Equilibrium Cell   PT1 : Pressure Transducer
GMI : Gas-Mercury Interface   PT2 : Pressure Transducer

Figure D-1

Simplified Diagram Showing Necessary Corrections
to Pressure Readings

Table D-1

Typical Calibration Corrections for the Pressure Transducer (PT1)

Trans. Press. (psia)	D. W. Press. (psia)	Trans. Corr.* (psia)
64.80	49.94	-0.63
94.40	79.90	-0.27
143.90	129.84	0.17
194.00	179.78	0.01
243.70	229.71	0.24
264.00	249.69	-0.08
293.90	279.65	-0.02
393.80	379.53	-0.04
443.70	429.46	-0.01
543.60	529.34	-0.03
643.40	629.22	0.05
743.40	729.09	-0.08
843.00	829.05	0.28
943.00	928.85	0.08
1042.60	1028.72	0.35
1142.60	1128.60	0.23
1242.20	1228.45	0.48
1342.20	1328.32	0.35
1441.90	1428.20	0.53
1541.60	1528.07	0.70

* (Trans. Corr.) = (D. W. Press.) + Pa - (Trans. Corr.) where Pa is the atmospheric pressure at calibration condition (14.23 psia).

$\mathcal{Z}$

VITA

Naif A. Darwish

Candidate for the Degree of

Doctor of Philosophy

Thesis: BINARY VAPOR-LIQUID PHASE EQUILIBRIUM FOR METHANE IN SELECTED HEAVY NORMAL PARAFFINS, NAPHTHENES, AND AROMATICS

Major Field: Chemical Engineering

Biographical:

Personal Data: Born in Bardala Palistine, April 27, 1957, the son of Abdulaziz A. Darwish and Tarfeh M. Farhan.

Education: Attended elementary school in Al-Huson, Jordan; graduated in 1976 from Al-Huson High School. Received the Bachelor of Science degree in Chemical Engineering from Kuwait University in Kuwait in June 1981. Received Master of Science in Mechanical Engineering from Yarmouk University in Jordan in December 1983. Completed the requirements for Doctor of Philosophy degree in May, 1991.

Professional Experience: Graduate teaching assistant, Mechanical Engineering Department, Yarmouk University-Jordan, 1981-1983. Lecturer, Chemical Engineering Department, University of Petroleum and Minerals, Dahran, Saudia Arabia, 1984-1985. Graduate Research assistant, School of Chemical Engineering, Oklahoma State University, 1987-1991.